Molecular analysis of chromosome movement by microtubule depolymerisation-coupled pulling

Philip Auckland

A thesis submitted for the degree of Doctor of Philosophy
in Interdisciplinary Biomedical Research

Warwick Medical School, The University of Warwick,
October 2016

Contents

Chapter 3: *Congressing kinetochores require progressive loading of Ska complexes to prevent force dependent detachment*

Chapter 4: *Distinct contributions of the Ska complex, CENP-F and CENP-E to depolymerisation-coupled pulling*

Bancroft, J., P. Auckland, C.P. Samora, and A.D. McAinsh. 2015. Chromosome congression is promoted by CENP-Q- and CENP-E-dependent pathways. *J Cell Sci*. 128:171-184.

Auckland, P., and A.D. McAinsh. 2015. Building an integrated model of chromosome congression. *J Cell Sci*. 128:3363-3374.

Auckland, P., Clarke, N.I., Royle, S.J., and McAinsh, A.D. 2017. Congressing kinetochores progressively load Ska complexes to prevent force-dependent detachment. *J Cell Biol*.

Figures and tables

Abbreviations

DCP – depolymerisation-coupled pulling

SAC – Spindle assembly checkpoint

Ska – Spindle and kinetochore associated

CENP – Centromere protein

siRNA – Small interfering RNA

IF – Immunofluorescence

SBF-SEM – Serial block face scanning electron microscopy

Ab - antibody

Declaration

This thesis is submitted to the University of Warwick in support of my application for the degree of Doctor of Philosophy. It has been composed by myself and has not been submitted in any previous application for any degree.

Parts of the introduction and results have been published by the author, and can be found here:

Auckland, P., and A.D. McAinsh. 2015. Building an integrated model of chromosome congression. *J Cell Sci*. 128:3363-3374.

Bancroft, J., P. Auckland, C.P. Samora, and A.D. McAinsh. 2015. Chromosome congression is promoted by CENP-Q- and CENP-E-dependent pathways. *J Cell Sci*. 128:171-184.

Auckland, P., Clarke, N.I., Royle, S.J., and McAinsh, A.D. 2017. Congressing kinetochores progressively load Ska complexes to prevent force-dependent detachment. *J Cell Biol*.

Inclusion of published work

In appendix 2 I have included three papers to which I have contributed. The first “chromosome congression is promoted by CENP-Q and CENP-E dependent pathways” (Bancroft et al., 2015). Here, I conducted all experiments for figures five and six, and contributed to manuscript preparation. The second “building an integrated model of chromosome congression” (Auckland and McAinsh, 2015). Here, I produced all figures and wrote the manuscript under the supervision of Prof Andrew D. McAinsh. The third, “congressing kinetochores progressively load Ska complexes to prevent force-dependent detachment” (Auckland et al, 2017). Here I conducted all experiments with the exception of the electron microscopy and prepared the manuscript with Prof Andrew D. McAinsh.

Summary

The alignment of all chromosomes at the spindle equator is a universal feature of mitosis in metazoans. Kinetochores mediate this migratory event by either sliding chromosomes along the lattice of spindle microtubules (lateral sliding) or by coupling them to depolymerising microtubule plus-ends (depolymerisation-coupled pulling, DCP). While a robust molecular description of the lateral sliding mechanism has been generated both *in vivo* and *in vitro* over the past decade, similar models of DCP are lacking. This may represent the comparable complexity of DCP, where multiple redundant kinetochore factors contribute to specific DCP sub-steps that together enable congression. Moreover, unlike the lateral sliding motor CENP-E, many candidate DCP factors have pleiotropic roles in the kinetochore and convincingly separating these *in vivo* is complex. Here, we discuss how combining high-resolution kinetochore tracking with specific molecular perturbations enables the assignment of distinct DCP functions to kinetochore components. This enables us to build an integrated model of chromosome congression *in vivo*, which acts downstream of the well established microtubule attachment machinery. We also resolve some of the previously reported discrepancies associated with depletion of kinetochore proteins. Finally, this work identifies a previously overlooked step in wild-type congression.

Chapter 1: *Introduction*

1.1 *Overview of mitosis*

The field of cell division began with the 17th century discovery of *cellula* – small chambers that make up cork (Hooke, 1665). After nearly two centuries of research, this idea evolved into 'cell theory', a proposal by German biologists Matthias J. Schleden and Theodor Schwaan, which stated that all living organisms are composed of microscopic units (cells) that are generated by *de novo* synthesis (M.J.Schleden, 1838; Schwaan, 1839). Despite being an accepted model for nearly 50 years, several lines of evidence contradicted this 'free cell formation' proposal. Including earlier findings of cell multiplication by binary fission (Paweletz, 2001; Remak, 1855; von Mohl, 1835), and pioneering work on animal cell division by Walther Flemming (Flemming, 1882; Paweletz, 2001). Building on the first observations of metaphase and anaphase by Anton Schneider (Schneider, 1873), Flemming published an extensive description of mitosis called "Cell substance, nucleus and cell division" in 1882 (Flemming, 1882; Paweletz, 2001) (Fig 1). Here, he described the rearrangement of 'nuclear threads' during 'karyomitosis' (threadlike metamorphosis of the nucleus). This process was subdivided into progressive and regressive phases. The progressive phase began once threads could be observed in the nucleus, and continued until all threads where aligned at the cell equator. As the

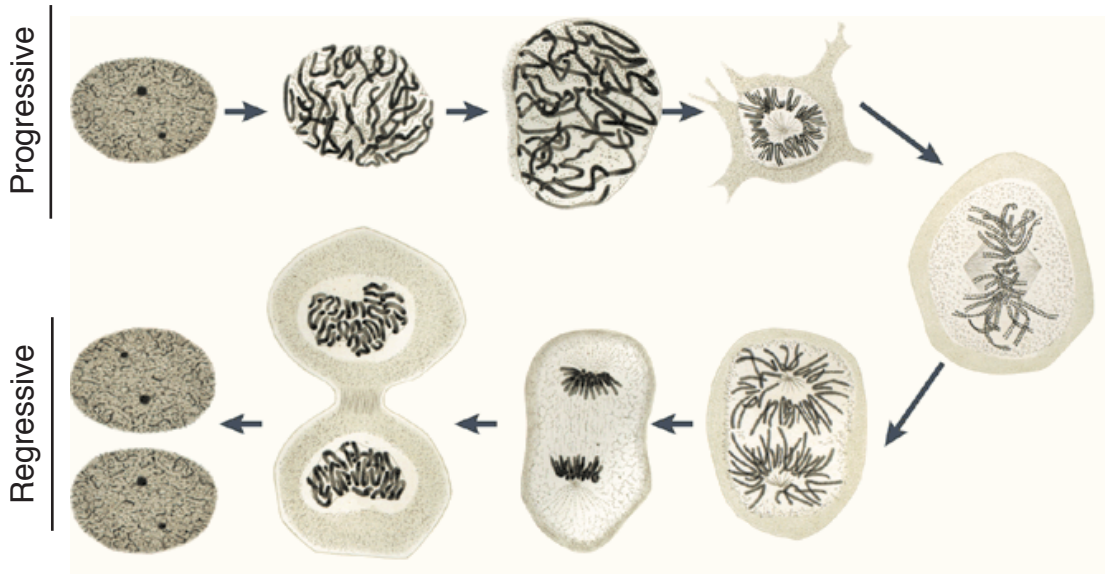

Figure 1: The stages of mitosis by Walther Flemming

Images from Walther Flemming's 1882 description of mitosis. Here, he described the rearrangement of 'nuclear threads' during 'karyomitosis' (threadlike metamorphosis of the nucleus). This process was subdivided into progressive and regressive phases. The progressive phase began once threads could be observed in the nucleus, and continued until all threads where aligned at the cell equator. As the threads began to separate, the cell entered the regressive phase, which encompassed all subsequent mitotic stages until the formation of daughter nuclei. Adapted from Paweletz, 2001.

threads began to separate, the cell entered the regressive phase, which encompassed all subsequent mitotic stages until the formation of daughter nuclei (Flemming, 1882; Paweletz, 2001). In 1888, these threads were renamed ‘Chromosomen’ (stainable bodies) (Waldeyer, 1888).

Now, mitosis is defined as the equal segregation of replicated DNA from a single parent into two daughter cells. Importantly, this division creates two progeny that are genetically identical to one another and the parent cell, which differentiates this process from meiosis and the production of gametes (McIntosh, 2016). Mitotic cell division can be observed in all eukaryotes, and follows a series of highly conserved steps (Fig 2) (McIntosh, 2016). It begins with prophase, where the long thin chromatin strands supercoil into compact chromosomes and the nucleolus disappears. In open mitosis, which is used by somatic cells of higher eukaryotes, the nuclear envelope then breaks down (NEB) scattering the condensed chromosomes throughout the cell. This cell is now said to have entered prometaphase. Simultaneously with NEB, two structures known as centrosomes, which nucleate dynamic tube-like polymers called microtubules, move to opposite ends (poles) of the cell. Microtubules grow from these foci at either pole forming the mitotic spindle, which in turn bind chromosomes via the kinetochore, a large protein machine that assembles on the centromere of each sister chromatid (Fig 2). For a detailed structural description of the kinetochore see appendix 1. The two kinetochores on sister chromatids are in a mirrored orientation, a geometry that favours

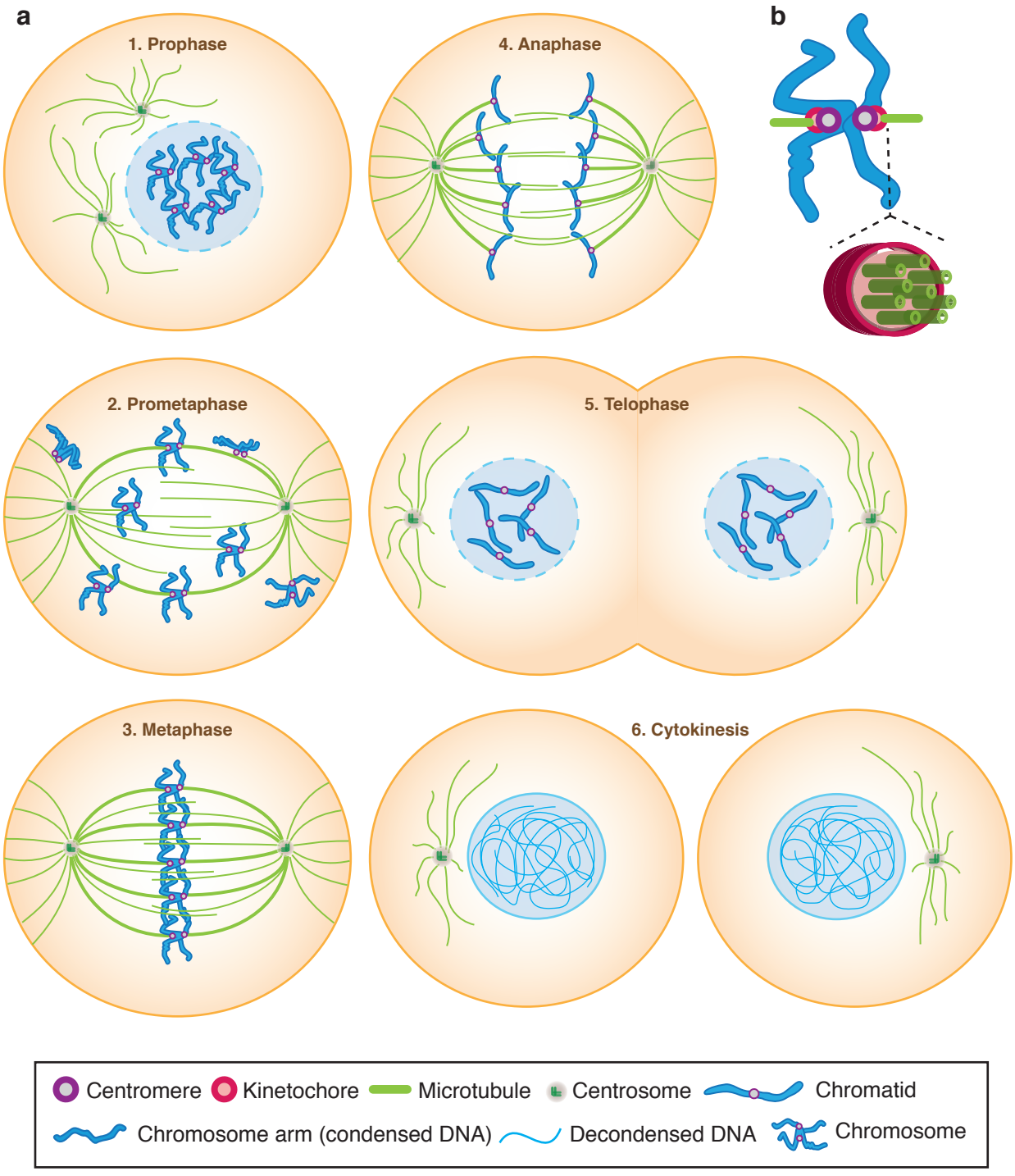

Figure 2: An overview of mitosis

(a) Cartoon representation of mitosis. For detailed description see section 1.1. Briefly, mitosis beings with prophase (1), where the chromosomes condense, nuclear envelope breaks down and centrosomes move to opposite poles of the cell. Once the nuclear envelope is lost and the chromosomes are scattered throughout the cell, it is said to have entered prometaphase (2). Here, dynamic tube-like polymers called microtubules grow from the centrosomes at either pole, and interact with chromosomes via a large centromere associated protein structure called the kinetochore. These kinetochore-microtubule attachments generate a force that aligns chromosomes at the spindle equator, an imaginary plane equidistant from either pole. Once all chromosomes have aligned, the cell is said to have entered metaphase (3). Following a short pause, the cell enters anaphase (4). Here, the cohesion between sister chromatids is broken and their attached microtubules dissemble, pulling them to opposite poles of the cell. Once the two chromatin masses have reached either pole, the cell enters telophase (5), where nuclear envelopes reform and the DNA decondenses. The cell is then physically cleaved in a process called cytokinesis (6). (b) Cartoon representation of the kinetochore-microtubule attachment interface.

each kinetochore making a single attachment to microtubules emanating from the pole it faces. Once bound to microtubules, the leading kinetochore generates a directional force that aligns chromosomes at the spindle equator, an imaginary plane equally distant from either pole. This migratory event is termed congression, and once complete for all chromosomes the cell is said to have entered metaphase. Following a short time lag associated with the silencing of the spindle checkpoint, the cell enters anaphase. Here, the cohesion between sister-chromatids is broken and the K-fiber bound to each kinetochore depolymerises, which results in the segregation of chromatids to opposite poles. Once all chromatids are positioned at either pole the cell enters telophase, where a nuclear envelope reforms around each chromatin mass and the DNA de-condenses. The parental cell is then divided via contraction of a membrane tethered actomyosin ring prior to being physically cleaved into two daughter cells, a process termed cytokinesis.

1.2 *Introduction to chromosome congression*

Congression is the process by which chromosomes are aligned at the spindle equator during mitosis. This event is highly conserved among animal cells and has independently evolved in several lineages (Nicklas and Arana, 1992; Pereira and Maiato, 2012). Suggesting that it is critical for accurate chromosome segregation. The mechanics of congression have

been the focus of considerable research for almost half a century, and this has seen what appears to be a simplistic migratory event grow into a complex multi-modal system of mediators, spatial cues and chromosome states.

The myriad of challenges presented during congression can be highlighted by looking at its end-point, metaphase. Here, all chromosomes are aligned at the spindle equator, an imaginary plane equidistant from either pole, with sister kinetochores in a bi-oriented state (Fig 3). Also known as an amphitelic attachment, bi-orientation describes the formation of single, end-on kinetochore-microtubule attachments to opposite spindle poles (Fig 3). In contrast, early prometaphase cells appear tumultuous, with chromosomes distributed throughout the cytoplasm following NEB (Fig 3). This creates several problems that must be overcome. First, kinetochores must not only bind microtubules, but also bind in a conformation that permits migration through the spindle. As such, erroneous attachments must be destabilised, and the attachment status of all chromosomes must be communicated. Second, peripheral chromosomes require relocating into the spindle, enabling interaction with microtubules emanating from opposite poles. Finally, the kinetochore-microtubule attachment must generate a directional force that moves chromosomes toward the spindle equator. Here, I will introduce both the kinetochore-centric and non-kinetochore

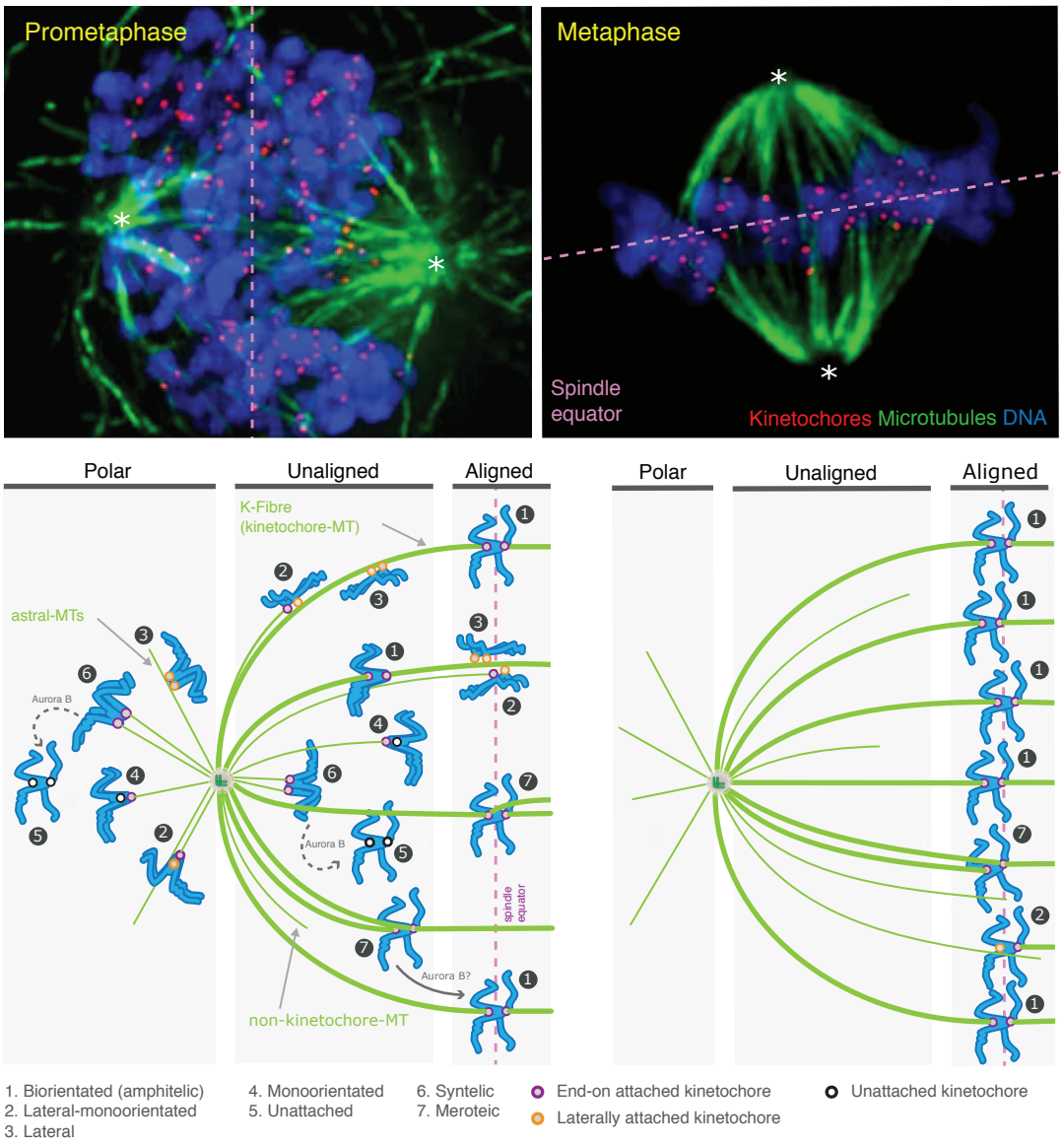

Figure 3: Kinetochore states in prometaphase and metaphase

Top left, immunofluorescence image of a prometaphase HeLa cell stained for kinetochores (CENP-A, red), microtubules (α-tubulin, green) and DNA (DAPI, blue). Chromosomes are distributed throughout the early spindle, and a subpopulation is already positioned at the spindle equator (dotted line), which is located halfway between the two spindle poles (asterisks). Bottom left, cartoon representation of the various spindle positions and attachment states occupied by prometaphase chromosomes. Chromosomes are categorised as polar if they are located behind the pole within the astral region, unaligned if they are located between the pole and equator, and aligned if they are positioned at the equator. Within these regions, kinetochores attach to spindle microtubules in numerous orientations; (1) bi-orientated (amphitelic), where sister kinetochores are bound to opposite spindle poles, (2) lateral-monoorientated, where one kinetochore in the sister pair is attached end-on and the other is bound to the wall of a pre-existing microtubule bundle, (3) lateral, where both sister kinetochores are bound to the wall of a pre-existing microtubule bundle, (4) monoorientated, where one sister kinetochore is attached end-on and the other unattached, (5) unattached, where both sister kinetochores are unbound, (6) syntelic, where both sister kinetochores are attached end-on to a single pole, (7) merotelic, where one sister in a bi-orientated pair forms a second attachment to its distal pole. These erroneous attachments (6 and 7) are actively destabilised by Aurora B, enabling reattachment in a conformation that permits congression. Top right, immunofluorescence image of a metaphase HeLa cell. Bottom right, cartoon representation of the position and attachment states of metaphase chromosomes. Kinetochore pairs are located at the spindle equator and are predominantly bi-orientated (1); however, merotelic (7) and lateral-monoorientated (2) attachments can persist within this region at a low frequency (Cimini et al., 2003; Magidson et al., 2011). Asterisks in the images denote the position of the spindle poles.

mechanisms that generate force, sense position and regulate attachment to permit the timely and accurate congression of all chromosomes.

1.3 *Kinetochores as the force generator*

In principal, two mitotic structures could generate the force that aligns chromosomes at the spindle equator: (1) kinetochores and (2) microtubules. Prior to electron microscopy (EM) studies formally identifying kinetochores as a distinct structure assembled on the centromere (Brinkley and Stubblefield, 1966), models of congression proposed that microtubule bundles (termed spindle fibres, now known as K-fibres) mediated force-generation. The first manifestation of this idea was the 'polar repulsion' model published by Darlington in 1937 (Darlington, 1937). Here, it was proposed that the arrangement of chromosomes at the spindle equator was "due to repulsion from the poles acting on the centromeres", and that the strength of this repulsion was inversely proportional to distance from the pole. As the repulsive force from either pole would be approximately equal at the spindle equator, chromosomes would migrate to, and remain in, this region (Darlington, 1937). This force is now known as polar ejection force (PEF), which is generated by the walking of chromatin-associated kinesin along non-kinetochore microtubules (see section 1.6.2) (Ault et al., 1991). However, while having a role in chromosome position sensing, the principal PEF generator Kid (Kif22) is dispensable for congression (Levesque and

Compton, 2001). An alternative idea is that K-fibres pull chromosomes. This concept formed the basis of the 'traction fibre' model suggested by Östergren in 1951. Here, Östergren proposed that centromeres are pulled towards their attached pole with a force proportional to K-fibre length (Östergren, 1951). Congression to the equator would then occur autonomously as this is where the antagonistic forces are balanced. Despite gaining some experimental evidence (Hays and Salmon, 1990; Hays et al., 1982; Östergren, 1945), several key observations discounted this model. If chromosome position at the spindle equator was maintained by the balancing of antagonistic forces, the severing of a metaphase K-fibre should move the sister-pair towards to pole attached to the undamaged K-fibre. However, UV microbeam studies in Blood Lilly, Newt and Kangaroo cells demonstrated that the sister-pair only moved a short distance off the equator in certain cases (Czaban et al., 1993; Spurck et al., 1990). Thus, the maintenance of chromosomes at the metaphase plate cannot be due to the balancing of K-fiber pulling forces (Czaban et al., 1993; Spurck et al., 1990). Moreover, early microtubule labelling studies demonstrated that K-fibers were relatively stable with the exception of one highly dynamic focus, which was located proximal to the kinetochore at the microtubule plus-ends. Within this region, changes in microtubule polymerisation were coupled to kinetochore movement, with K-fiber depolymerisation associated with poleward (P, towards the attached pole) motion, and K-fiber polymerisation associated with away-from-the-pole (AP, away from the attached pole)

motion (Cassimeris and Salmon, 1991; Centonze and Borisy, 1991; Mitchison et al., 1986; Mitchison and Salmon, 1992; Shelden and Wadsworth, 1992; Wise et al., 1991). Thus, models of K-fibre force generation could not account for several experimental observations, and the kinetochore became the primary force-generating candidate.

A key question remained unanswered; are chromosomes pulled and/or pushed to the equator? Insight into this problem came from early computational tracking of kinetochores, which discovered a behaviour termed 'directional instability'. Here, both mono-oriented and bi-oriented sister-pairs would oscillate relative to their associated pole(s), suggesting that kinetochores existed in different force-generating states (Cassimeris et al., 1994; Skibbens et al., 1993). To investigate how kinetochore state was correlated with movement, Skibbens and colleagues used centromere deformation to infer whether a kinetochore was subject to a pull or push. They found that during P movement the centromere was frequently stretched poleward, while during AP movement it was flattened or indented. This suggested that P motion corresponded to a pull, and AP to a push or neutral state (Skibbens et al., 1993). In contrast, later studies showed that both kinetochores were on average equally stretched (Waters et al., 1996). Direct evidence that a pulling force mediated chromosome congression came from laser ablation studies. When a congressing bi-oriented kinetochore-pair was severed between the sisters, the P kinetochore continued migration toward the equator, whereas the AP kinetochore

stopped and switched to P motion (Khodjakov and Rieder, 1996). Moreover, when the P kinetochore was destroyed on a congressing bi-oriented sister-pair, the chromosome stopped, paused, and the AP sister switched to P motion (Khodjakov and Rieder, 1996). Based on these observations, a model of congression arose where a P-kinetochore generated pulling force aligned chromosomes at the spindle equator (Khodjakov and Rieder, 1996 ; Skibbens et al., 1993; Waters et al., 1996). Two mechanisms were proposed for how the P-kinetochore produced a pulling force. The first, termed the 'pac-man' model, suggested that kinetochores catalyse the depolymerisation of K-fiber microtubules, which allows the pulling of chromosomes through the maintenance of attachment to the shortening fibre (Gorbsky et al., 1987; Mitchison et al., 1986). The second, termed the 'pole-ward flux' model, suggested that a combination of microtubule minus-end depolymerisation at the pole and motor driven microtubule sliding generated a pulling force (Mitchison, 1989). Importantly, an 80% reduction in flux had no effect on congression in human cells (Ganem et al., 2005), and chromosome velocity during alignment is faster than flux in several model organisms (Pereira and Maiato, 2012; Skibbens et al., 1993). Together, these data suggest that flux does not significantly contribute to congression. Moreover, work in flies showed that the 'pac-man' mechanism was responsible for the poleward movement of chromosomes in anaphase (Brust-Mascher and Scholey, 2002; Rogers et al., 2004). As such, the coupling of the P-kinetochore to depolymerising

microtubules is thought to be the dominant force generating mechanism that aligns bi-oriented sister-pairs. From here, I use the term depolymerisation-coupled pulling (DCP) to describe this process.

1.4 *Molecular mechanisms of depolymerisation-coupled pulling*

Kinetochore movement via DCP can be thought of as a series of sequential events that are all essential for congression to the spindle equator. First, the kinetochore needs to form an end-on attachment to the plus-ends of spindle microtubules, and then remain stably attached as they depolymerise to generate force. Once migration has initiated, the kinetochore-pair must ensure that a polymerisation bias is sustained between sisters, as the K-fibers attached to the P and AP kinetochores must shorten and grow, respectively (Fig. 4a-c).

1.4.1 *Physically coupling to depolymerising microtubules*

A microtubule can be thought of as a store of torsional and chemical energy that can be harnessed to do mechanical work. Microtubule depolymerisation generates both structural and energetic changes at the plus-end that are harnessed by kinetochore components to generate force. In terms of structure, when the stabilising GTP cap of a growing microtubule is lost and the filament disassembles, individual protofilaments

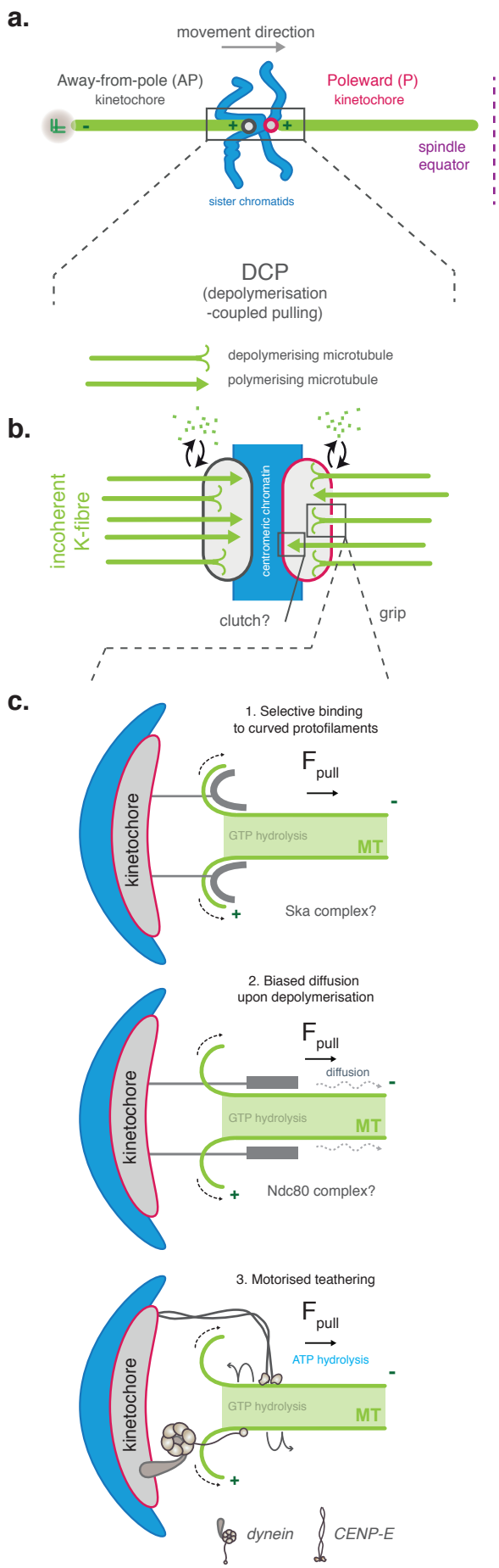

Figure 4: Mechanics of depolymerisation-coupled pulling

(A) Chromosomes that form amphitelic attachments away from the spindle equator utilisedepolymerisation-coupled pulling (DCP) to congress. During this movement, kinetochores are described as moving poleward (P) if they move towards their attached pole (shown in red), and away-from -the-pole (AP) if moving away from their attached pole (shown in dark grey). (B) The force required for DCP is generated by microtubule depolymerisation at the P kinetochore, which pulls the chromosome towards the equator. This implies that there is a polymerisation or depolymerisation bias between K-fibres that are attached to the P and AP kinetochores, with P K-fibres in a net depolymerising state and AP K-fibres in a net polymerising state. Owing to the incoherent nature of the K-fibre, the P kinetochore might selectively disengage from polymerising microtubules using a clutch-like mechanism. (C) Three potential mechanisms have been proposed for how kinetochores grip depolymerising microtubules (see main text for details): (i) selective binding to curved protofilaments, a unique structural feature of depolymerising microtubules; (ii) biased diffusion along the microtubule lattice upon depolymerisation; and (iii) motorised tethering in which kinetochore-tethered kinesin (top) and/or dynein (bottom) step along the microtubule. MT, microtubule.

are thought to peel away from the lattice in a ‘rams-horn’ like conformation (Simon and Salmon, 1990). Early observations from grasshopper spermatocytes suggested this bending could generate up to 7pN per kinetochore-bound microtubule, with similar values later being calculated from centromere stretching in yeast (Nicklas, 1988; Powers et al., 2009). In contrast, experimentally conjugating glass beads to tubulin polymers *in vitro* suggested this force might be significantly higher (65pN) (Grishchuk et al., 2005). Regardless of its magnitude, this force acts in the P direction, and could therefore be used to pull chromosomes (Fig 4a-c). Importantly, EM studies in cells have subsequently identified ‘fibrils’ connecting the centromere to curving protofilaments, providing the first evidence that protofilament bending may indeed be linked to poleward kinetochore movement in mammalian systems (McIntosh et al., 2008). However, the molecular mediator(s) remains obscure. In contrast, work in yeast has identified the oligomeric Dam1 complex, which forms a force-coupling ring around microtubules *in vitro* (Grishchuk et al., 2008; Miranda et al., 2005; Umbreit et al., 2014; Westermann et al., 2005), and is required for microtubule attachment *in vivo* (Cheeseman et al., 2001; Umbreit et al., 2014). Despite lacking any true vertebrate homologue, the spindle and kinetochore associated (Ska) complex is suggested to be functionally analogous to Dam1, and therefore represents the best protofilament-coupling candidate in these organisms. This idea has emerged because the Ska complex can track with depolymerising microtubule plus-ends *in vitro*,

and transduce this force to beads coated in the complex (Fig. 4c) (Schmidt et al., 2012; Welburn et al., 2009). Moreover, the Ska complex binds microtubules via the electrostatic interaction of several basic patches in Ska1 and Ska3 with regions of tubulin that are accessible in straight and curved lattice configurations (Abad et al., 2014; Abad et al., 2016). This suggests that the complex can bind both structural states, unlike the end-on attachment factor Ndc80, whose binding cleft is obscured by filament curvature (Alushin et al., 2012). In agreement, biochemical analysis showed that the Ska complex has an equal affinity for curved and straight microtubules, whereas a truncated monomeric Ndc80 specifically binds the latter (Schmidt et al., 2012). Nevertheless, the function of the Ska complex in cells is poorly defined. While some report that small interfering (si) RNA depletion of any Ska subunit causes a severe congression defect, which was associated with reduced K-fiber stability (Chan et al., 2012; Gaitanos et al., 2009; Schmidt et al., 2012; Welburn et al., 2009), others reported a robust metaphase arrest with few misaligned kinetochore-pairs (Abad et al., 2014; Hanisch et al., 2006; Jeyaprakash et al., 2012; Theis et al., 2009), which lead to the downstream failure of sister cohesion and the asynchronous separation of chromatids (known as cohesion fatigue) (Sivakumar et al., 2014; Sivakumar et al., 2016). This phenotype was probably misinterpreted in fixed images as the failure of congression (Schmidt et al., 2012; Welburn et al., 2009), and may be associated with the proposed role of Ska1 in PP1 recruitment to the kinetochore and

anaphase onset (Sivakumar et al., 2014; Sivakumar et al., 2016). It must be noted however, that more recent studies are far less deterministic in the reporting of Ska depletion phenotypes (Abad et al., 2016; Redli et al., 2016), with pleotropic observations being attributed to inter-experimental variation in siRNA efficiency. Thus, a detailed analysis of kinetochore fates in cells depleted of Ska via multiple techniques is required to shed more light on the function of this complex.

In addition to Ska, CENP-F has been proposed to function as another link between curved protofilaments and the centromere (Volkov et al., 2015). CENP-F relocates from the nuclear envelope to the kinetochore during mitosis (Liao H. et al., 1995), where it binds microtubules via two domains located at opposite ends of the protein (Volkov et al., 2015). Biochemical analysis suggested that these MTBDs couple the kinetochore to specific microtubule structures. In this regard, the N-terminal MTBD displays a preference for curved filaments over straight microtubules, while the C-terminal MTBD does the opposite (Volkov et al., 2015). Nevertheless, both regions track depolymerising microtubule plus-ends *in vitro* and can transduce this force to beads, suggesting they may both contribute to force-generation at end-on attached kinetochores (Volkov et al., 2015). In terms of mechanics, the N-terminal MTBD is likely analogous to Ska, whereas the C-terminal MTBD may utilize biased diffusion, as described for Ndc80 (see below). The function of CENP-F at end-on attached kinetochores in cells is, however, unclear. This is primarily due to its proposed structural roles in the

kinetochore, where it is implicated in the recruitment of dynein and CENP-E (Bomont et al., 2005; Vergnolle and Taylor, 2007; Yang et al., 2005). These loading dependencies may entirely account for the observed congression defect in CENP-F depleted cells. However, by tracking the fate of unaligned bi-oriented kinetochore-pairs located between the pole and metaphase plate, another CENP-E loading protein, CENP-Q, was shown to have an independent role in DCP (Bancroft et al., 2015). As such, the possibility exists that CENP-F directly contributes to DCP, a hypothesis that can be tested by following the fates of a specific kinetochore subgroup when depleted of the protein.

In addition to structural modification, microtubule depolymerisation also creates an energy gradient away from the plus-end. Proteins that diffuse along microtubules can utilize this gradient to bias their diffusion along the lattice during filament disassembly, and therefore generate a P force. This is because it is more energetically favorable for these molecules to move to adjacent tubulin dimers, away from the dissembling plus-end, as opposed to detaching (Hill, 1985; Vladimirou et al., 2011) (Fig. 4c). This idea underpinned the ‘Hill’s sleeve’ model, a theoretical proposal of how kinetochores could track with dynamic microtubules (Hill, 1985). One molecule that may function in a manner reminiscent of a ‘Hill’s sleeve’ is the KMN component Ndc80/Hec1. Ndc80 binds microtubules via multiple positively charged regions in both its unstructured N-terminal tail and calponin homology (CH) domains (Alushin et al., 2012; Alushin et al., 2010;

Miller et al., 2008; Tooley et al., 2011). Ndc80 forms a cooperative complex with Nuf2, Spc24 and Spc25 at the kinetochore (the Ndc80 complex), and loss of this complex in all tested systems leads to the abrogation of end-on kinetochore-microtubule attachment (Cheeseman and Desai, 2008). This does not implicate Ndc80 in force generation *per se*, as it may act solely as an attachment factor. However, *in vitro* reconstitution of the entire complex on dynamic microtubules demonstrated that diffusing ensembles could track with depolymerising plus-ends, and that single complexes could 'bounce' off the tip back to the lattice without dissociating (Powers et al., 2009). Moreover, beads coated with physiological levels of the complex could persistently attach to depolymerising plus-ends and transduce force (Powers et al., 2009). This suggested that the Ndc80 complex has attachment independent functions, at least *in vitro*. It must be noted, however, that a truncated monomeric Ndc80 complex (consisting of Ndc80 and Nuf2 microtubule binding and adjacent regions) does not display similar behavior (Schmidt et al., 2012). Nevertheless, vertebrate kinetochores contain at least nine Ndc80 complexes per kinetochore-microtubule (Johnston et al., 2010), which can self-oligomerize into arrays (Alushin et al., 2010). Therefore, the possibility exists that the complex forms a higher order force-coupling structure that operates via biased diffusion at end-on attached kinetochores

Interestingly, the protofilament binding and biased diffusion pathways are partially interconnected, as the Ndc80 loop region facilitates the loading of

the Ska complex to kinetochores (Zhang et al., 2012), and the Ska complex can couple monomeric Ndc80 to depolymerising plus-ends *in vitro* (Schmidt et al., 2012). Similarly, Dam1, the proposed Ska functional homologue in yeast, also acts as a processivity factor for Ndc80 *in vitro* (Lampert et al., 2010; Tien et al., 2010). Moreover, EM analysis of purified kinetochores showed that Dam1 and Ndc80 physically interact, however, this appears to be mediated by calponin homology (CH) domains and not the loop, as suggested for the Ska-Ndc80 interaction (Gonen et al., 2012; Zhang et al., 2012). Therefore, in both vertebrates and yeast, the Ndc80 complex appears to be upstream in this pathway, and likely forms an initial end-on attachment to microtubules while recruiting the Ska/Dam1 complex. Together, these factors then link microtubule depolymerisation to chromosome migration via protofilament binding and biased diffusion pathways, respectively. CENP-F potentially contributes to both pathways via the interaction of distinct MTBDs with specific regions on the tubulin heterodimer. Nevertheless, analysis of mutants deficient in specific functions will be required to truly determine if Ndc80 has an attachment independent role in congression.

1.4.2 *Coordinating microtubule dynamics*

The persistent migration of a bi-oriented kinetochore-pair towards the spindle equator suggests that a polymerisation differential exists between

the P and AP K-fibres (Fig 4a,b), as one microtubule bundle must shorten while the other elongates. Consistent with this notion, work in *Xenopus* extracts using end-binding (EB) protein 1 as a marker of microtubule polymerisation showed high levels of polymerisation at the AP K-fibre relative to the P K-fibre (Tirnauer et al., 2002). In contrast, EM analysis of K-fibres in Ptk1 and S2 cells demonstrated that the bundles are incoherent, containing microtubules in both polymerising and depolymerising states (VandenBeldt et al., 2006). A finding that was confirmed in recent work that combined kinetochore tracking with EB3 labelling in HeLa cells (Armond et al., 2015). As such, the P-kinetochore must prevent polymerising microtubules from generating an antagonistic force that could impede chromosome movement. Interestingly, it has been proposed that kinetochores exert a pushing force during bipolar spindle assembly via the prometaphase pathway in HeLa cells (Toso et al., 2009).

In this model, the authors suggest that kinetochores push against the centrosomes via the incorporation of tubulin at K-fiber plus-ends during microtubule flux (Toso et al., 2009). Therefore, end-on attached kinetochores may indeed have force-generating states, as suggested by early tracking experiments (Skibbens et al., 1993). However, both kinetochore pushing and flux have largely been eliminated as contributors to the congression of bi-oriented sister-pairs (Ganem et al., 2005; Khodjakov and Rieder, 1996 ; Levesque and Compton, 2001), which raises the possibility that kinetochores may temporally switch from pushing to

pulling states. Such a state switch could be facilitated by two changes; (1) the alteration of kinetochore microtubule binding properties such that depolymerising filaments are specifically engaged with (Fig 4b), and (2) limiting microtubule polymerisation such that any pushing interactions are avoided. As the latter mechanism could switch the entire K-fiber into a depolymerising state, it would require the tight regulation of microtubule dynamics to account for the observed incoherent nature. In this regard, several plus-end tracking proteins and molecular motors are known to be regulators of microtubule dynamics (Cross and McAinsh, 2014; Ferreira et al., 2014), However, only the kinesin-8 Kif18A and kinesin-13 mitotic centromere-associated kinesin (MCAK) have been shown to directly affect the balance of microtubule dynamics within the K-fiber (Armond et al., 2015).

Kif18A is a highly processive plus-end directed motor that accumulates at the K-fibre plus-end, forming a comet-like gradient from this focus in a manner dependent on K-fibre length (Stumpff et al., 2008; Stumpff et al., 2012). Early studies suggested that Kif18A depletion lead to a severe congression defect (Mayr et al., 2007). However, subsequent work that employed high-resolution kinetochore tracking revealed that these misaligned chromosomes are end-on attached, under tension and oscillating (Stumpff et al., 2008; Stumpff et al., 2012). Thus, Kif18A depleted kinetochores are qualitatively indistinguishable from metaphase kinetochores, with the exception of a broad distribution about the spindle

equator. This suggests that congression has been successful, and that these kinetochores instead have a position sensing defect (see section 1.7). Nevertheless, it must be noted that these pseudo-metaphase kinetochores in Kif18A depleted cells display numerous oscillation abnormalities. Including an increase in velocity, (Jaqaman et al., 2010; Stumpff et al., 2011; Stumpff et al., 2008; Stumpff et al., 2012), a decrease in switching frequency, which, however, is disputed (Jaqaman et al., 2010; Stumpff et al., 2008), and loss of spatially controlled directional switching (Stumpff et al., 2012). These defects may explain the reported increase in polymerisation bias between AP and P kinetochores, which is proposed to dampen the AP resistive force that would otherwise slow the sister-pair (Armond et al., 2015). In agreement, Kif18A is suggested to suppress microtubule dynamics at the AP kinetochore and stimulate direction switching with *in vivo* (Du et al., 2010; Stumpff et al., 2008; Stumpff et al., 2012).

MCAK is a non-motile kinesin that functions as a microtubule depolymerase (Hunter et al., 2003). *In vitro*, MCAK can couple to, and generate tension at, both microtubule ends (Oguchi et al., 2011). However, no such behavior has been described *in vivo*. MCAK has been shown to localise to both the centromere and microtubule plus-ends, and demonstrates a bias to the P-kinetochore during congression (Honnappa et al., 2009; Kline-Smith et al., 2004). Abrogation of MCAK has been proposed to cause congression defects (Kline-Smith et al., 2004; Shrestha and Draviam, 2013). However,

this effect is inconsistently reported in the literature, particularly in studies investigating the role of MCAK in metaphase kinetochore dynamics, where congression appears to have completed (Armond et al., 2015; Jaqaman et al., 2010). At metaphase, MCAK has been shown to regulate kinetochore oscillation dynamics, with depleted sister-pairs displaying a decrease in directional coordination and a reduction in velocity (Jaqaman et al., 2010; Wordeman et al., 2007). This is consistent with the reported loss of polymerisation bias between AP and P-sisters in MCAK depleted cells, which implies that the K-fiber that is bound to the P kinetochore (which is mediating DCP) has fewer depolymerising microtubules (Armond et al., 2015). Thus, while MCAK is required for the regulation of kinetochore movement during metaphase, its role in congression is currently unclear. Some caution is necessary here as current models of kinetochore dynamics are derived from the analysis of metaphase chromosomes. While many concepts are likely conserved, these models may not be immediately transferrable to congressing kinetochores. Indeed, prometaphase K-fibers are less stable that those in metaphase cells (Kabeche and Compton, 2013), and the composition of unaligned and aligned kinetochores is known to differ (Gudimchuk et al., 2013; Kline-Smith et al., 2004; Schmidt et al., 2010). Moreover, periods of persistent movement are considerably longer during congression (~2min compared to 10-60 secs in metaphase (Jaqaman et al., 2010; Khodjakov et al., 1999)). Therefore, a detailed analysis of microtubule dynamics and subunit composition at single

congressing kinetochores, with emphasis on differentiating AP and P states, is required to fully decipher the mechanics that underpin DCP.

1.5 *Congression in the absence of end-on pulling*

1.5.1 *Lateral sliding*

The formation a bi-oriented attachment was originally thought to be an essential prerequisite for congression. On the contrary, congression can also occur before bi-orientation, via the motor dependent sliding of kinetochores along the microtubule sidewall (Fig 5). Chromosomes that are located in the spindle periphery following NEB initially migrate to their proximal pole prior to ejection towards the spindle equator. This movement is driven by the kinetochore-bound dynein, a minus-end directed motor that steps towards the pole (Barisic et al., 2014; Li et al., 2007; Savoian et al., 2000; Yang et al., 2007) (Fig. 5, Step 1). Subsequent equatorially directed motion is driven CENP-E, a high processive plus-end directed motor that is enriched at polar chromosomes (Gudimchuk et al., 2013; Kapoor et al., 2006; Kim et al., 2008; Wood et al., 1997) (Fig. 5, Steps 2 and 3). The lateral sliding of chromosomes was first demonstrated in a study that used single kinetochore tracking and correlative EM to analyse the behaviour and attachment state of congressing sister-pairs in PtK1 cells. Here, kinetochore-pairs were observed to glide toward the spindle equator

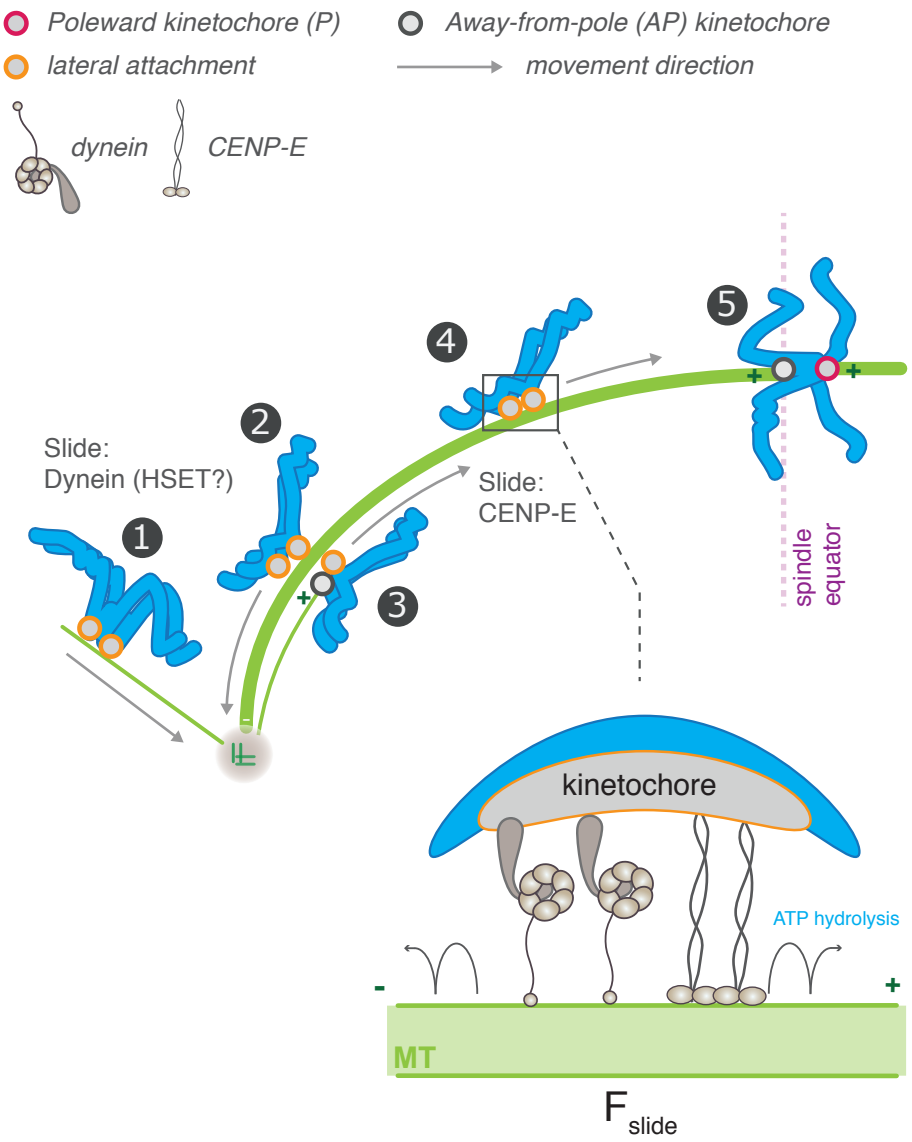

Figure 5: Congression of laterall attached kinetochores

Congression can take place prior to bi-orientation, mediated by the motor proteins dynein and CENP-E. These motors form lateral attachments with the microtubule lattice, and walk along the microtubule toward the minus-end (dynein, steps 1 and 2) or plus-end (CENP-E, steps 3 and 4). HSET has also been implicated in minusend-directed polewards movement, however the mechanism remains unknown. These migratory events contribute to distinct steps of congression, with chromosomes first being moved polewards by dynein (steps 1 and 2), before being ejected towards the equator by CENP-E (steps 3 and 4). Motor driven congression often fails to maintain chromosomes at the spindle equator, and as such, these lateral attachments are converted into the default end-on attachment state during the formation of the metaphase plate (step 5). MT, microtubule.

alongside the mature K-fibre of an aligned bi-oriented chromosome, a movement that was facilitated by a force-generating lateral interaction between the P-kinetochore and K-fibre (Kapoor et al., 2006) (Fig. 5, Chr 2). This behaviour was abolished by CENP-E depletion, establishing that CENP-E drives a bi-orientation independent congression mechanism (Kapoor et al., 2006). Further validation of this model came from studies that specifically enriched for the lateral sliding pathway. Here, DCP was prevented by abrogating end-on attachment with depletion of the Ndc80 complex component Nuf2 (Cai et al., 2009). Remarkably, CENP-E mediated lateral sliding could align all chromosomes in 50% of cells when the minus-end directed motor HSET was also depleted (Cai et al., 2009). Similar observations were made when the major end-on attachment factor Ndc80 was codepleted with MCAK (Iemura and Tanaka, 2015). Interestingly, these studies highlighted that MCAK and HSET depletion could suppress an unknown P force, and allow for CENP-E mediated congression in the absence of end-on attachment, but how? The current idea is that this effect is indirect, as HSET and MCAK both negatively regulate the stability of microtubules required for CENP-E sliding toward the equator (Iemura and Tanaka, 2015).

Somewhat unexpectedly, CENP-E has been implicated in the DCP mechanism *in vivo*. In an experiment designed to simulate DCP, where end-on attached sisters are transported by depolymerising astral microtubules (in response to nocodazole) towards a monopole, CENP-E

inhibition was found to perturb microtubule tracking (Gudimchuk et al., 2013). Moreover, CENP-E was shown to track with polymerising and depolymerising microtubules *in vitro*, and can transduce the force from filament disassembly to beads (Gudimchuk et al., 2013). Together, these data provided compelling evidence that the motor contributes to DCP (Fig 3c). However, 80% of bi-oriented kinetochore pairs in a bipolar spindle successfully congressed when depleted of CENP-E (Bancroft et al., 2015), and CENP-E is not required for the oscillation of aligned sister-pairs (Jaqaman et al., 2010). Nevertheless, microtubule dynamics at aligned kinetochore-pairs are perturbed when CENP-E is inhibited or depleted (Maffini et al., 2009). It must be noted that CENP-E is significantly reduced at aligned sisters when compared to polar kinetochores. As such, the primary function of CENP-E appears to be as a lateral sliding mediator that congresses peripheral chromosomes (Barisic et al., 2014).

1.5.2 *The polar ejection force*

The existence of a polar ejection force (PEF) was proposed by Darlington in 1937. This idea formed the basis of his ‘polar repulsion’ model of congression (Darlington, 1937), which stated that centromeres are repelled from the poles with a force inversely proportional to their proximity (Darlington, 1937). While failing to account for congression (Levesque and Compton, 2001), the existence of the PEF was later demonstrated by laser

cutting experiments (Rieder et al., 1986). Here, an acentric chromosome fragment was shown to be actively transported away from its proximal pole (Rieder et al., 1986). This behaviour was abolished by the addition of nocodazole, suggesting that microtubules were critical for PEF generation (Ault et al., 1991). Importantly, these studies also showed that the PEF was exerted along chromosomes arms, as oppose to the centromere as originally predicted (Darlington, 1937). Consistent with this, both *in vivo* and *in vitro* suites later showed that plus-end directed chromosome arm associated kinesins (chromokinesins) Kif4a and Kid create the PEF (Antonio et al., 2000; Bieling et al., 2010; Brouhard and Hunt, 2005; Funabiki and Murray, 2000; Levesque and Compton, 2001; Yajima et al., 2003). Thus, the PEF is an AP force generated by the plus-end directed walking of chromatin-tethered kinesin along microtubules. As microtubule concentration is proportional to proximity to the pole, the strength of the PEF is inversely proportional to distance from the pole (Cane et al., 2013). In terms of congression, the individual depletion of Kif4a or Kid has little effect. In contrast, their co-depletion results in significant alignment defects, suggesting these motors may have independent and/or coordinated functions (Wandke et al., 2012). In this regard, Kid, the principal PEF generator, is dispensable for chromosome alignment, but has a role in the control of aligned kinetochore dynamics and kinetochore position sensing (Levesque and Compton, 2001; Stumpff et al., 2012; Wandke et al., 2012). With respect to the former, Kid depletion decreases the velocity of, and

increases the rate of directional switching at, aligned kinetochore-pairs. In contrast, the function of Kif4a is less well characterised. It has been suggested to antagonise Kid by reducing microtubule dynamicity in early mitosis via the suppression of polymerisation, a finding that suggests it may have a PEF independent function (Wandke et al., 2012). Indeed, this may involve the regulation of antiparallel microtubule overlaps, a well documented function of Kif4a in cytokinesis (Nunes Bastos et al., 2013). Nevertheless, several studies have implicated Kif4a and kinesin-4 motors in PEF generation, although more work is necessary to tease out the specific contribution (Antonio et al., 2000; Bieling et al., 2010; Brouhard and Hunt, 2005; Funabiki and Murray, 2000; Levesque and Compton, 2001; Yajima et al., 2003).

1.6 *Coupling congression with position sensing in the spindle*

How do kinetochores sense their position in the spindle and feedback this information to regulate force-generating mechanisms? Early ideas focused on coordinated kinetochore states in response to tension; however, such a model failed to consider any integration of spatial information and kinetochore behaviour during congression could be recapitulated with no external modulation of behaviour (Khodjakov et al., 1999), i.e. congression could be achieved with no kinetochore mediated position-sensing. Nevertheless, several other asymmetric cues exist that could bias both

DCP and lateral sliding mechanisms toward the equator (Fig 6). One such mechanism is the opposing regulation of microtubule dynamics at bi-oriented kinetochore pairs by the motor proteins MCAK and Kif18A (see section 1.5.2). Here, MCAK accumulates at the P-kinetochore (Kline-Smith et al., 2004), enhancing microtubule depolymerisation at this force generating interface, which causes chromosomes to move at an increased velocity toward the equator (Jaqaman et al., 2010) (Fig 6a). Once at the metaphase plate, MCAK in unloaded from this region and accumulates in the inner-centromere (Kline-Smith et al., 2004), where it generates a symmetrical P-force that favours positional equilibrium. Simultaneously, the length dependent accumulation of Kif18A at the AP attached K-fibre promotes an AP-to-P state switch at chromosomes moving away from the equator (Fig 6b) (Stumpff et al., 2012). Mechanistically, the high Kif18A concentration at the AP K-fibre acts to suppress microtubule dynamics until the GTP cap is eventually compromised, which leads to microtubule depolymerisation and directional switching. Once aligned at the equator, the Kif18A concentration gradient at each sister is roughly identical, favouring the maintenance of position via quasi-periodic oscillation. Thus, Kif18A senses K-fiber length whilst MCAK senses kinetochore position. Recently, the importance of this Kif18A positioning mechanism and the requirement for chromosome congression have been questioned (Czechanski et al., 2015). Here, mouse embryonic fibroblasts (MEF) derived from animals homozygous for a Kif18A motor domain mutation

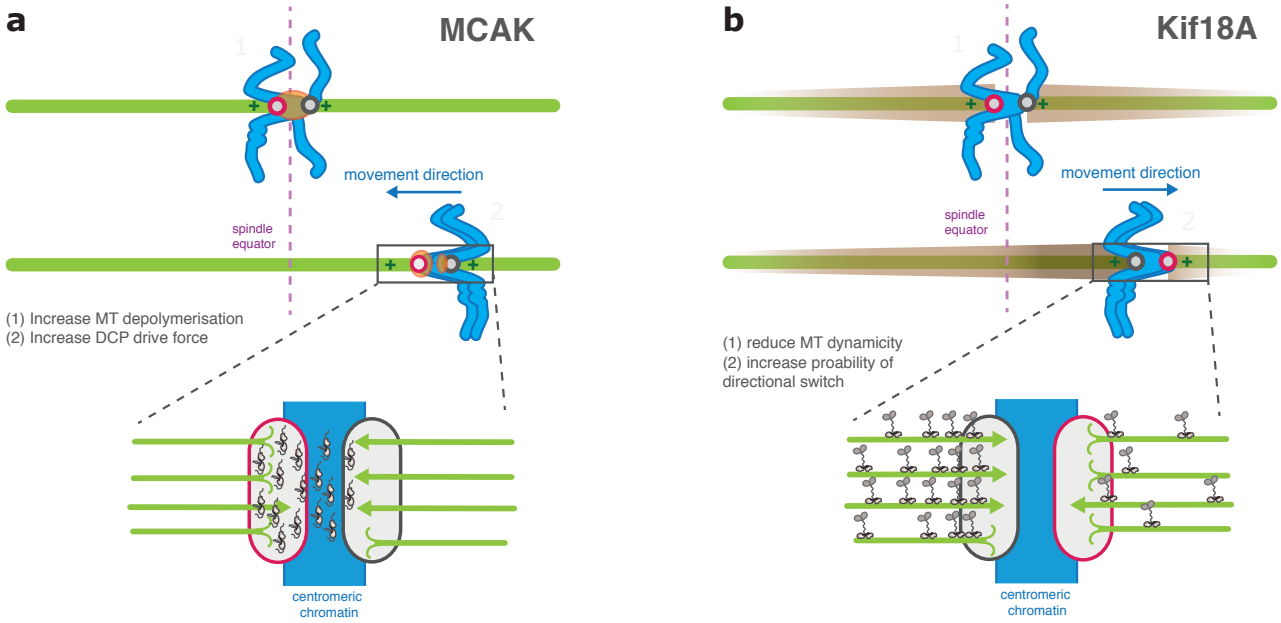

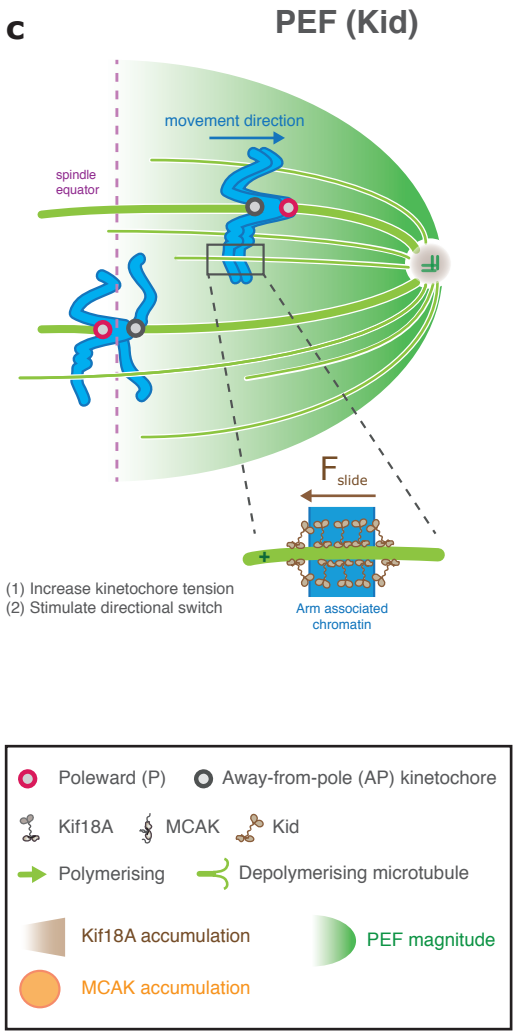

Figure 6: Biased congression towrds the spindle equator

(A) Role of MACK in biased congression. At aligned kinetochore pairs (1), the microtubule depolymerase MCAK localises to the inner-centromere. In contrast, at unaligned kinetochore pairs undergoing congression (2) MCAK displays a bias to the P kinetochore, suggesting that it might augment the DCP-mediated drive force and enhance migration towards the spindle equator. (B) Kif18A forms a concentration gradient along the K-fibre (illustrated by the brown 'cloud') and accumulates at the outer-kinetochore. Here, it acts to suppress microtubule dynamics and promote directional switching. At aligned kinetochore pairs, its concentration is comparable between sisters and so it promotes maintenance of this position (1); however, at unaligned kinetochore pairs, Kif18A promotes switching of the AP kinetochore into a P state, resulting in its migration towards the spindle equator (2). (C) The PEF is generated by plus-end-directed kinesins that are associated with chromosome arms (for instance Kid), which interact with spindle microtubules and walk towards the spindle equator (directionality indicated by Fslide). This force therefore decays with increasing distance from the pole and reducing microtubule density. Aligned kinetochore pairs are positioned equidistantly from either pole and therefore experience a more symmetrical PEF (1). Unaligned kinetochore pairs, however, experience an increase in PEF as they move towards a pole, which increases kinetochore tension and promotes their directional switching towards the equator (2).
MT, microtubule.

(Kif18A^{gcd2}) successfully progressed through mitosis, entering anaphase with seemingly unaligned chromosomes (Czechanski et al., 2015). However, as previously mentioned, kinetochore tracking experiments have revealed that sister-pairs form bioriented attachments and oscillate with perturbed dynamics about the spindle equator in Kif18A depleted cells (Stumpff et al., 2008). This leads to the formation of a broad 'pseudo-metaphase plate', and suggests that congression has completed. Further work is needed to determine the impact of this pseudo-plate affects the fidelity of mitosis in this cell type, as it is known to be highly detrimental in HeLa cells (Czechanski et al., 2015).

An alternative idea is that chemical gradients throughout the spindle guide chromosome movement. In this regard, Plk1 and RanGTP concentration gradients have been shown to control spindle position (Kiyomitsu and Cheeseman, 2012), and Aurora A forms a gradient from the pole that is required for attachment error correction (Ye et al., 2015). Abrogation of the RanGTP gradient that forms around aligned chromosomes using a dominant negative RanT24N mutant had no effect on congression (Barisic et al., 2015). In contrast, polar Aurora A is suggested to bias the lateral sliding of chromosomes toward the equator via direct regulation of CENP-E (Kim et al, 2010). Here, the phosphorylation of CENP-E at the pole is proposed to abrogate its interaction with PP1, a factor that is required for stable CENP-E-microtubule binding. This is suggested to bias congression toward the equator as the PP1 deficient phospho-CENP-E only efficiently

walks on stabilised K-fibre microtubules that are oriented toward the equator (Kim et al., 2010). It must be noted, however, that while CENP-E mediated congression requires some form of stabilised microtubules, it is not dependent upon K-fibres (Cai et al., 2009; Iemura and Tanaka, 2015), and a new model of directionality based on the 'tubulin code' has been proposed (see below) (Barisic et al., 2015).

As already discussed, the PEF, a decaying AP force field that emanates from each aster, is symmetrical about the spindle equator and could therefore bias chromosome migration toward this region (Cane et al., 2013). The principal PEF generator, Kid, has been shown to induce a position dependent increase in tension at kinetochores approaching the pole, which promotes directional switching (Fig. 6c) (Stumpff et al., 2012). However, its depletion has no effect on congression (Levesque and Compton, 2001), probably because Kif18A mediates the dominant position sensing mechanism and can compensate for its loss (Stumpff et al., 2012). Recently, the 'tubulin code' has been suggested to bias CENP-E stepping toward the equator, and therefore impose directionality on the lateral sliding mechanism (Barisic et al., 2015). Here, Barisic and colleagues found that microtubules oriented toward the equator are enriched with detyrosinated tubulin. Abrogation of this modification resulted in aberrant chromosome movements that were dependent upon CENP-E. Moreover, *in vitro*, CENP-E was observed to be more processive and to carry higher loads on detyrosinated microtubules. As such, the authors proposed a model where

CENP-E transports pole proximal chromosomes preferentially on detyrosinated microtubule tracks, which are orientated toward the spindle equator (Barisic et al., 2015).

1.7 *Coupling congression with attachment regulation and signalling*

1.7.1 *Correcting erroneous kinetochore-microtubule attachments*

Despite geometric constraints favouring sister-kinetochores forming bi-oriented attachments (Cimini et al., 2003; Loncarek et al., 2007), errors in microtubule attachment are frequenting during prometaphase (Ault and Rieder, 1992). If left uncorrected, these errors would lead to segregation defects (Cimini et al., 2001). As such, kinetochores employ a correction mechanism that selectively destabilises erroneous attachments while promoting bi-orientation, ensuring that all kinetochores are in an anaphase compatible configuration prior to segregation. The current model, termed the “spatial separation” model, dictates that attachment stability is directly dependent upon tension across the centromere. This is based on classic observations in grasshopper spermatocytes, which showed that the normally unstable unipolar attachments could be stabilised by the application of tension (Nicklas and Koch, 1969). In molecular terms, insights into this pathway came from increase-in-ploidy screens (Ipl) in

yeast, which identified the kinase Ipl1 (Chan and Botstein, 1993). Critically, it was demonstrated that Ipl1 promoted attachment turnover in the absence of tension (Tanaka et al., 2002). The vertebrate homologue of Ipl1 is Aurora B, a ser/thr kinase that is a member of the CPC located at the inner-centromere (see appendix 1 for a structural description of the CPC) (Adams et al., 2000). In agreement with models of Ipl1, small molecule inhibition of Aurora B leads to the stabilisation of incorrect attachments, which are subsequently corrected upon inhibitor washout (Hauf et al., 2003; Lampson et al., 2004). Given the centromeric localisation of Aurora B, it was suggested that substrate proximity to the kinase was critical for attachment correction, and this was related to the tension. Indeed, the formation of a bi-oriented attachment is thought to exert enough tension to physically separate Aurora B from its substrates in the outer-kinetochore. As erroneous attachments fail to generate sufficient tension, these substrates are in close proximity to the kinase and can therefore be phosphorylated (Andrews et al., 2004; Cimini et al., 2006; Tanaka et al., 2002). This idea is supported by two key lines of experimental evidence; (1) A FRET based biosensor that reports Aurora B phosphorylation is constitutively phosphorylated when positioned close to the centromere, irrespectively of tension, however, if positioned at the outer-kinetochore it is dephosphorylated when under tension (Welburn et al., 2010). It must be noted that similar behaviour is observed for endogenous Aurora B substrates (Welburn et al., 2010). (2) By artificially positioning Aurora B

closer to the outer-kinetochore, and therefore forcing constitutive phosphorylation within this region, microtubule attachments can be destabilised in a tension independent manner (Liu et al., 2009). A key prediction of this model is that Aurora B phosphorylation of outer-kinetochore proteins must alter their microtubule affinity, which in turn allows for the correction of erroneous attachments. Indeed, experimental evidence suggests that this is achieved via two mechanisms. First, by negatively regulating microtubule binding regions within the kinetochore. Specifically, this involves the phosphorylation of key attachment proteins Ndc80 and Knl1, which antagonises their electrostatic interaction with tubulin and therefore decreases microtubule affinity (Cheeseman et al., 2006; Ciferri et al., 2008; Guimaraes et al., 2008; Miller et al., 2008; Welburn et al., 2010; Zaytsev et al., 2015). Second, by regulating the composition of the kinetochore. In this regard, Aurora B phosphorylation of the microtubule binding Ska and ASTRIN/SKAP complexes antagonises their recruitment (Chan et al., 2012; Schmidt et al., 2010). Thus, Aurora B targets a myriad of microtubule binding proteins, which causes a global reduction in microtubule affinity at low-tension kinetochores.

The spatial separation model is not, however, without caveats. At low-tension kinetochores, the N-terminus of Ndc80, which contains the principal error correction target site, is >100nm from Aurora B (Smith et al., 2016). Therefore it is unclear how the kinase physically interacts with this substrate. One idea is that an active pool of Aurora B diffuses from the

centromere. This is based on findings that show the activation of Aurora B by INCENP occurs in trans, and this concentrates active kinase at the centromere (Bishop and Schumacher, 2002; Honda et al., 2003; Kelly et al., 2007; Sessa et al., 2005). This pool then turns over with a $t_{1/2}$ of ~50s (Ahonen et al., 2009; Murata-Hori and Wang, 2002), releasing active kinase that diffuses away from the centromere that is eventually deactivated by cytoplasmic phosphatases (Kelly et al., 2007). Thus generating a phospho-gradient. However, it is still unclear if a soluble pool of diffusing kinase can act on this length scale. Moreover, while syntelically attached kinetochores (both sisters bound to the same pole) fail to generate tension, merotelic attachments (one sister in a bi-oriented pair bound to both poles; see Fig 3) are under tension (Gregan et al., 2011) and are therefore invisible to the correction machinery. Aurora B is required for the correction of merotelic attachments, as its inhibition leads to an increase in these errors (Cimini et al., 2006; Knowlton et al., 2006), however, the mechanism of correction is less clear. It has been suggested that the merotelically attached sister is deformed, with the second (incorrect) attachment site projecting towards the inner-centromere (Cimini et al., 2004). This could bring it in close proximity to Aurora B, leading to its destabilisation. Moreover, the CPC has been shown to enrich at merotelically attached sister-pairs (Knowlton et al., 2006), suggesting there may be an additional detection mechanism that acts upstream of Aurora B that concentrates it at these errors. Indeed, sister-separation in response to tension cannot be the only regulatory

mechanism, an idea that is supported by several observations; (1) metaphase kinetochores display a phenomenon termed ‘breathing’, where the inter-sister separation oscillates (Jaqaman et al., 2010). During this oscillation, there are periods of low tension that are comparable to unattached or erroneously attached kinetochore-pairs. Importantly however, the bi-oriented sister-pair at low tension does not appear to activate error correction. (2) Metaphase kinetochores treated with taxol (to induce centromeric relaxation) do not display a significant increase in outer-kinetochore phosphorylation by Aurora B (DeLuca et al., 2011), and (3) the level of Ndc80 dephosphorylation between prometaphase and metaphase cannot be explained by changes in intra-kinetochore distance. As moving Ndc80 significantly further from Aurora B via the induction of kinetochore ‘hyper-stretch’ has little effect on its phosphorylation state (Suzuki et al., 2014). Therefore, once a bi-oriented attachment has formed, the dynamics of outer-kinetochore phosphorylation, and the tension independent maintenance of attachment, cannot be explained by changes in subunit separation at the inter- or intra-kinetochore level. This suggests that error correction is antagonised or abrogated after bi-orientation by a biochemical event. This may involve Knl1 mediated recruitment of PP1 (DeLuca et al., 2011; Liu et al., 2010), which creates a stabilising region of dephosphorylation within the outer-kinetochore. Therefore, while tension is contributory to correction, particularly at syntelic attachments, additional molecular signals must be involved in the correction and communication of

attachment status. In this regard, a recent study has shown that Aurora A, which is concentrated at the poles, contributes to error correction by phosphorylating Ndc80 at identical sites to Aurora B. This counteracts the stabilising effect of the PEF within this region, which could otherwise promote erroneous attachment (Ye et al., 2015). While this contributes to the knowledge of correction mediators, work focusing on precise molecular alterations induced by bi-orientation is needed to describe how error correction is regulated independently of spatial separation.

1.7.2 *The spindle assembly checkpoint*

The accurate transmission of genetic material between cellular generations is absolutely dependent upon kinetochore-pairs forming bi-oriented attachments prior to anaphase. As described above, one mechanism to promote bi-orientation is Aurora B mediated error correction, which destabilises erroneous attachments in response to a lack of tension. A second mechanism is a signalling cascade termed the spindle assembly checkpoint (SAC), which senses kinetochore attachment status and directly inhibits anaphase until all sister-pairs are in a bi-oriented state. The major SAC effectors, budding uninhibited by benzimidazole (Bub1, Bub2 and Bub3) and mitotic arrest deficient (Mad1, Mad2 and Mad3) proteins were originally identified in yeast screens (Hoyt et al., 1991; Li and Murray, 1991). Early models suggested that these mediators generated a switch-

like SAC signal, as a single unattached kinetochore could delay anaphase (Rieder et al., 1995). However, later work showed that the duration of the cell cycle delay could be influenced by the size of the defect (Rieder and Maiato, 2004; Weaver, 2003). As such, the SAC can be thought of as a graded signal, with more severe defects eliciting a stronger response (Collin et al., 2013; Dick and Gerlich, 2013). The SAC delays mitotic progression by generating a soluble 'wait-anaphase' signal, whose biological manifestation is the mitotic checkpoint complex (MCC), consisting of cell division control (Cdc) protein 20, Mad2, Bub1-related protein (BubR1) and Bub3 (Sudakin, 2001). The MCC inhibits the anaphase promoting complex / cyclosome (APC/C), an E3 ubiquitin ligase bound to is cofactor Cdc20, through direct inactivation of Cdc20. The APC/C triggers anaphase onset and mitotic exit by targeting two key proteins for degradation; (1) securin, which protects sister-chromatid cohesin from proteolytic cleavage, and (2) cyclin B, the mitotic cyclin dependent kinase (Cdk) 1 cofactor (Oliveira et al., 2010). Thus, the primary aim of an unattached kinetochore is to generate MCC, and therefore halt mitosis in prometaphase/metaphase. This is achieved by catalysing a key step in MCC formation (Howell et al., 2000; Howell et al., 2004; Shah et al., 2004); the conformational activation of soluble Mad2 from a free 'open' form (O-Mad2) to a Cdc20 bound 'closed' form (C-Mad2) (Luo and Yu, 2008). This catalysis is mediated kinetochore tethered C-Mad2 (Luo and Yu, 2008), whose loading is dependent upon Mad1. Therefore, a vital step in SAC

signalling is the loading of Mad1:C-Mad2 to kinetochores. A process that involves a complex, phospho-dependent cascade that begins with the conserved kinases Aurora B and Mps1, and is followed by the recruitment of the Bub1:Bub3 and BubR1:Bub3 complexes, then finally kinetochore association of Mad1:Mad2 heterotetramers (Chen, 2002; Howell et al., 2004; Kiyomitsu et al., 2007; London and Biggins, 2014a; London et al., 2012; Sharp-Baker and Chen, 2001; Shepperd et al., 2012; Yamagishi et al., 2012). Here, Mps1 is recruited to the kinetochore via direct interaction with Ndc80 CH domains (Dou et al., 2015; Hiruma et al., 2015; Kemmler et al., 2009; Zhejian et al., 2015; Zhu et al., 2013). The Ndc80 docked Mps1 then phosphorylates Knl1 at several MELT (Met-Glu-Leu-Thr) motifs, which targets Bub1 to the kinetochore (London et al., 2012; Shepperd et al., 2012; Yamagishi et al., 2012). Both Bub3, and the BubR1:Bub3 complex do not demonstrate sufficient affinity to phospho-MELTs (pMELTs) for this interaction alone to facilitate their recruitment (Overlack et al., 2015; Primorac et al., 2013; Zhang et al., 2015). Therefore, in addition to the pMELT interaction, Bub1 directly binds with Bub3 (forming the Bub1:Bub3 complex) and with BubR1 via a GLEBS domain to enable their loading (Overlack et al., 2015; Primorac et al., 2013; Sharp-Baker and Chen, 2001). The kinetochore association of Bub1 and BubR1 is also enhanced in a pMELT independent way, via interaction with KI motifs in Knl1 (Krenn et al., 2014; Krenn et al., 2012). While not essential for their localisation, this interaction is proposed to act as a sensitised switch that recruits enough

Bub protein to generate a SAC signal, while preventing BubR1 mediated stabilisation of microtubule attachment. This may function to maximise a kinetochores ability to simultaneously signal the SAC and correct attachment errors (London and Biggins, 2014b).

Despite Bub1:Bub3 loading to kinetochores being required for checkpoint activity, its localisation does not necessarily correlate with SAC activity. Indeed, some Bub1 is retained at anaphase kinetochores (Howell et al., 2004; Sharp-Baker and Chen, 2001), albeit at a reduced level when compared to prometaphase. In contrast, the association of Mad1:Mad2 heterotetramers strictly correlates with SAC signalling. A relationship that was demonstrated by artificially tethering Mad1 to kinetochores, which led to constitutive SAC activation (Kuijt et al., 2014; Maldonado and Kapoor, 2011). The recruitment of Mad1 in human kinetochores is dependent upon two independent pathways. This first involves Bub1, which interacts with an RLK motif in Mad1. This pathway is solely required for Mad1 recruitment in budding yeast and *C. elegans* (London and Biggins, 2014a; Moyle et al., 2014). However, an RLK mutant that abrogated Mad1 loading in these model organisms, only reduced kinetochore Mad1 levels by ~50% in HeLa cells (Kim et al., 2012). Moreover, Knl1 depletion in RPE1 and HeLa cells had no effect on an unattached kinetochores ability to generate a checkpoint signal, despite Bub1 being absent (Silio et al., 2015). Therefore, a Knl1-Bub independent pathway for Mad1 loading must operate at these kinetochores. In this regard, the RZZ complex has been implicated in the

recruitment Mad1:Mad2 to unattached kinetochores (Silio et al., 2015), a process that may be dependent upon the direct interaction of spindly with Mad1 (Yamamoto et al., 2008). Thus, human kinetochores possess two independent routes for Mad1:Mad2 kinetochore recruitment.

Once a stable end-on attachment has formed, the checkpoint must be silenced to enable mitotic progression. Current models suggest that this is achieved by unloading Mad1:Mad2 from the kinetochore, which halts cytoplasmic Mad2 conversation and therefore abrogates MCC formation. This is achieved by two mechanisms: (1) kinetochore tethered dynein strips Mad1:Mad2 and BubR1 upon microtubule binding (Gassmann et al., 2010; Howell, 2001), and (2) Knl1 bound PP1 antagonises key SAC phosphorylation events, which leads to the dissociation of Bub1:Bub3 from the kinetochore (London et al., 2012; Meadows et al., 2011; Pinsky et al., 2009; Rosenberg et al., 2011; Vanoosthuyse and Hardwick, 2009; Zhang et al., 2014), thereby silencing the checkpoint upstream of Mad1:Mad2.

1.8 *Integrating the current models of chromosome congression*

While recent work has begun to decipher the mechanistic details of individual congression pathways, how these are integrated throughout the spindle during prometaphase is still poorly understood. Below, we set out a working model of congression based on the advances discussed above (Fig 7). Immediately following NEB, chromosomes pre-positioned at the

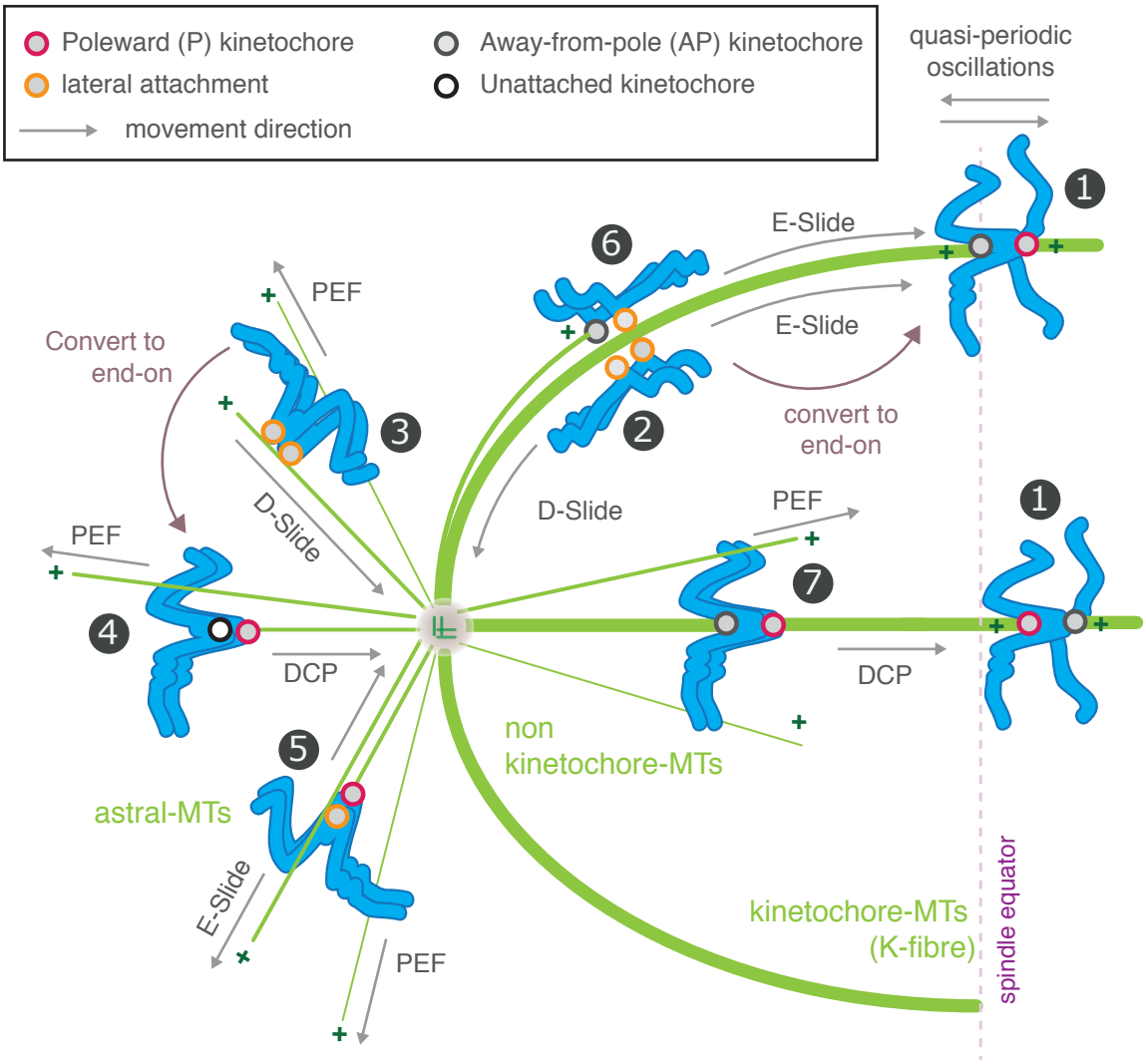

Figure 7: An integrated model of chromosome congression

After nuclear envelope breakdown, chromosomes can be positioned throughout the cytoplasm and the nascent spindle, resulting in the formation of various microtubule attachments (1 to 7). Chromosomes at the spindle equator instantaneously biorientate, and do not require congression (1). Chromosomes that are positioned behind the pole or in the spindle periphery first move poleward through the action of dynein (D-slide) (2 and 3), or by DCP if a monoorientated attachment has formed (4 and 5). Within the polar region, an MCAK-dependent pathway operates to actively convert lateral attachments into monoorientated ones. Once at the pole, lateral (2) and monoorientated or lateral (6) chromosomes are transported to the spindle equator by CENP-E sliding (E-slide). This pathway often fails to maintain chromosomes at the metaphase plate and is not compatible with anaphase – as such, these chromosomes are converted into the default amphitelic state at the equator by PP1-mediated dephosphorylation of CENP-E (1). Pole-proximal chromosomes within the spindle can also bi-orientate and congress by DCP (7). These kinetochores are subject to the spatial control mechanisms outlined in Fig. 5 and Barisic et al. (2015).

equator by the polar ejection force instantaneously form bi-oriented attachments (step 1, Fig 7) (Barisic et al., 2014; Magidson et al., 2011). The remaining chromosomes are distributed throughout the spindle, and interact with microtubules in a myriad of conformations (steps 2-7, Fig 7). Any erroneous attachments (merotelic/syntelic attachments) are immediately destabilised by Aurora B mediated phosphorylation of outer-kinetochore proteins, rendering the sister-pair unattached (Lampson and Cheeseman, 2011). Now, spindle position dictates how chromosomes are moved to the equator. Those positioned in the spindle periphery are first moved toward their proximal pole via either dynein mediated sliding (steps 2 & 3, Fig. 7) (Barisic et al., 2014; Li et al., 2007; Yang et al., 2007), or DCP if a monoorientated attachment has formed (steps 4 & 5, Fig. 7) (Bancroft et al., 2015). Here, both mechanisms overcome an AP force generated by the PEF and CENP-E, suggesting that dynein and DCP are dominant within this region (steps 3 – 5, Fig. 7) (Bancroft et al., 2015; Barisic et al., 2014). Moreover, lateral kinetochore-microtubule attachments are actively converted to an end-on state about the pole, a process that depends on CENP-E and MCAK in mammalian cells (Shrestha and Draviam, 2013), and Dynein in *C. elegans* (Cheerambathur et al., 2013) (step 3, Fig. 7). In summary, the initial poleward transport yields a population of laterally attached or monoorientated kinetochore pairs in close proximity to the pole. From here, laterally attached sister-pairs migrate toward the equator via CENP-E mediated sliding (steps 2 & 6, Fig. 7) (Barisic et al., 2014; Kapoor

et al., 2006), a process that is guided by microtubule detyrosination and Aurora A phosphorylation of CENP-E (Barisic et al., 2015; Kim et al., 2010). As lateral attachments are not compatible with anaphase, these are actively converted to the default end-on state about the equator via PP1 recruitment to CENP-E (Kim et al., 2010). Finally, chromosomes that bi-orient between the pole and spindle equator congress via DCP (step 7, Fig. 7) (see section 1.6 for a description of directional control). Taken together, both CENP-E-mediated sliding and DCP move chromosomes from the pole to spindle equator. Here, DCP appears to be the prominent mechanism as clear lateral sliding events were observed in a quarter of Ptk1 cells (Kapoor et al., 2006), and only 15-20% of congression events were CENP-E dependent in U2OS and HeLa cells (Bancroft et al., 2015; Barisic et al., 2014). Nevertheless, both mechanisms act in conjunction with the instantaneous biorientation of kinetochores early in mitosis to provide a robust, multi-layered system that ensures all chromosomes congress in preparation for anaphase.

1.9 *Thesis aim*

The mechanistic contributors to DCP are currently only described *in vitro*. The function of these factors at kinetochores in cells, and how they are regulated is currently unknown. Here, we sought to assign precise contributions of kinetochore components to DCP *in vivo*, and determine how these contributions are regulated by post-translational modification.

Chapter 2: *Materials and methods*

2.1 *Cell culture and drug treatments*

HeLa-Kyoto (K) cells were grown in a humidified incubator at 37ºC and 5% CO_2 in Dulbecco's modified Eagle's medium (DMEM) (Gibco) containing 10% foetal calf serum (FCS), 100U ml^{-1} penicillin and 100 μg ml^{-1} streptomycin. This was supplemented with 0.1 μg ml^{-1} puromycin (Invitrogen) for the maintenance of the eGFP-CENP-A cell line. The HeLa H2B-GFP cell line was maintained in non-selective media. The hTERT-RPE1 eGFP-CENP-A cell line was maintained in DMEM/F-12 medium containing 10% fetal calf serum (FCS), 2.3 gl^{-1} sodium bicarbonate, 100 U/ml penicillin and 100 μg ml^{-1} streptomycin. For drug treatment conditions, see table 1.

2.2 *siRNA*

siRNA oligonucleotides (53 nM) were transfected using oligofectamine (Invitrogen) according to the manufacturer's guidelines and analysed at 48 hr. Briefly, two tubes were prepared, the first (tube 1) containing 150 μl Optimem (Gibco) and 4.5 μl RNA duplex, and the second (tube 2) containing 36 μl Optimem (Gibco) and 9.5 μl oligofectamine (Invitrogen). These were incubated separately for 5 min at room temperature, tube 2

Drug	Use	Conditions	Manufacturer	Reference
ZM447439 (ZM1)	Aurora B inhibitor	2 μM, 10 min	Tocris	Ditchfield *et al* 2003, JCB
MG132	Proteasome inhibitor	1μM, 90 min	Sigma	Tsubuki *et al* 1996, J. Biochem
Nocodazole	Microtubule depolymerisation	330nM, 16 hr	Tocris	De Brabnder *et al* 1977, Cell Biol Int Rep
Taxol	Microtubule stabilisation	100nM, 1 hr	Sigma	Wani *et al* 1971, J Am Chem Soc

Table 1: Drug details

Target	RNAi oligo sequence (5' - 3') All sequences + 3'-tt	Manufacturer	Reference
Control	GGA CCU GGA GGU CUG CUG U	Sigma	Samora *et al* 2010, NCB
Ska1	CCC GCT TAA CCT ATA ATC A	Qiagen	Hanisch *et al* 2006, EMBO
Ska1 pool	CCG CUU AAC CUA UAA UCA A UAU AGU GGA AGC UGA CAU A UCA AUG GUG UUC CUU CGU A GGA CUU ACU CGU UAU GUU A	Thermo-Fischer	Schmidt *et al* 2012, Dev Cell
CENP-Q	GGU CUG GCA UUA CUA CAG GAA GA	Invitrogen	Bancroft *et al* 2015, JCS
CENP-E	ACU CUU ACU GCU CUC CAG U	Ambion	Bancroft *et al* 2015, JCS
MCAK	GAU CCA ACG CAG UAA UGG U	Invitrogen	Cassimeris & Morabito 2004, Mol Biol Cell
CENP-F	AAG AGA AGA CCC CAA GUC AUC	Sigma	Johnson *et al* 2004, JCS

Table 2: siRNA oligonucleotides

was then added to tube 1 and incubated for a further 25 min at room temperature. The final mix (200 μl) was then added to cells in a 35 mm dish containing 1.5 ml minimal essential medium (MEM) (Gibco) at ~60% confluency. The media was replaced at 24 hr with 2 ml DMEM. RNAi oligonucleotide sequences are displayed in table 2.

2.3 *Plasmid construction*

2.3.1 *Construction methodology*

The CENP-Q phospho-mutants (created by James Bancroft) were generated with site-directed mutagenesis using siRNA resistant CENP-Q-eGFP (pMC308) as a template vector. To generate tagRFP-FKBP-Ska1, eGFP was first replaced with tagRFP in pEGFP-C1 (Clontech) using NheI and XhoI creating tagRFP-C1 (pMC387). FKBP12 was then inserted in the XhoI and HindIII restriction sites creating tagRFP-FKBP (pMC390) (all PCR primers, conditions and vectors can be found in table 3). Next, full length siRNA resistant Ska1 was ligated into pMC390 using PstI/MfeI to create tagRFP-FKBP-Ska1(RIP) (pMC393). Ska1 was rendered resistant to the Ska1 siRNA oligonucleotide using site directed mutagenesis with the primer pairs shown in table 4. For Ska1 loading analysis, FKBP was cut from pMC393 and replaced with PCR amplified tagRFP using XhoI and HindIII sites, creating 2xtagRFP-Ska1(RIP) (pMC463). To generate 2xtagRFP-Ska1ΔMTBD, Ska1 1-132 was amplified using PCR and cloned into pMC390 using PstI/MfeI sites, creating tagRFP-FKBP-Ska1ΔMTBD.

Primer name	Sequence 5'-3''	Use	Site	Annealing temp used	Supplier
FKBP-Xho1	AATCTCGAGATGGGAGTGCAGGTGGAA	Inserting FKBP into tag-RFP-C1, creating tagRFP-FKBP (pMC390)	Xho1	60°C	Sigma
FKBP-HindIII	TCGAAGCTTTTCCAGTTTTAGAAGCTC	Inserting FKBP into tag-RFP-C1, creating tagRFP-FKBP (pMC390)	HindIII	60°C	Sigma
Ska1-PtsI	ATTCTGCAGATGGCCTCGTCAGATCTG	Inserting Ska1 into tagRFP-FKBP, creating tagRFP-FKBP-Ska1 (pMC393)	PtsI	60°C	Sigma
Ska1-MfeI	CAACAATTGTCAGGTTATAACATAACG	Inserting Ska1 into tagRFP-FKBP, creating tagRFP-FKBP-Ska1 (pMC393)	MfeI	60°C	Sigma
tagRFP-XhoI	ATCTCGAGATGGTGTCTAAGGGCGAA	Replacing FKBP in pMC393 with tagRFP, creating 2xtagRFP-Ska1 (pMC463)	XhoI	68°C	Sigma
tagRFP-HindIII	CGAAGCTTATTAAGTTTGTGCCCCAG	Replacing FKBP in pMC393 with tagRFP, creating 2xtagRFP-Ska1 (pMC463)	HindIII	68°C	Sigma
Ska1ΔMTBD-Mfe1	TTCTGCAGATGGCCTCGTCAGATCTG	Replacing Ska1with Ska1ΔMTBD in pMC393, creating tagRFP-FKBP-Ska1ΔMTBD	MfeI	60°C	Sigma
Ska1ΔMTBD-PstI	AACAATTGTCATTGCTCTTTGGGAGGCTT	Replacing Ska1with Ska1ΔMTBD in pMC393, creating tagRFP-FKBP-Ska1ΔMTBD	PstI	60°C	Sigma

Table 3: PCR primers for cloning

The FKBP was then replaced with tagRFP as in pMC463, creating pMC464.

Primer name	Sequence 5'-3'	Use	Annealing temp	Supplier
Ska1-ProN1-FW	CTTCGTACATGAAATCCCGGTTAACCTATAATCAAATTAA	Protecting Ska1 against Hanisch *et al* siRNA, round 1	55°C	Sigma
Ska1-ProN1-RV	TTAATTTGATTATAGGTTAACCGGGATTTCATGTACGAAG	Protecting Ska1 against Hanisch *et al* siRNA, round 1	55°C	Sigma
Ska1-ProN2-FW	ATGAAATCCCGGTTAACCTACAATCAAATTAATGATGTTA	Protecting Ska1 against Hanisch *et al* siRNA, round 2	58°C	Sigma
Ska1-ProN2-RV	TAACATCATTAATTTGATTGTAGGTTAACCGGGATTTCAT	Protecting Ska1 against Hanisch *et al* siRNA, round 2	58°C	Sigma
Ska1-ProN3-FW	AATCCCGGTTAACCTACAACCAAATTAATGATGTTATTAA	Protecting Ska1 against Hanisch *et al* siRNA, round 3	62°C	Sigma
Ska1-ProN3-RV	TTAATAACATCATTAATTTGGTTGTAGGTTAACCGGGATT	Protecting Ska1 against Hanisch *et al* siRNA, round 3	62°C	Sigma

Table 4: PCR primers for site directed mutagenesis

Primer name	Sequence 5'-3'	Use	Supplier
tagRFP-FKBP-seq	AGAATCAAGGAG GCCGACAAA	Sequencing the FKBP inserted into pMC387	Sigma
Ska1-Seq-FW	CTGACTATATCTC CAGATTAT	Sequencing Ska1 insertion into pMC390 and Ska1ΔMTBD cloning	Sigma
Ska1-Seq-RV	AGGGGGAGGTGT GGGAGGTTT	Sequencing Ska1 insertion into pMC390	Sigma
2xtagRFP-Seq	TAGGTTCCTGGCC ACAGTTTC	Sequencing the replacement of FKBP in pMC393 with tagRFP	Sigma

Table 5: Primers for sequencing

2.3.2 PCR

For gene amplification, the following protocol was employed for all reactions, with only the annealing temperature varying between primer sets (see tables 3 & 4 for sequences and annealing temperatures). (1) Initial denaturation at 98°C for 30 s, (2) denaturation at 98°C for 10 s, (3) annealing for 30 s, (4) extension at 72°C for 20 s then return to step two for 34 cycles, (5) final extension at 72°C for 10 min. This was modified for site-directed mutagenesis, where samples were annealed for 50 s and extended for 12 min at 68°C for a total for 20 cycles. In all cases, the reaction mix was made of 20 ng of template DNA, 1 μM of each primer, 2 mM dNTPs, 5μl 10X buffer (for pfu Ultra II polymerase) or 10 μl 5X buffer (phusion polymerase) and 1 μl of enzyme, added last. For typical amplification Phusion polymerase (NEB) was used, which was replaced with pfu Ultra II polymerase (Agilent) for site-directed mutagenesis.

Amplification products were separated on a 1% agarose gel and purified using a QIAquick extraction kit (Qiagen). For site directed mutagenesis, the PCR product was incubated with Dpn1 (NEB) for 1 hr at 37°C, and directly transformed into bacteria.

2.3.3 *Restriction digests*

1.25 μg of DNA was digested using equal units of enzyme (total 1 μl) in a total reaction volume of 50 μl. This was incubated for 2 hr at 37°C.

2.3.4 *DNA ligation*

Digested DNA fragments were ligated in a 1:3 molar ratio (vector:insert) with 1 μl T4 DNA ligase (Invitrogen) in a total reaction volume of 10 μl. This was incubated for 1 hr at room temperature.

2.3.5 *Bacterial transformation*

For transformation, the entire ligation reaction volume (10 μl) or 15 μl of a site-directed mutagenesis reaction was incubated with 100 μl super-competent DH5α cells on ice for 5 min. The cells were then shocked at 42°C for 90 s and returned to ice for 5 min. For kanamycin resistant plasmids, 900 μl of liquid broth (LB) without selective antibiotic was added and the bacteria were cured for 1 hr at 37°C. After curing, the bacteria were pelleted by spinning at 8000 rpm for 2 min at room temperature, resuspended in 200 μl LB, plated on resistant agar and incubated for >16

hr at 37°C. For Ampicillin resistant plasmids, the curing step was skipped, and cells were plated directly onto selective agar after the second incubation on ice. Colonies were picked and amplified in 5 ml LB containing selective antibiotic for ~16 hr at 37°C. Plasmid DNA was prepared using a mini-prep kit (Qiagen).

2.3.6 *Sequencing*

All constructs were confirmed by sequencing (Source Bioscience). With plasmid DNA sent at 100 ng/μl, and primers at 3.2pmol/μl (primer sequences are shown in table 5).

2.4 *Transient transfections*

Plasmid DNA for transfection was produced using a maxi-prep kit (Qiagen) from 200 ml of overnight culture. Cells in a 35 mm dish at ~60% confluency were transfected with 1 μg of plasmid using Fugene6 (Roche) according to manufacturers instructions. Briefly, in a total reaction volume of 100 μl, 4 μl of Fugene6 was added to an appropriate volume of Optimem (Gibgo) and incubated for 5min at room temperature. Plasmid DNA was then added, and the reaction was incubated for a further 20 min at room temperature, after which the entire reaction was then added to cells in 1.5 ml DMEM. Cells were analyzed at 48 hr, with 500 μl of fresh DMEM added at 24 hr.

2.5 *siRNA rescue experiments*

For both CENP-Q and Ska1 rescue experiments, cells were grown to ~35%

confluency in a 35 mm dish. At this point, cells were treated either CENP-Q, Ska1 or control siRNA for 12 hr as in 2.2. The media was then changed to DMEM, and the cells transfected with 1 μg of vector DNA as in 2.3 and incubated for a further 48 hr.

2.6 *CRISPR Cas9*

To target Ska1 exon 1, the guide 5' TAATTGTTCCAGATCTGACG 3' (Ska1 GuideA, generated using genome-enginerring.org) was cloned into the human codon optimized SpCas9 and chimeric guide expression plasmid (Addgene pX330) using Bbs1 as previously described (Ran et al., 2013). Cells were transfected with 1.5 µg of plasmid using Fugene6 (Roche) in 1.5 ml DMEM as in 2.3. After 24 hr, 500 μl of fresh DMEM was added and the cells were grown for a further 24 hr, at which point the media was replaced with 2 ml of DMEM containing selective antibiotic if necessary and grown for another 24 hr. Cells were imaged, harvested or fixed after a total of 72 hr transfection. For SURVEYOR analysis of guide induced indel mutation, HeLa K cells were harvested from a single 35mm dish after guide transfection for 72 hr and genomic DNA extracted using a QIAamp DNA blood mini kit (Qiagen). A ~1 kb fragment containing the target site was amplified using PCR with the following primer pair (designed using the CHOP CHOP tool) 5' TTAGACCCTCCCCTTCTCTCTC 3' and 5' CGCTTTTGTCAGAACACATCTC 3'. The product was denatured, reannealed and digested with T7 endonuclease as previously described

(Ran et al., 2013), and visualized on a 2% agarose gel using a UV transillumintor.

2.7 *Immunofluorescence microscopy*

For CENP-A, Ska1, Hec1PSer55, CENP-F, Bub1, CENP-E and Plk1 staining, cells were fixed for 10 min at room temperature with 20 mM PIPES pH 6.8, 10 mM EGTA, 1 mM $MgCl_2$, 0.2% Triton X-100 and 4% formaldehyde (PTEMF). For anti-MCAK antibodies cells were fixed for 10 min at -20ºC in methanol. In both cases, the cells were then washed three times in PBS for 5 min before blocking in 3% BSA in PBS for 30 min. Cells were then incubated for 1 hr with primary antibodies (see table 6 for antibody concentrations), and washed three times in PBS for 5 min. Secondary antibodies were AlexaFlour-conjugated antibodies (Invitrogen) used at 1/500 for 30 min. For α-tubulin staining, cells were extracted for 30 sec in 80 mM PIPES pH 6.8, 1mM $MgCl_2$, 4mM EGTA and 0.5% Triton X-100 and then fixed by adding gluteraldehyde at 0.5% for 10 min. Gluteraldehyde autofluorescence was quenched in 0.1% $NaBH_4$ for 7 min. Cells were then washed three times in PBS for 5 min, followed by blocking in TBS containing 0.1% Triton X-100 and 2% BSA for 10 min. Cells were incubated with α-tubulin primary antibody for 30 min, followed by four 5 min washes in TBS containing 0.1% Triton X-100 and then incubated with 647-nm AlexaFlour-conjugated secondary antibodies (Invitrogen) in TBS containing 0.1% Triton X-100 and 2% BSA for 30 min. Three-dimensional

image stacks were acquired (75 x 0.2 μm z-sections) using an 100x oil NA 1.4 objective on an Olympus Deltavision Elite microscope (Applied Precision) equipped with a DAPI, fluorescein isothioyanate (FITC), Rhodamine or Texas Red and Cy5 filter set, solid state light source and a CoolSNAP HQ2 camera (Roper Scientific). Image stacks were deconvolved using SoftWorx, and fluorescence-intensity measurements were made manually after background subtraction and normalization to the CENP-A or CREST signal. Staining intensity distributions were compared using a two-sample t-test in R.

2.8 *Live-cell imaging*

To film kinetochore fates in the HeLa-K eGFP-CENP-A cell line, cells were seeded in fluorodishes (World Precision) and imaged in DMEM supplemented with 10% FCS, 100U ml^{-1} penicillin, 100 μg ml^{-1} streptomycin and 0.1 μg ml^{-1} puromycin. Detailed imaging conditions are described elsewhere (Jaqaman et al., 2010): Briefly, three-dimensional image stacks (25 x 0.5 μm *z*-sections) were acquired every 7.5 s using an 100x oil NA 1.4 objective on an Olympus Deltavision Elite microscope (Applied Precision), equipped with a eGFP and mCherry filter set, Quad-mCherry

Antibody	Target (uniprot ID)	Working Concentration	Supplier
Ms anti-CENP-A	Centromere protein A (p49450)	1/500	Abcam
Rb anti-Ska1	Spindle and kinetochore protein 1 (Q96DB8)	1/400	Abcam
Rb anti-Hec1pSer55	Phosphorylated serine 55 in Hec1, a member of the Ndc80 complex (Q014777)	1/300	Thermo
Ms anti-CENP-F	Centromere protein F (p49457)	1/200	Abcam
Ms anti-Bub1	Bub1 (O43683)	1/500	Abcam
Rb anti-CENP-E	Centromere protein E (Q02224)	1/1500	Meraldi lab
Hu CREST antisera	Centromere proteins A, B and C	1/250	Antibodies Inc
Ms anti-Plk1	Polo-like-kinase 1 (p53350)	1/250	Santa-Cruz
Ms anti-α-tubulin	Alpha-tubulin (Q71u36)	1/1000	Sigma
Rb anti-MCAK	Mitotic centromere associated kinesin (Q99661)	1/500	Cytoskeleton

Table 6: Primary antibodies for immunofluorescence

dichroic mirror, solid-state light source and CoolSNAP HQ2 camera (Roper Scientific). The environment was tightly controlled at 37ºC and 5% CO_2 using a stage-top incubator (Tokai Hit) and a weather station (Precision Control). Camera pixels were binned at 1_1, giving an effective pixel size of

64 nm in the lateral direction. Image stacks were deconvolved using SoftWorx (Applied Precision) and kinetochore fates were determined manually. Measurements of kinetochore velocity were taken manually from tracks of persistent movement that lasted at least 3 time frames. To film kinetochore fates in the hTERT-RPE1 eGFP-CENP-A cell line, cells were seeded in fluorodishes (World Precision) and imaged in Leibovitz L-15 supplemented with 10% foetal calf serum. Three-dimensional image stacks (25 z-sections, 0.5 μm) were acquired every 2 s for 5 min using a 100X 1.4 NA oil objective on a confocal spinning-disk microscope (VOX Ultraview; PerkinElmer) equipped with a Hamamatsu ORCA-R2 camera, controlled by Volocity 6.0 (Perki-nElmer) running on a Windows 7 64-bit (Microsoft) PC (IBM). Images were deconvolved with Huygens 4.1 (SVI) using a point spread function (PSF) measured from micro-bead images (using the Huygens 4.1 PSF distiller), and visualized in Fiji. Kinetochore fates were determined manually.

2.9 *Electron microscopy*

For correlative light electron microscopy (CLEM) experiments, HeLa-K eGFP-CENP-A expressing cells were imaged on gridded glass MatTek dishes (P35G-1.5-14-CGRD, Mat-Tek Corporation, Ashland, MA, USA) using a Deltavision microscope as described above. The photo-etched grid coordinate containing the cell of interest was recorded using brightfield illumination at 20x. The same cell was then relocated and live cell imaging

was acquired at 100x. Kinetochore pairs of interest where tracked as described above and once the congression event had occurred, cells were immediately chemically fixed in 3% glutaraldehyde, 0.5% paraformaldehyde and 0.1% tannic acid in 0.05 M phosphate buffer pH 7.4 for 1 h and processed for SBF-SEM. Here, samples were processed and images segmented as previously described (Nixon et al., 2016). Briefly, cells were post-fixed in reduced osmium (2% osmium tetroxide, 1.5% potassium ferrocyanide) for 1 h, incubated in 0.1% thiocarbohydrazide in dH_2O for 20 mins, followed by incubation in 2% osmium tetroxide in dH_2O for 30 mins, before being incubated overnight in 1% uranyl acetate dH_2O at 4°C. Cells were incubated in Walton's lead aspartate at 60°C for 30 mins and then dehydrated in grade series ethanol before being infiltrated and embedded in EPON 812 hard premixed resin (TAAB). Once the resin had fully polymerized, the coverslip was removed and the cell of interest was located using previously acquired grid co-ordinates. The block of resin containing the cell of interest was then excised and mounted on to a cryo pin using Silver Dag (Agar Scientific). Excess resin was trimmed away with an Ultramicrotome (Leica Microsystems, Milton Keynes, UK) leaving a 200 µm x 200 µm block face. To reduce charging the block was first painted with silver conductive paste (TAAB), before 10 nm gold/palladium was evaporated onto it (Quorum Technologies, East Sussex, UK). Imaging was done using Gatan 3View System and Digital Micrograph software (Gatan, Abingdon,UK) and FEI Quanta 250 (FEI, Eindhoven, Netherlands). To image the whole cell including all chromosomes and visualize both

microtubules and kinetochores at a resolution of ~5nm in x and y and 60nm in z the following imaging parameters were used; 4000 x 4000 frame size,12 µs dwell time, 2.3 KeV, 50Pa and a magnification of 9500x. Kinetochores were identified in the images as electron dense regions on chromatin that span 2-3 z-slices (120-180nm).

2.10 *Figure preparation*

Data were visualized using either excel (Microsoft) or R. Immunofluorescence images were prepared using SoftWorx (Applied Precision), with scale bars added in Fiji. Movie stills were prepared in Fiji. Rendering of the electron micrographs was carried out by Nicholas Clarke in Imaris (Bitplane). All figures were generated using illustrator (Adobe).

Chapter 3: *Congressing kinetochores require progressive loading of Ska complexes to prevent force dependent detachment*

3.1 *Introduction*

As discussed in 1.3, two kinetochore properties that involve microtubule binding are required for congression via DCP, (1) the formation of end-on microtubule attachments, and (2) the tracking of depolymerising microtubule plus-end to generate force. It is well established that Hec1, a subunit of the Ndc80 complex is the major end-on attachment factor (Cheeseman et al., 2006), and this is conserved across all tested organisms (Cheeseman and Desai, 2008). However, it remains unclear as to what factors are responsible for plus-end tracking, and by what mechanism - biased diffusion or curved protofilament binding. The Ska complex has been suggested to be one factor that mediates the coupling of end-on attached kinetochores to curving protofilaments based on *in vitro* data (Abad et al., 2014; Jeyaprakash et al., 2012; Schmidt et al., 2012; Welburn et al., 2009), however, convincing *in vivo* assessment of its role is lacking.

3.2: *The Ska complex is required for the maintenance of bi-orientation during congression*

To follow the behaviour of congressing chromosomes we imaged HeLa cells expressing eGFP-CENP-A at 7.5s intervals for 5min. Because kinetochores utilise two distinct congression mechanisms, we sought to sub-sample for sister-pairs utilising DCP. To do so, we employed three criteria; (1) the kinetochore axis (K-K axis) was no more than 45° relative to the local microtubule path (from here termed oriented), a geometry where end-on attachment to both poles is possible, (2) we only followed kinetochore-pairs located between the pole and spindle equator at t=0s, as lateral sliding is largely restricted to peripheral chromosomes (Barisic et al., 2014), and (3) we confirmed the sister-pair was undergoing cycles of breathing, a characteristic of bi-orientation (Cai et al., 2009) (Fig 8a). These kinetochores appeared bi-oriented based on gluteraldehyde fixation and α-tubulin staining (Fig 8b). Nevertheless, to further confirm their attachment state, we filmed sisters-pairs as they congressed and then fixed/processed the cell for serial block face scanning electron microscopy (SBF-SEM) (Fig8d-g). Here, both kinetochores and microtubule structures were clearly visible in the SBF-SEM images, allowing us to correlate the live cell and SEM data. Importantly, microtubule fibres terminated at both the P and AP kinetochores on the sister-pair that we had tracked, confirming that such chromosomes are congressing via DCP (Fig8d-g).

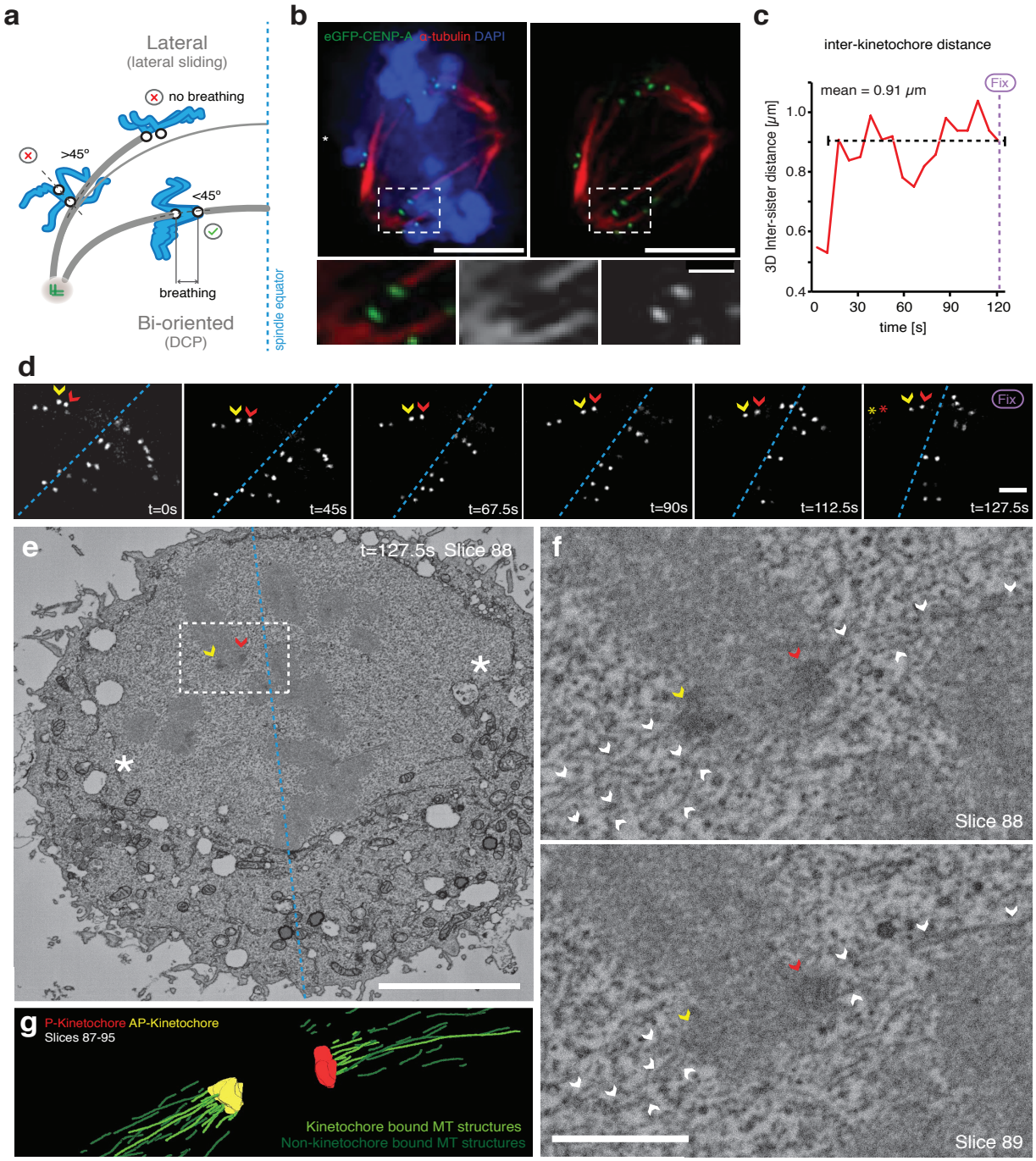

Figure 8: Congressing chromosomes that are oriented and breathing are bi-oriented

(a) Schematic showing the selection criteria used to sample for kinetochore pairs that are congressing via DCP. (b) Image of a prometaphase HeLa cell expressing eGFP-CENP-A stained with DAPI and an Ab against α-tubulin. Zoom boxes depict an unaligned kinetochore-pair that has formed a bi-oriented attachment. Scale bar 5μm (top) 1μm (bottom). (c) Measurement of 3D inter-sister distance over time for the congressing kinetochore-pair depicted in (d) showing that it is undergoing inter-kinetochore breathing (av=0.91μm) following attachment (seen as rise in inter -kinetochore distance at t=15s). (d) Movie stills of an eGFP-CENP-A marked kinetochore-pair congressing to the metaphase plate. The cell was fixed at t=127.5 s and processed for SBF-SEM. Red and yellow arrows depict the P and AP kinetochores, red and yellow stars indicate the position of the kinetochore pair at t=0s, dotted blue line indicates the metaphase plate periphery. Scale bar 1μm. (e) A single slice (84) from an SBF-SEM stack of the cell displayed in (d) after fixation at t=127.5 s. Red and yellow arrows depict the P and AP kinetochores. Dotted blue line indicates the metaphase plate periphery. White asterisks depict the spindle poles. Scale bar 5 μm. (f) Zoom of the white box in (d). Here, the congressing kinetochore pair followed in (c,d) can clearly be seen with end-on microtubule attachment at both sisters, confirming that it is bi-oriented. White arrows indicate microtubules, red and yellow arrows depict the P and AP kinetochores. Scale bar 1 μm. (g) Rendered image of slices 77-100 from the SBF-SEM stack of the cell depicted in (d-f).

By tracking the behaviour of individual bi-oriented kinetochore-pairs, we documented three phenotypes associated with DCP, (1) successfully congressing to the spindle equator (74.3 ±3.3%), (2) stalling, where the sister-pair would persist in an immobile state (6.8 ±2.4%), and (3) 'flipping' (18.8 ±3%), where the sister-pair would initiate congression but then rotate through 90° relative to the spindle axis as it approached the metaphase plate (Fig 9a). This phenotype is distinct from the previously reported 'kinetochore wobbling' by Magidson and colleagues (Magidson et al., 2011), where laterally attached kinetochore-pairs in early prometaphase changed their orientation by >45° in the absence of directed motion. We then sought to investigate how these phenotypes differed in cells depleted of Ska1. We found a dramatic reduction in successful congression to the spindle equator (to 10.7 ±1%), which corresponded with a large increase in kinetochore flipping (to 70 ±3.7%; Fig 9a-d). Importantly, the flipping phenotype was not the consequence of a change in attachment state because the fraction of unaligned bi-oriented kinetochores in control and Ska1-depleted cells was unchanged (Fig 10a,b).

To rule out siRNA off target effects, we transfected cells depleted of Ska1 with an siRNA resistant tagRFP-FKBP-Ska1 transgene. This successfully rescued the flipping phenotype, with 63% (±8.5%, n=57 kinetochore pairs from 29 cells) of unaligned bi-oriented kinetochore-pairs now successfully congressing to the spindle equator (Fig 11a,b). To validate this phenotype independently of siRNA, we targeted the first exon of Ska1 using CRISPR

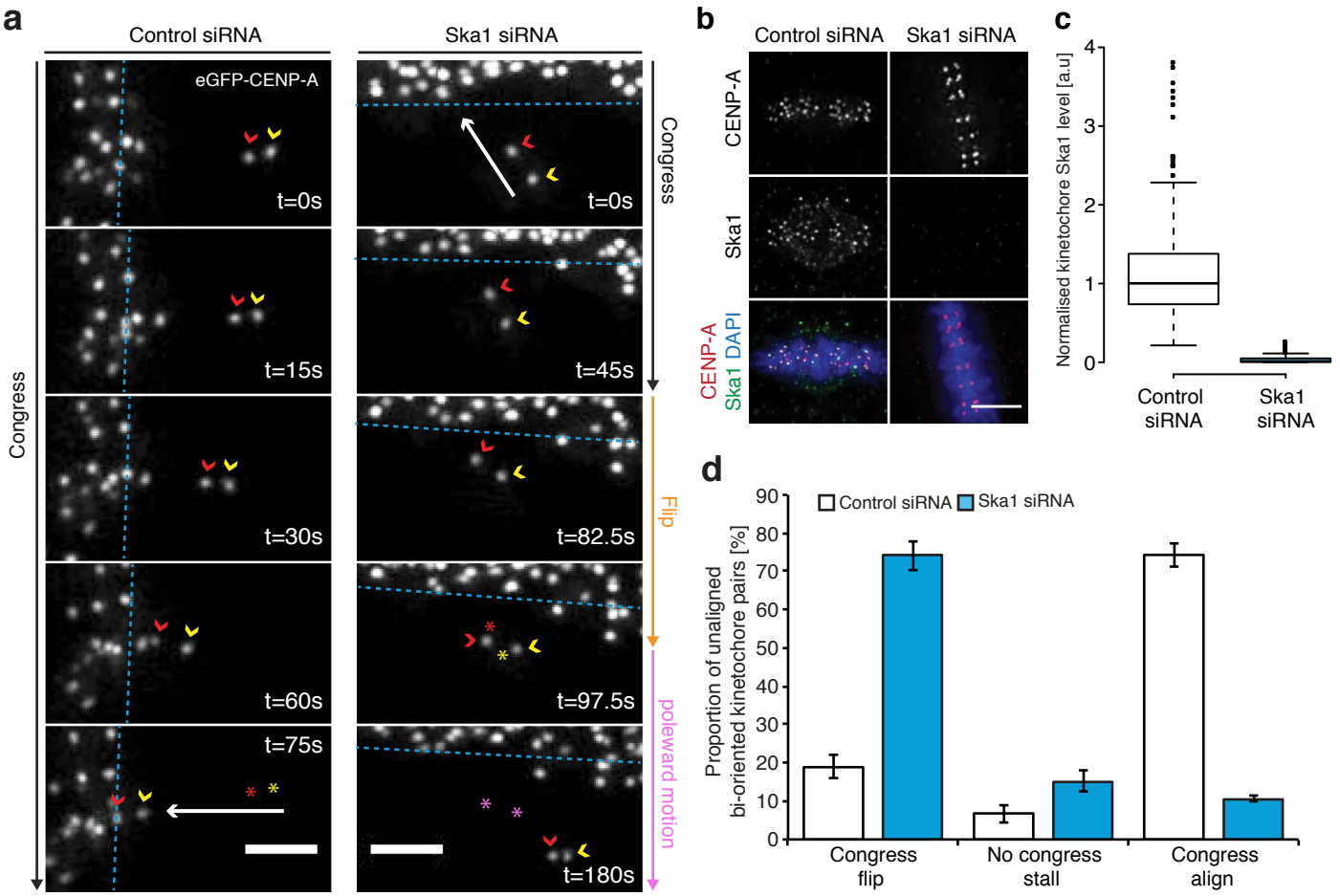

Figure 9: The Ska complex is required for the maintenance of bi-orientation during congression

(a) Example image sequence of a sister kinetochore-pair labelled with eGFP-CENP-A congressing to the metaphase plate in a cell treated with control siRNA (left), or initiating congression toward the metaphase plate in a Ska1 depleted cell, but then rotating through 90° relative to the spindle axis, a phenomenon we have termed 'flipping' (right). Red and yellow arrows indicate the P and AP kinetochores. Red and yellow stars indicate the position of the kinetochore pair at t=0 (control) and pre-flip (Ska1 siRNA), pink stars indicate the post-flip position of the Ska1 depleted kinetochore-pair. Dotted blue line indicates the metaphase plate periphery. Scale bar 2 μm. (b) Immunofluorescence images of HeLa K cells treated with control or Ska1 siRNA and stained with DAPI and antibodies against CENP-A and Ska1. Scale bar 5μm. (c) Quantification of kinetochore Ska1 staining intensity in cells treated with either control or Ska1 siRNA. (d) Quantification of unaligned bi-oriented kinetochore-pair behaviour in eGFP-CENP-A expressing cells treated with control or Ska1 siRNA. Error bars ± SD.

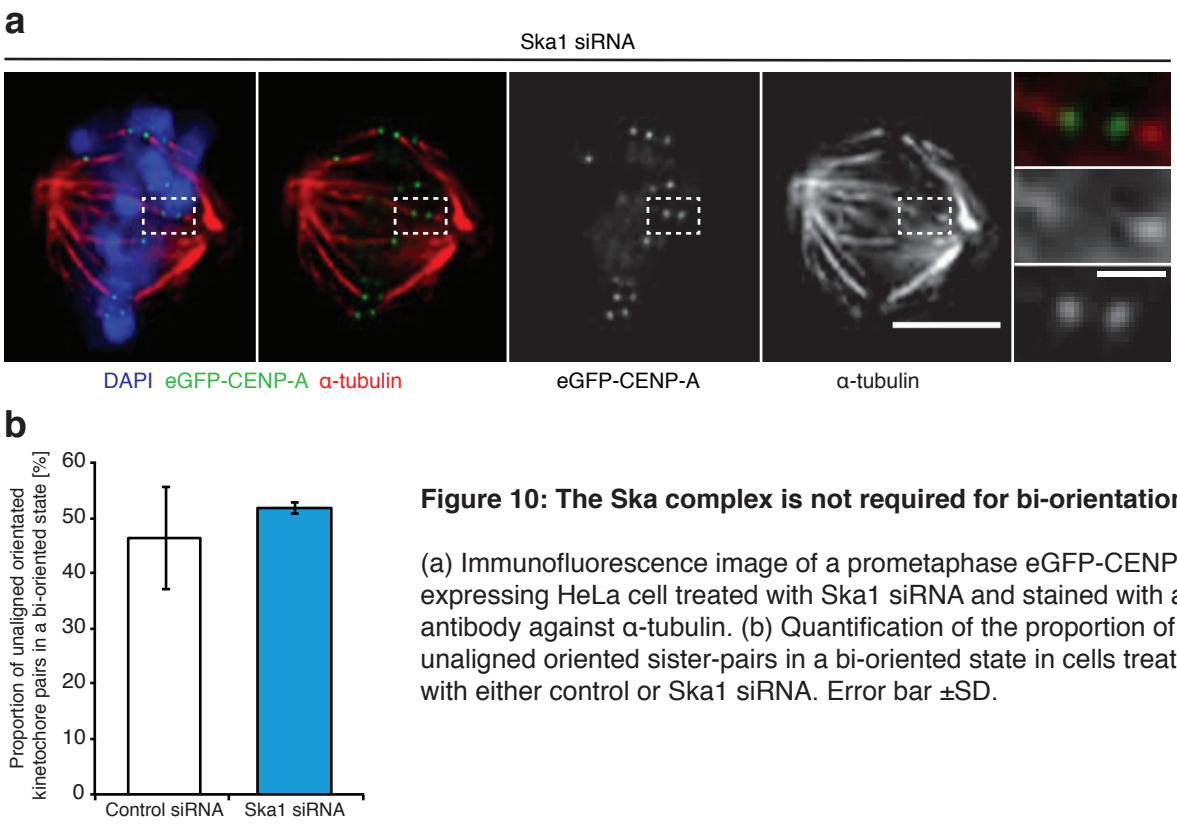

Figure 10: The Ska complex is not required for bi-orientation

(a) Immunofluorescence image of a prometaphase eGFP-CENP-A expressing HeLa cell treated with Ska1 siRNA and stained with an antibody against α-tubulin. (b) Quantification of the proportion of unaligned oriented sister-pairs in a bi-oriented state in cells treated with either control or Ska1 siRNA. Error bar ±SD.

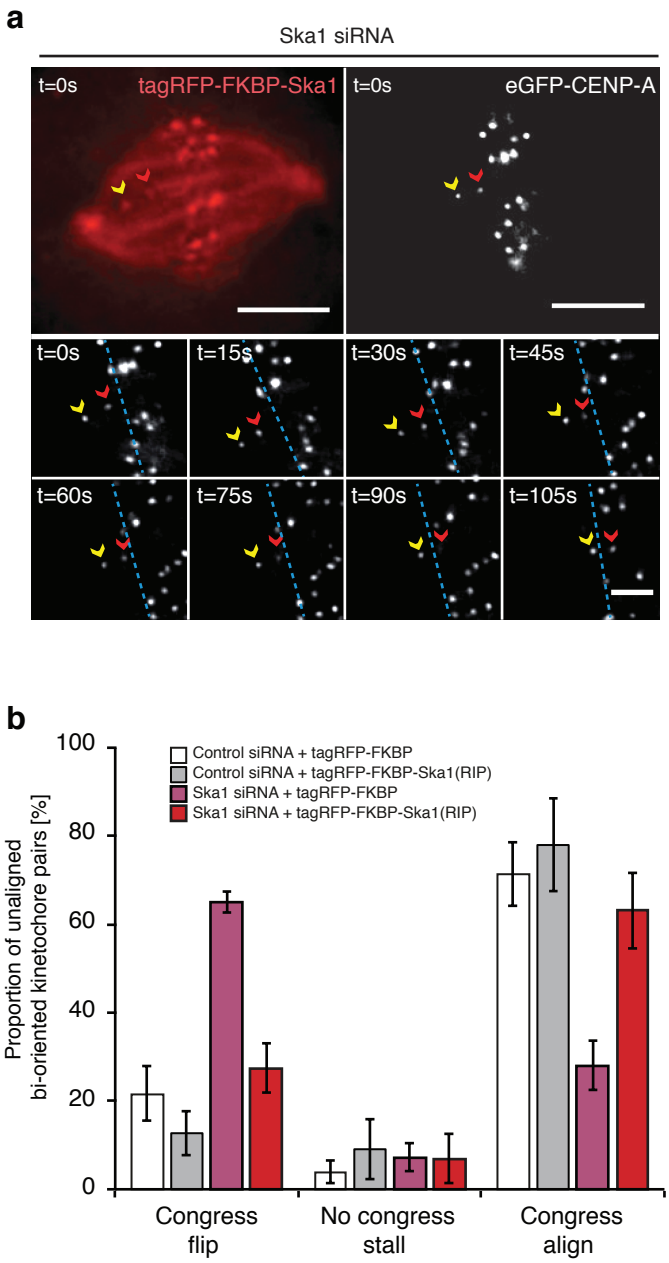

Figure 11: Rescue of the Ska1 depletion phenotype

(a) Example trajectory of a congressing bi-oriented kinetochore-pair labelled with eGFP-CENP-A in a cell depleted of Ska1 and subsequently rescued with an siRNA resistant tagRFP-FKBP-Ska1 transgene. Red and yellow arrows indicate the P and AP kinetochores respectively. Dotted blue line indicates the metaphase plate periphery. Scale bars 5 μm (top) and 1 μm (bottom).
(b) Quantification of unaligned bi-oriented kinetochore behaviour during the Ska1 siRNA rescue experiment shown in a. Error bars ±SD.

Cas9. SURVEYOR analysis confirmed that transfection with the Ska1 targeted Cas9 (Ska1 guideA) for 72hr induced an indel mutation at the desired locus (Fig 12a). Moreover, quantitative immunofluorescence revealed that ~20% of cells transfected with Ska1 guideA demonstrated a >95% reduction in Ska1 signal at kinetochores (Fig 12b-d) (n=200 kinetochore pairs from 20 cells). In agreement with our siRNA data, kinetochore flipping was augmented in CRISPR treated cells (to 41% ±5.1%, n=191 kinetochore pair from 60 cells) (Fig 12e,f). The lower rate of flipping observed in CRISPR treated cells compared to those treated with Ska1 siRNA reflects the penetrance of the two methods, as we cannot positively select for cells where Cas9 targeting was successful. Taken together, these data demonstrate that the Ska complex is required for the maintenance of bi-orientation during congression.

3.3 *Kinetochore flipping corresponds to lead sister detachment*

The rotation of a bi-oriented kinetochore pair through 90° relative to the spindle axis suggests that flipping corresponds to microtubule detachment at the sister-pair. To confirm this, we measured the eGFP-CENP-A based inter-sister distance at the two time points before and after a flip event in cells depleted of Ska1. This demonstrated a significant reduction in inter-sister distance after a flip event (from 900 nm (±195 nm) before the flip to 740nm (±190 nm), n=47 flip events from 39 cells) to a level comparable to

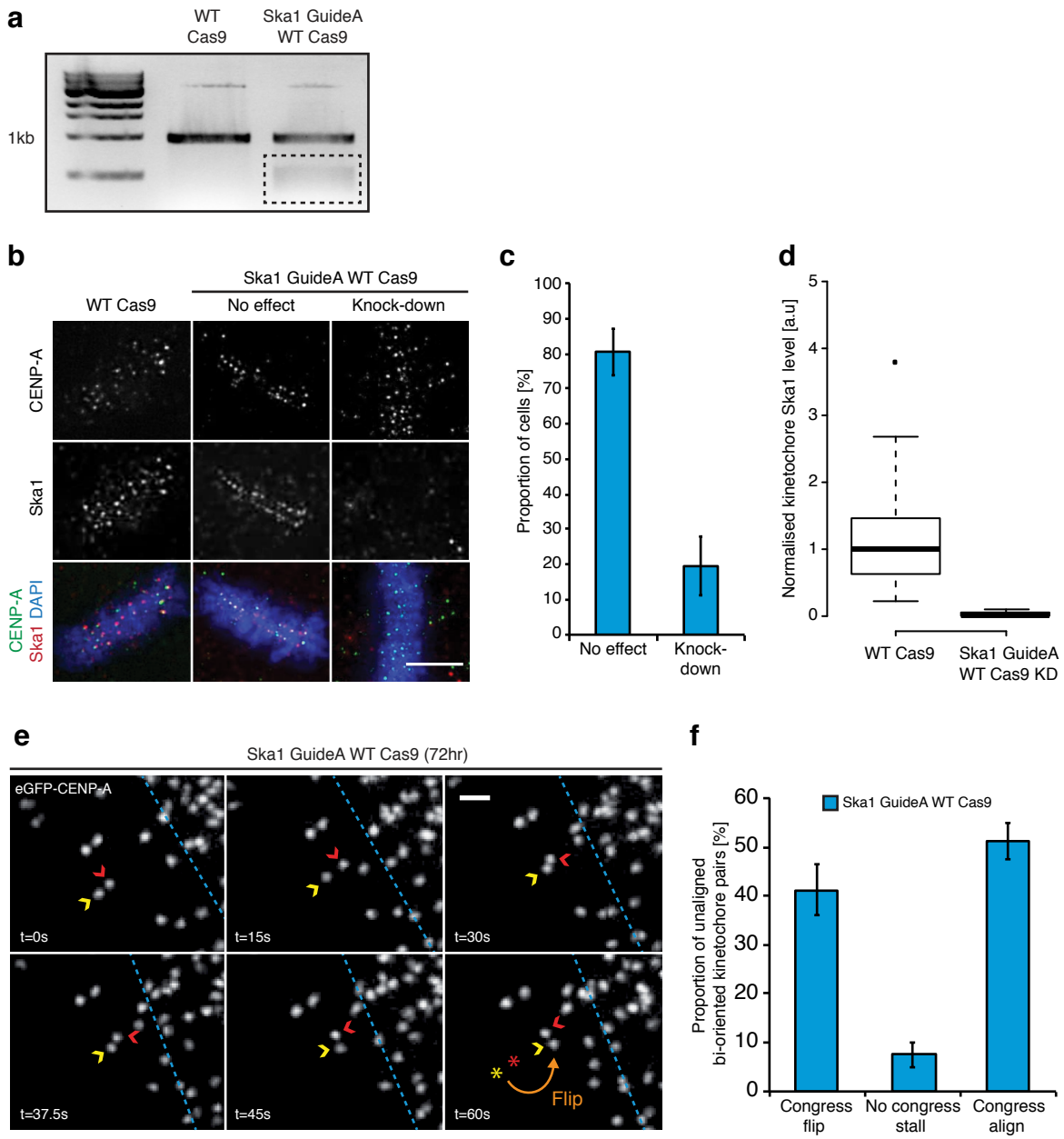

Figure 12: Validation of Ska complex function using CRSPR Cas9

(a) Inverted agarose gel image of the Ska1 SURVEYOR T7 endonuclease digest. Black box highlights the laddering pattern indicative of indel mutation at the target locus. (b) Immunofluorescence images of HeLa K cells transfected with WT Cas9 or Ska1 GuideA WT Cas9 for 72 hr and stained with antibodies against CENP-A and Ska1. In the Ska1 GuideA WT Cas9 transfected cells, we identified two clear phenotypes, (1) no change in Ska1 staining intensity at kinetochores, and (2) knock-down of Ska1. Scale bar 5μm. (c) Quantification of the proportion of cells displaying no change and knock-down of kinetochore Ska1 staining after transfection of Ska1 GuideA WT Cas9 for 72hr.
(d) Quantification of Ska1 kinetochore staining in HeLa K cells transfected with WT Cas9 or Ska1 GuideA WT Cas9 and displaying a knock-down phenotype. Intensity measurements were taken relative to CENP-A following background subtraction (e) Example trajectory of a flipping kinetochore pair labelled with eGFP-CENP-A in a cell treated with Ska1 GuideA WTCas9. Red and yellow arrows indicate the P and AP kinetochores respectively. Dotted blue line indicates the metaphase plate periphery. Scale bar 1 μm. (f) Quantification of unaligned bi-oriented kinetochore behaviour in cells treated with Ska1 GuideA WTCas9 for 72hr. Error bar ±SD.

that measured at unattached (tensionless) kinetochores in the presence of the microtubule depolymerising drug nocodazole (~700nm) (Fig 13a). Given the proposed role of the Ska complex in DCP, where force generation occurs at the P kinetochore (Auckland and McAinsh, 2015), we sought to identify if there was a P/AP bias in the flipping kinetochore. By counting which kinetochore rotated around it sister, we found that microtubule detachment occurred at the P kinetochore in ~90% of cases (Fig 13b) (n=39 flip events from 37 cells). To confirm this, we followed a congressing kinetochore-pair depleted of Ska1, and when a flip initiated, flowed in gluteraldehyde to fix the sample. As depicted in fig 13c, the P kinetochore can be seen rotated around its sister and not bound to a K-fiber, whereas the AP-kinetochore is still attached to microtubules (Fig 13c). Taken together, these data demonstrate that kinetochore flipping corresponds to microtubule detachment at the P kinetochore during congression.

3.4 *Force dependent release of the leading kinetochore*

Currently, our data suggests that the Ska complex is required to maintain lead kinetochore attachment at bi-oriented kinetochore-pair undergoing congression. However, the mechanism of detachment remains unclear. One possibility is that we are observing Aurora B mediated error correction, which acts to destabilize erroneous attachments in response to a lack of

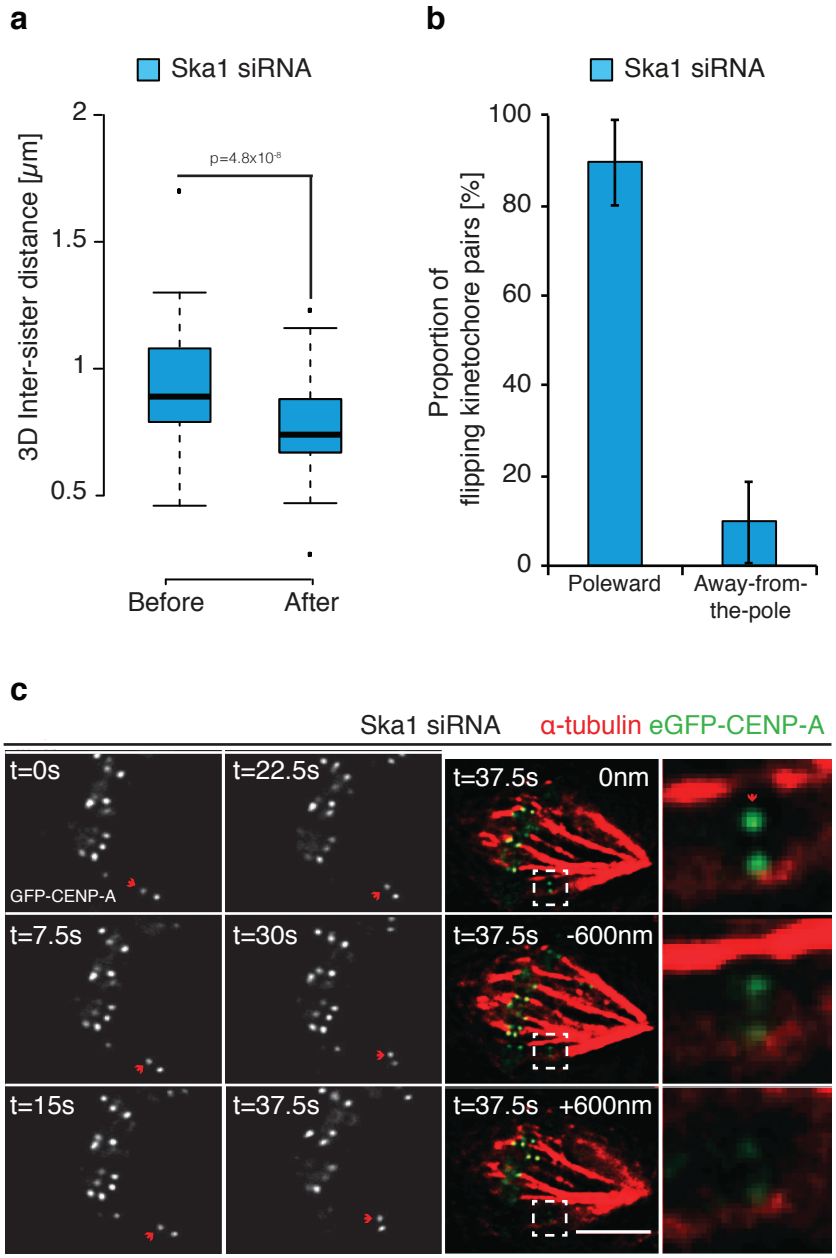

Figure 13: Kinetochore flipping coresponds to lead sister detachment

(a) Quantification of inter-kinetochore distance before and after the flip event in eGFP-CENP-A cells treated with Ska1 siRNA. Measurements were taken manually from the two time frames preceding the initiation of a flip and the two proceeding the 90°rotation. (b) The proportion of flip events that occurred at the either P or AP kinetochore in cells treated with Ska1 siRNA. The 'flipping' kinetochore was identified as the kinetochore that rotated ~90° around its roughly stationary sister. Error bars ±SD. (c) The lead sister is no longer associated with microtubules after a flip event. Cells expressing eGFP-CENP-A were depleted of Ska1 and an unaligned bi-oriented kinetochore pair was followed during a flip. Immediately after the 90° rotation was observed, the cell was fixed with gluteraldehyde and microtubules were visualised using an anti-α-tubulin antibody. Insets show a zoom of the flipped kinetochore at 0 nm, +600 nm and -600 nm. Red arrow indicates the lead (flipped) kinetochore. Scale bar 3μm.

tension (Lampson and Cheeseman, 2011). However, it has been reported that bi-oriented kinetochore-pairs irreversibly antagonise error correction due to recruitment of PP1 (DeLuca et al., 2011). Nevertheless, it is unknown whether this antagonism occurs once sister-pairs have congressed, or immediately after bi-orientation in a position-independent manner. To investigate this, quantified the phosphorylation of Ndc80 at serine 55 at bi-oriented sister-pairs that were either in an aligned or unaligned state. We found no difference in Ndc80pS55 levels between these two sister-pair subgroups (Fig 14a,b) (n = 256 aligned kinetochore pairs and 135 unaligned bi-oriented kinetochore pairs from 26 cells). Importantly, unlike their phospho-state, the rate of kinetochore flipping in control cells is not equal between these two groups. Instead, flipping is restricted to bi-oriented sister-pairs undergoing congression, a finding which suggests that an alternate mechanism underpins this process.
We did attempt to directly test the involvement of Aurora B by treating prometaphase cells with the inhibitor ZM1 (Ditchfield et al., 2003). However, this caused unaligned bi-oriented kinetochore pairs to stall, and as we have only observed flipping at chromosomes undergoing active congression this result is uninformative, other than implicating Aurora B activity in a force generation step (Fig 14c,d) (n=123 kinetochore pairs from 29 cells).

An alternative idea is that flipping results from the force dependent detachment of microtubules at the leading kinetochore. To test this, we

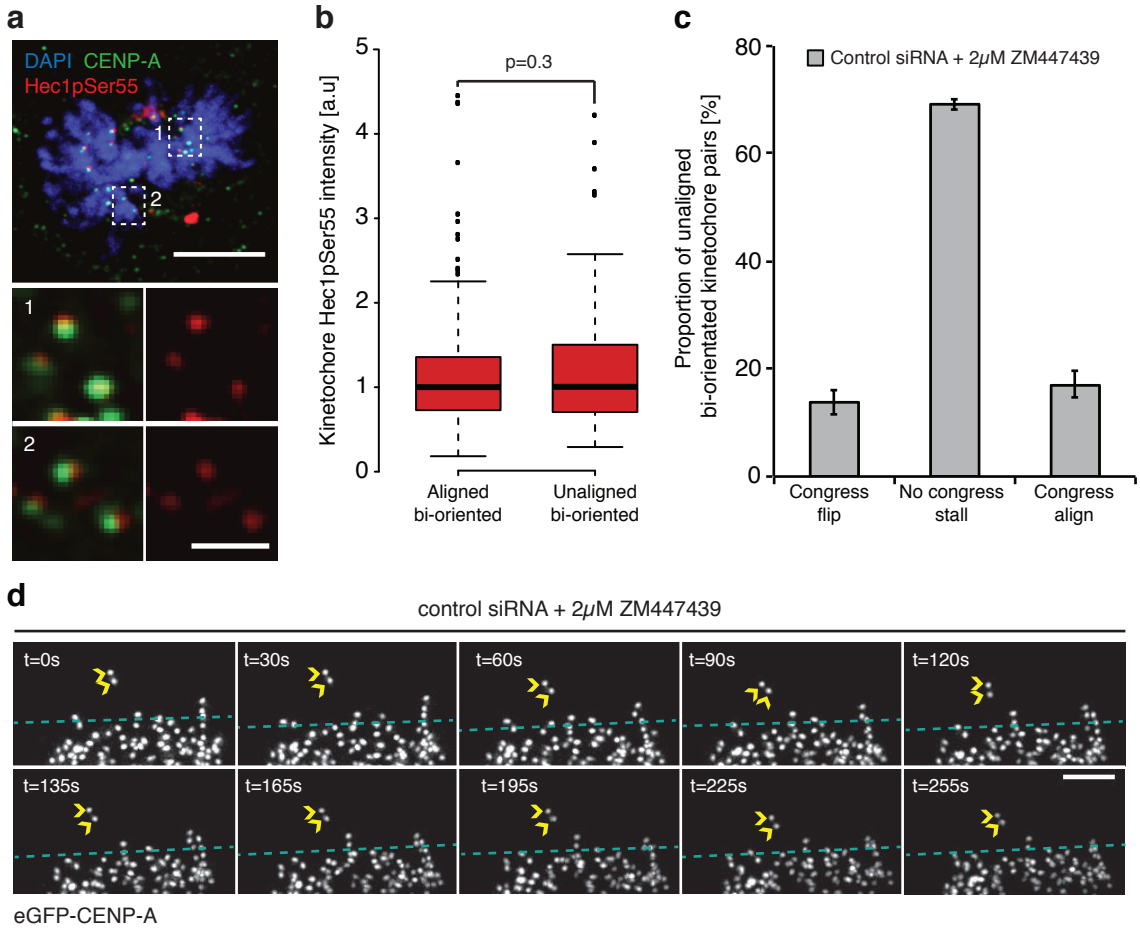

Figure 14: Testing the involvement of error correction in flipping

(a) Immunofluorescence image of a late prometaphase HeLa K cell stained with DAPI and antibodies against CENP-A and Hec1pSer55. Zoom boxes depict the staining intensities at aligned (1) and unaligned (2) bi-oriented kinetochore pairs respectively. In both cases the dual CENP-A and Hec1pSer55 signals (left) and individual Hec1pSer55 signal (right) are shown. Scale bar 5 μm. (b) Quantification of Hec1pSer55 staining at aligned bi-oriented and unaligned bi-oriented kinetochore pairs, respectively, in late prometaphase HeLa K cells relative to CENP-A after background subtraction. (c) Quantification of unaligned bi-oriented kinetochore behaviour in eGFP-CENP-A expressing cells treated with control siRNA and 2 μM ZM447439. Errors bars ± SD.(d) Example trajectory of a stalled kinetochore pair labelled with eGFP-CENP-A in a cell treated with control siRNA and 2 μM ZM447439. Blue line indicates the metaphase plate periphery. Scale bar 3 μm.

depleted the microtubule depolymerase kinesin-13 MCAK (Hunter et al., 2003), which reduces the velocity of oscillating metaphase kinetochores by altering the balance of microtubule polymerisation between the AP and P attached K-fibers (Armond et al., 2015; Jaqaman et al., 2010). Therefore in MCAK depleted cells, the P-kinetochore attached K-fiber is more likely to contain polymerising microtubules, which in turn reduces the depolymerising pool available for force generation. Quantitative immunofluorescence revealed that both proteins were efficiently depleted, reducing the centromeric/kinetochore signal by >95% (Fig 15a-d) (n=200 kinetochores from 20 cells per condition). Consistent with pervious reports of metaphase kinetochores (Jaqaman et al., 2010), MCAK depletion slowed the velocity of congressing kinetochores from 2.93 ± 1.2μm min^{-1} in control cells to 1.95 ± 0.8μm min^{-1} in MCAK depleted cells (Fig 15e) (n = at least 76 kinetochore pairs from 42 cells). We then compared the number of flip events in Ska1 and Ska1+MCAK double depleted cells, and found that MCAK co-depletion with Ska1 rescued the number of flip events from 63.1% (±2.7% n = 218 kinetochore pairs from 43 cells) to 38.3% (±5.6% n = 215 kinetochores from 76 cells), allowing more chromosomes to successfully congress (Fig 15f). Interpretation of this result is potentially confounded by the proposed role of MCAK in Aurora B mediated error correction (Lan et al., 2004). To address this, we treated with Ska1 depleted cells with 100nM taxol, which stabilises microtubules and reduces inter-sister tension (DeLuca et al., 2011). In agreement with our MCAK

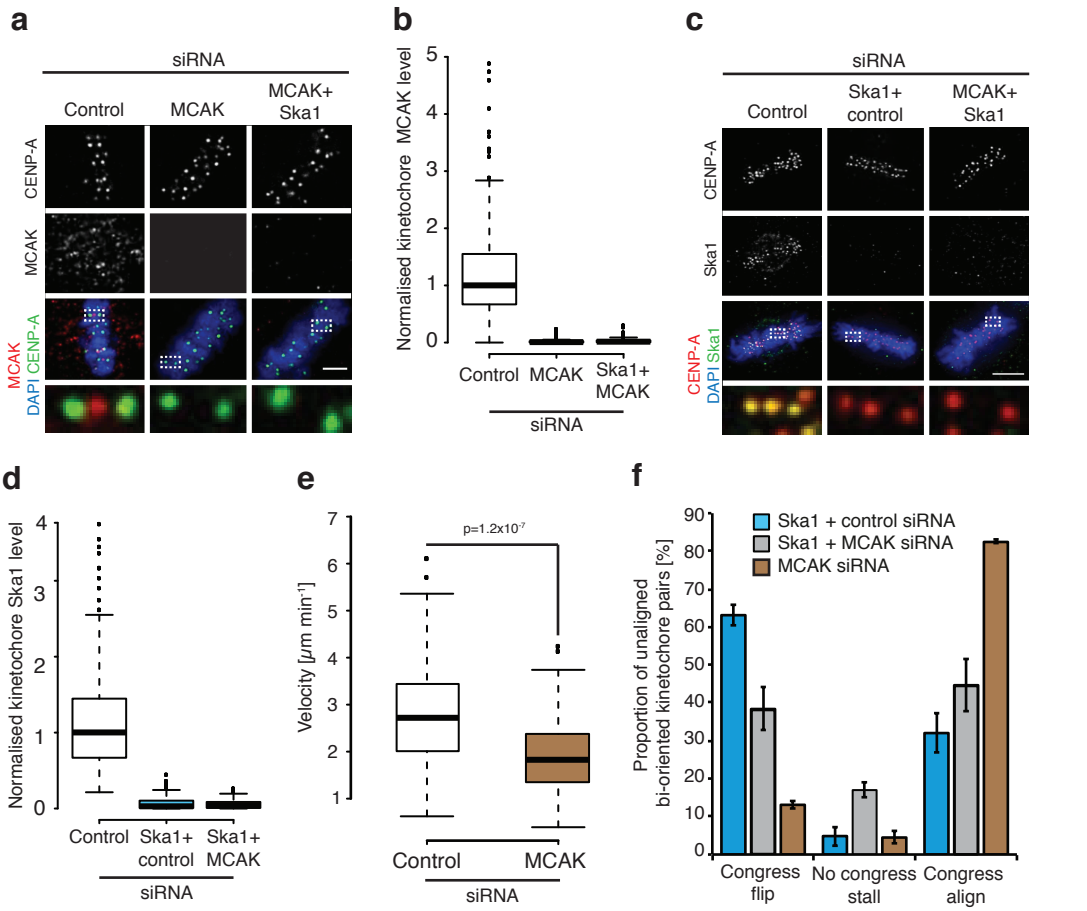

Figure 15: Force dependent release of the leading kinetochore

(a) Immunofluorescence images of a HeLa K cell treated with either control, MCAK or Ska1 + MCAK siRNA and stained with antibodies against CENP-A and MCAK. Zoom boxes depict the staining at individual kinetochores. Scale bar 5 μm. (b) Quantification of MCAK intensities in cells treated with control, MCAK or Ska1+MCAK siRNA. Intensity measurements were taken relative to CENP-A following background subtraction. (c) Left, immunofluorescence images of HeLa-K cells treated with either control, Ska1 + control or MCAK siRNA and stained with antibodies against CENP-A and Ska1. Insets show individual kinetochores. Scale bar 5μm. (d) Quantification of Ska1 staining intensities in cells treated with control, Ska1 + control or Ska1+MCAK siRNA. Intensity measurements were taken relative to CENP-A following background subtraction.(e) Quantification of kinetochore velocity during congression in eGFP-CENP-A expressing cells treated with control or MCAK siRNA. Measurements were taken from tracks of persistent movement that lasted at least three time frames. (f) Quantification of unaligned bi-oriented kinetochore behaviour in eGFP-CENP-A expressing cells treated with Ska1+control, MCAK or Ska1+MCAK siRNA. Error bars ±SD. (g) Quantification of unaligned bi-oriented kinetochore behaviour in cells depleted of Ska1 by siRNA and treated with DMSO or 100 nM taxol for 1 hr. Error bars ±SD.

data, treatment with taxol reduced the rate of flipping to 41.7% (±1.55% n = 127 kinetochore pairs from 38 cells), again allowing more chromosomes to successfully congress (Fig 15g). Thus, we favor a model where excess pulling force exerted on the P kinetochore microtubule attachment lead to its failure, causing the kinetochore pair to flip away from the spindle axis.

3.5 *Congression is coupled to an increase in microtubule occupancy at kinetochores*

We suspected that the increase in load on the P kinetochore may be related to the observation that metaphase kinetochores are bound to more microtubules that those in prometaphase (McEwen, 1997). However, this experiment did not rule out that differences were due to cell cycle effects. What is needed is a comparison of unaligned and congressed kinetochores in the same cell. To do this, we used our SBF-SEM images to quantify the number of microtubules terminating at bi-oriented kinetochore-pairs. We note that the resolution limit of SEM means that the observed microtubule fibres may reflect both single microtubules and small bundles. Hence, this assay reads out microtubule density rather than absolute microtubule number. We found a ~50% increase in microtubule density at aligned bi-oriented sister-pairs when compared to those that had not yet congressed (Fig 16a,b). To substantiate this finding we analysed prometaphase HeLa cells fixed using gluteraldehyde and stained with an α-tubulin antibody. This showed that the tubulin signal increased by ~27% at aligned bi-oriented sister-pairs (Fig 17a,b). A relationship that remains in Ska1

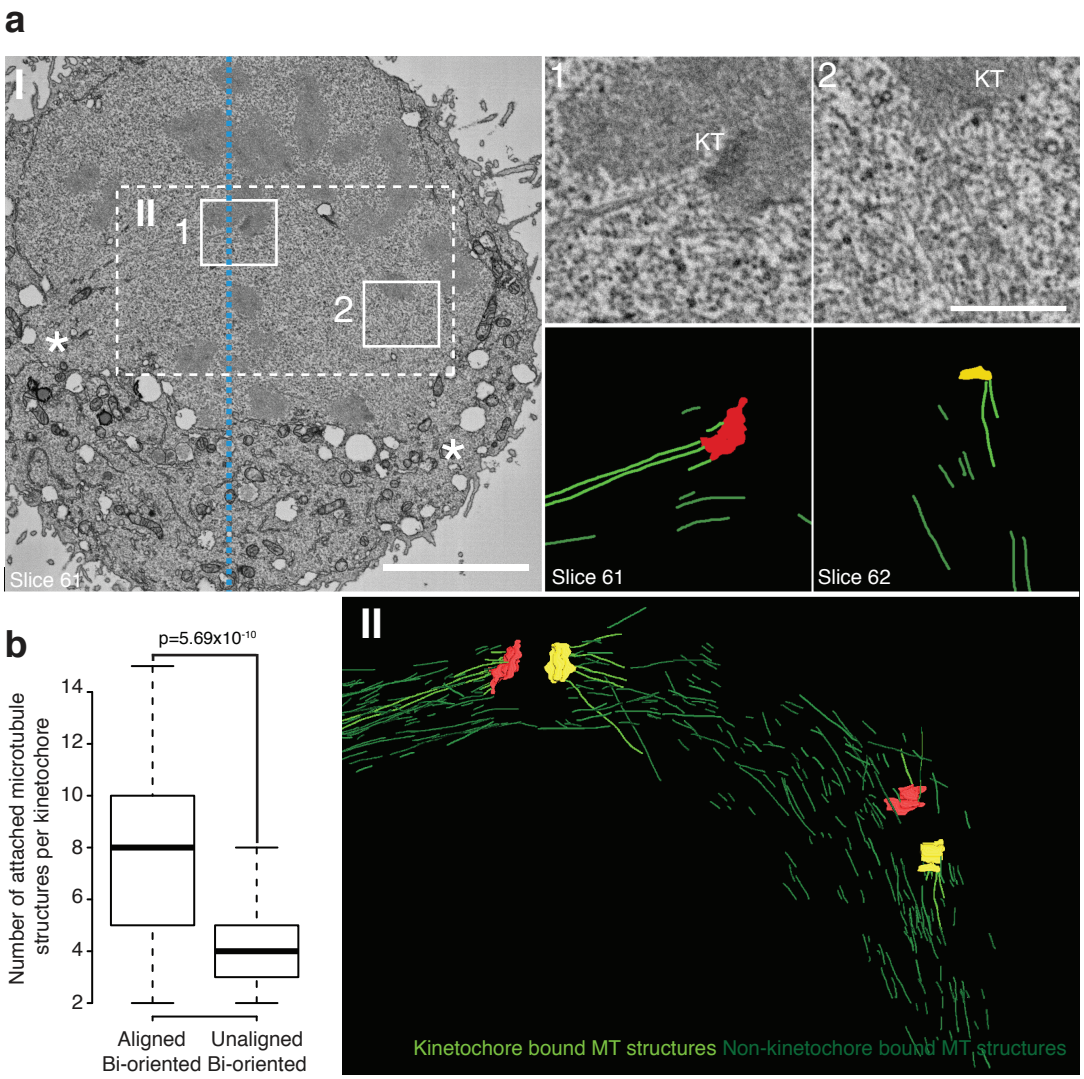

Figure 16: Congression is coupled to an increase in microtubule occupancy at kinetochores – EM analysis

(a) (I) Single slice from an SBF-SEM image of a prometaphase HeLa cell, boxes show aligned bi-oriented (1) an unaligned bi-oriented (2) kinetochore pairs. Zoom boxes display single slices and their associated segmentation. Kinetochore attached, and non-kinetochore attached microtubule structures are show in light green and dark green, respectively. Dotted blue line indicates the metaphase plate centre. White asterisks show the spindle pole positions. Scale bar 5 μm (left) 1μm (right) (II) Top, box depicting the spindle region used to render microtubule attachment at the sister-pairs indicated in (1) and (2). Bottom, z-projection (slices 56-65) of the kinetochore and microtubule model generated from the cell in (I). Kinetochore attached, and non-kinetochore attached microtubule structures are indicated in light green and dark green, respectively. (b) Quantification microtubule structures terminating at kinetochores in either aligned bi-oriented or unaligned bi-oriented state by SBF-SEM, n=100 aligned KT and 20 unaligned KT from 3 cells, p-value calculated using a two-sample t-test

Figure 17

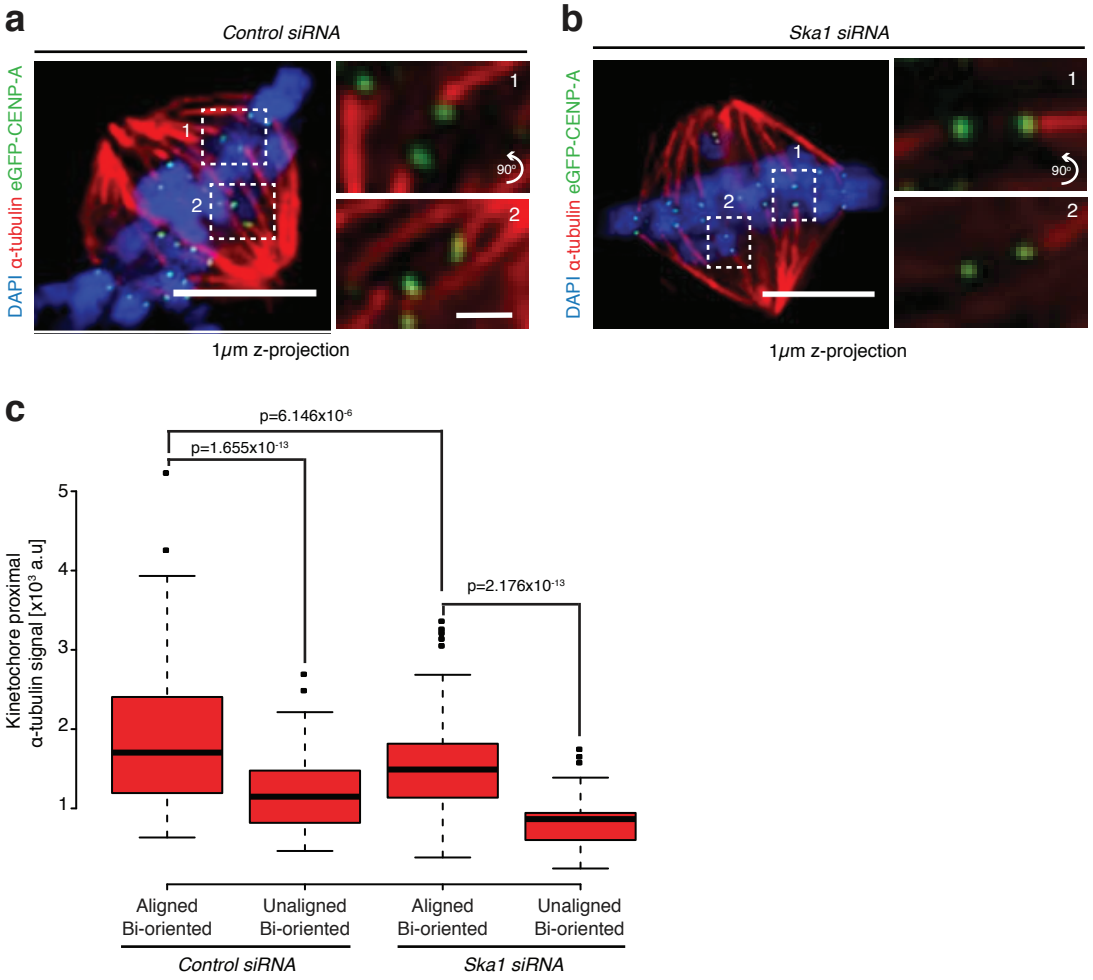

Figure 17: Congression is coupled to an increase in microtubule occupancy at kinetochores – IF analysis

Image of a prometaphase eGFP-CENP-A cell treated with control (a) or Ska1 (b) siRNA and stained with DAPI and anti-α-tubulin. Zoom boxes depict the staining intensities at aligned bi-oriented (1) and unaligned bi-oriented (2) kinetochore pairs, respectively. Scale bar 5μm (top) 1μm (bottom). (c) Quantification of kinetochore proximal α-tubulin signal at aligned bi-oriented an unaligned b-oriented kinetochore pairs in cells treated with either control or Ska1 siRNA, n (control) = 199 aligned KT and 75 unaligned KT from 20 cells, n (Ska1) = 152 aligned KT and 38 unaligned KT from 16 cells, p-value calculated using a two-sample t-test.

depleted cells (Fig 17a,b). We do note that depletion of Ska reduces the number of microtubules bound to the kinetochore, a finding that is consistent with previous work (Chan et al., 2012; Gaitanos et al., 2009; Raaijmakers et al., 2009). Together, these data demonstrate that kinetochores are recruiting additional microtubules in a Ska complex independent manner during congression.

3.6 *The fate of flipped kinetochore pairs*

During the initial analysis of the Ska complexes role in congression, we found that control siRNA treated cells have a ~20% baseline rate of flipping (Fig 9d), a finding that is consistent with observations in unperturbed HeLa cells expressing eGFP-CENP-A (Fig 18a) (flip rate of 22.3% ± 3.3%, n=134 kinetochore pairs from 43 cells). Importantly, kinetochore flipping can be detected in unperturbed RPE1 cells expressing eGFP-CENP-A (Fig 19a,b), however, due to the accelerated rate of congression its observation is less frequent.

In control siRNA treated HeLa cells, the flipping behavior is identical to that in Ska1 depleted cells, where the lead kinetochore detaches from its associated K-fiber, leading to a reduction in inter-sister separation (Fig 18b,c). Importantly however, the fate of flipping kinetochore pairs is distinct in Ska1 depleted and control cells. In Ska1 depleted cells, kinetochores flip, reattach to spindle microtubules and re-orient along the spindle axis.

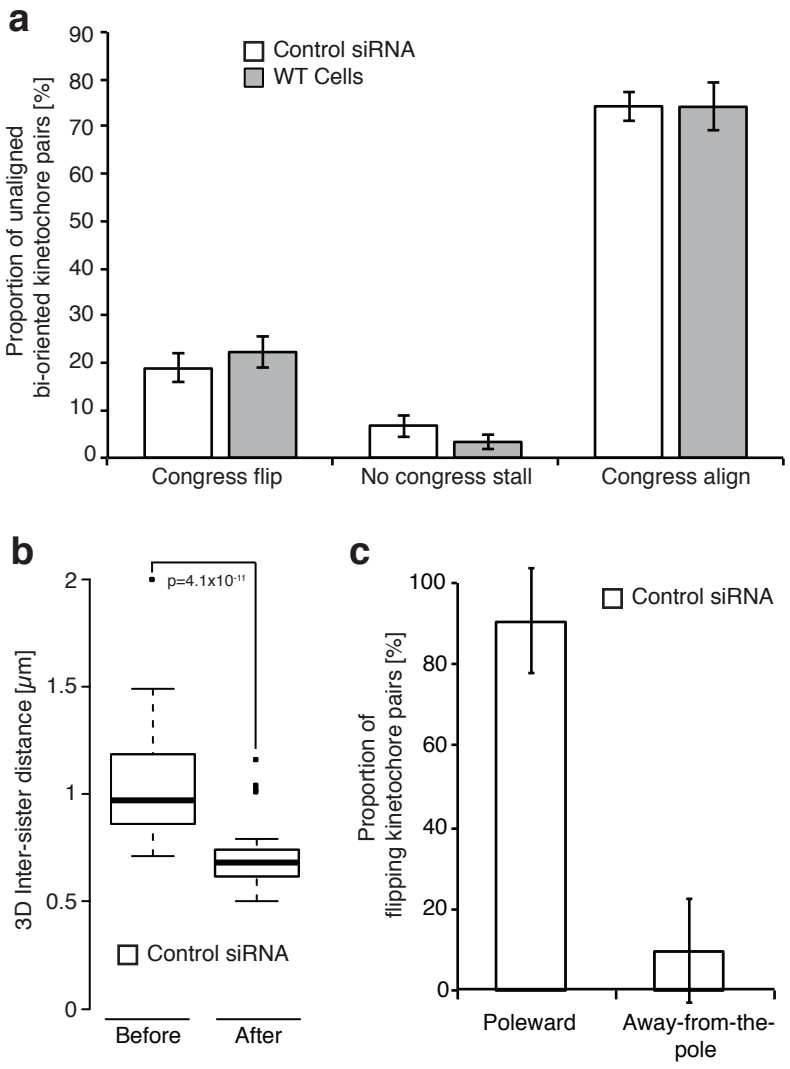

Figure 18: Flipping in unperturbed HeLa cells

(a) Quantification of unaligned bi-oriented kinetochore behaviour in wild type eGFP-CENP-A expressing and those treated control siRNA. Error bars ±SD. (b) Quantification of inter-kinetochore distance before and after the flip event in eGFP-CENP-A cells treated with control siRNA. Measurements were taken manually from the two time frames preceding the initiation of a flip and the two proceeding the 90° rotation. (c) The proportion of flip events that occurred at the either P or AP kinetochore in cells treated with control siRNA. The 'flipping' kinetochore was identified as the kinetochore that rotated ~90° around its roughly stationary sister. Error bars ±SD.

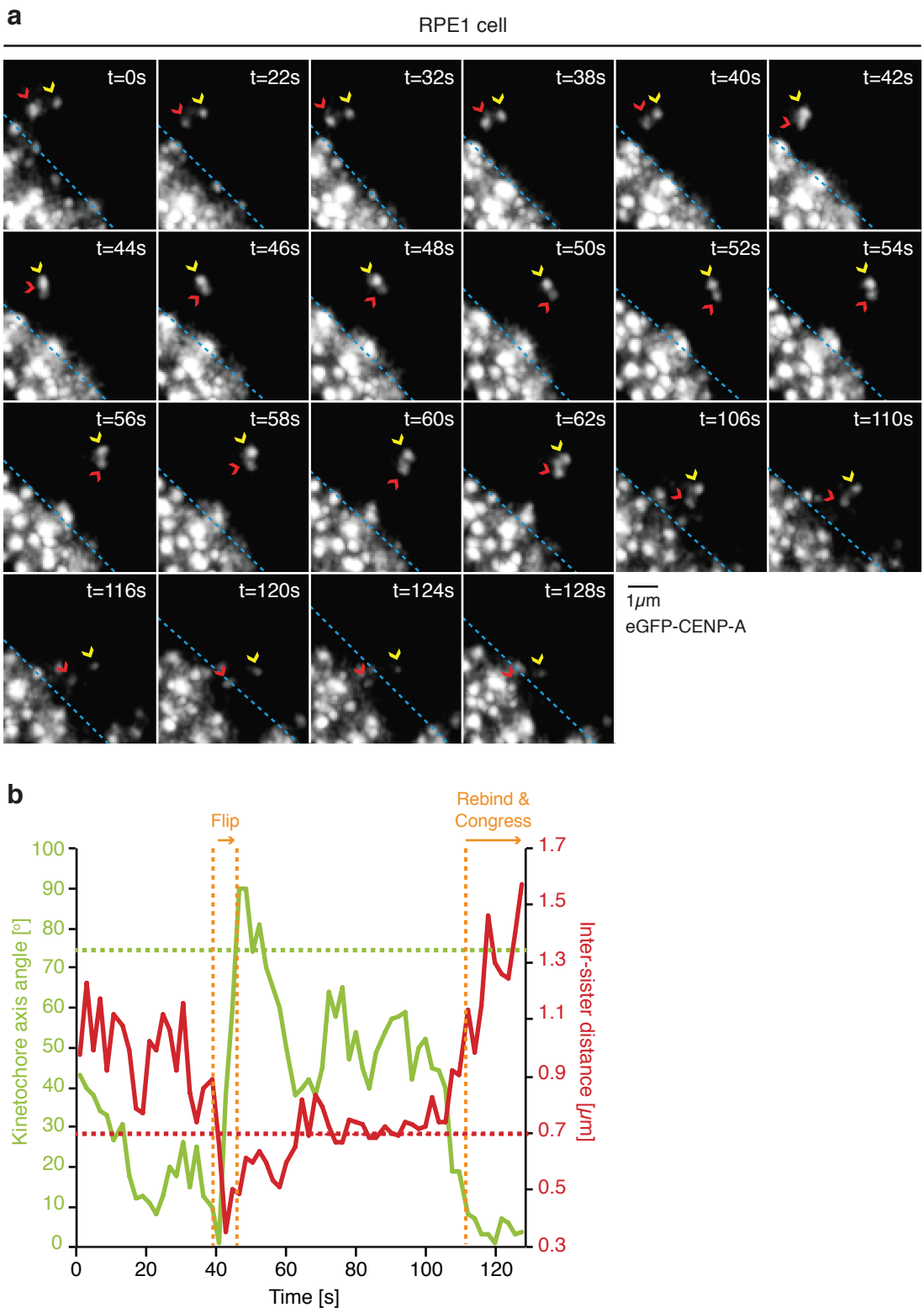

Figure 19: Flipping in an unperturbed RPE1 cell

(a) Example trajectory of a flipping kinetochore pair in an RPE1 cell expressing eGFP-CENP-A. Red and yellow arrows indicate the P and AP kinetochores, respectively. Blue dotted line indicates the metaphase plate periphery. Scale bar 1μm.(b) Plot of K-K axis angle and inter-sister distance (see Fig 16 for description of measurement) during a flip event followed by successful congression in the unperturbed RPE1 cell shown in (a). Dotted green line indicates a kinetochore axis angle of 75°. Dotted red line indicates the inter-sister distance in absence of microtubules (i.e. the rest length).

However, 42% (±6.4%, n=78 flip events from 55 cells) of these flipped kinetochore-pairs undergo a second flip event, and 91% (±8.7% n=78 flip events from 55 cells) of all flipped kinetochore-pairs fail to reach the spindle equator during the 5min movie (Fig 20a,c,d). This sequential flipping can be visualized by plotting the inter-sister distance and kinetochore-axis (K-K axis) angle of the sister-pair. Here, we observed a significant drop in inter-sister distance (indicative of detachment) that corresponded with a sharp increase in K-K axis angle during both flip events (Fig 20a,e,f). Importantly, this was preceded by a period of low K-K angle and inter-sister breathing about 1μm, demonstrating that the sister-pair was bi-oriented prior to the first flip, and reformed this attachment before the second flip. In contrast, only 15% (±6.2%, n=28 flip events from 27 cells) of flipped kinetochore-pairs in control cells undergo a second flip, and 61% (±1.7%, n=28 flip events from 27 cells) of flip events are followed by reattachment and successful congression (Fig 20b-e,g). Similarly, the flip event we observed in an RPE1 cell was followed reattachment and successful congression (Fig 19a,b). Given that we have only visualized a 5min snapshot of prometaphase (chosen to limit photodamage), it is likely that all flipped kinetochore-pairs in control cells reach the spindle equator. This is supported by 12hr time-lapse movies of HeLa cells expressing histone-2B-GFP, where 100% (n = 289 cells) of chromosomes in control cells congress by 24min, compared with 50% in Ska1 depleted cells (Fig 21a,b) (n = 149 cells). The resolution of attachment and subsequent congression post-flip in

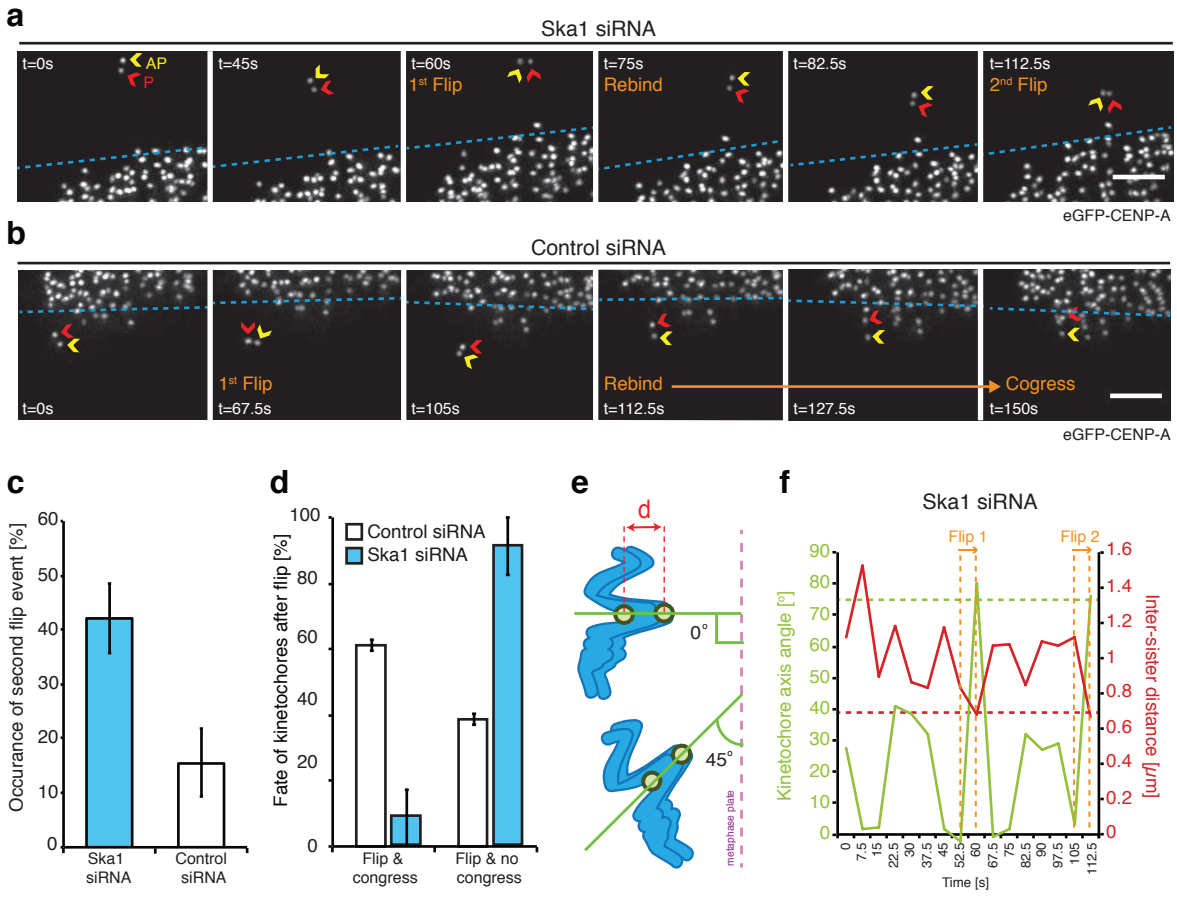

Figure 20: The fates of flipping kinetochore pairs

(a) Example trajectory of a Ska1 depleted kinetochore pair undergoing two sequential flip events (t=60 s & t=1 12.5 s) interspersed by a period of reorientation (t=75 s – t=82.5 s). Red and yellow arrows indicate the P and AP kinetochores respectively. Dotted blue line indicates the metaphase plate periphery. Scale bar 2 μm. (b) Example trajectory of a kinetochore pair undergoing a flip event followed by reorientation and successful congression in a cell treated with control siRNA. Red and yellow arrows indicate the P and AP kinetochores respectively. Dotted blue line indicates the metaphase plate periphery. Scale bar 2μm. (c) The proportion of flipped kinetochore pairs that undergo a second flip event in cells treated with control or Ska1 siRNA. Error bar ±SD. (d) Quantification of kinetochore pair fate after a flip event in cells treated with control or Ska1 siRNA. Error bar ±SD. (e) Schematic illustrating the measurement of kinetochore (K-K) axis angle relative to metaphase plate. The K-K axis angle has been normalised so that a perpendicular orientation to the metaphase plate is equal to 0. After a flip, when the kinetochore axis is parallel to the metaphase plate, the K-K angle is 90°. d indicates the inter-sister distance. (f) Plot of K-K axis angle and inter-sister distance during two sequential flip events in the Ska1 depleted kinetochore pair shown in panel (a). During both flip events, the K-K axis-angle can be observed to rotate ~90° while the inter-sister distance simultaneously drops to ~0.65μm, consistent with a loss of microtubule attachment. (g) Plot of K-K axis angle and inter-sister distance during a flip event followed by successful congression in the control siRNA treated kinetochore pair shown in panel (b). Dotted green line indicates a kinetochore axis angle of 75°. Dotted red line indicates the inter-sister distance in absence of microtubules.

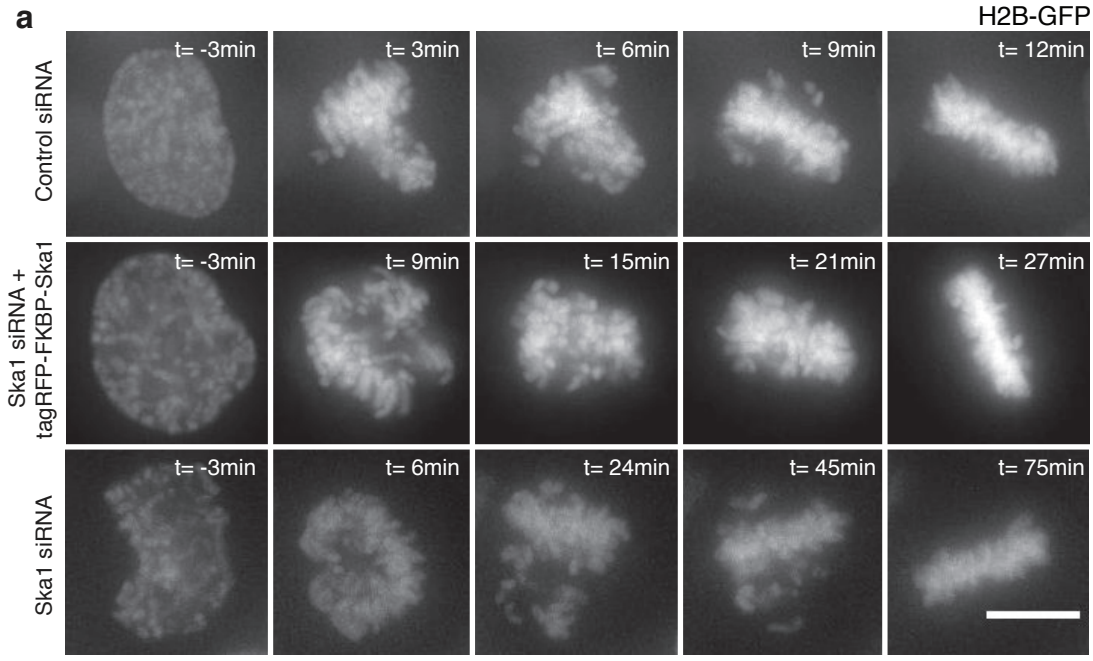

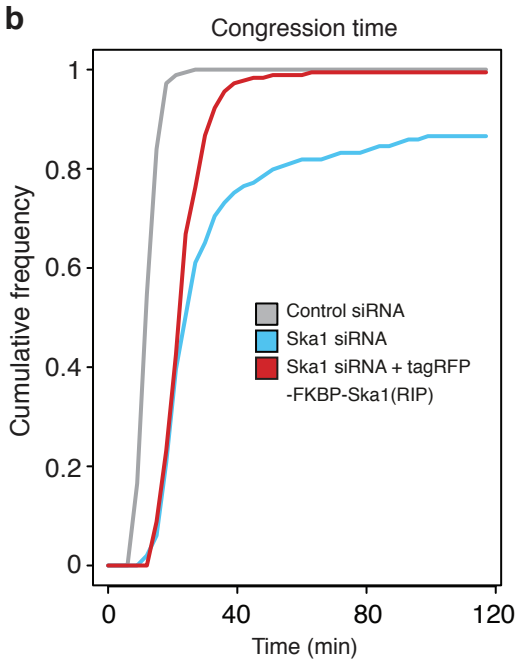

Figure 21: Congression timing in Ska1 depleted cells

(a) Example prometaphase trajectories of cells expressing histone-2B-GFP and treated with control siRNA, Ska1 siRNA or Ska1 siRNA and rescued with an siRNA protected tagRFP-FKBP-Ska1 transgene. Scale bar 20 μm. (b) Quantification of NEB -metaphase (congression) time for histone -2B-GFP expressing cells treated with control siRNA, Ska1 siRNA or Ska1 siRNA and rescued with an siRNA protected tagRFP-FKBP-Ska1 transgene.

control cells highlights two key points, (1) flipping does not represent a subset of defective kinetochores, and (2) flipping is a normal feature of mitosis in unperturbed human cells.

3.7 *Dynamic maturation of the Ska complex during congression*

Our data currently supports a model in which the Ska complex is required to limit the number of force dependent P-kinetochore detachment events during congression. From our immunostaining experiments, we noticed that the Ska1 staining intensity appeared to be lower at unaligned bi-oriented kinetochore-pairs when compared to those aligned at the spindle equator (Fig 22a,b) (n= at least 157 kinetochore from 37 cells per condition), a finding we confirmed in cells expressing a tagRFP-FKBP-Ska1 transgene (Fig 22c,d) (n= at least 53 kinetochores from 15 cells per condition). This raised the possibility that bi-oriented kinetochores progressively recruit the Ska complex as they congress. To test this, we took a single image of an unaligned bi-oriented kinetochore-pair in a cell expressing 2×tagRFP-Ska1, allowed it to congress to the spindle equator, and imaged the same kinetochore-pair once more. During this alignment, we found that the Ska complex intensity (relative to eGFP-CENP-A) increased by 178% (Fig 23a,b) (n=12 kinetochores from 10 cells). To confirm the calculated increase in 2×tagRFP-Ska1 intensity was not due to changes in eGFP-CENP-A levels during congression, we plotted the signal intensities for

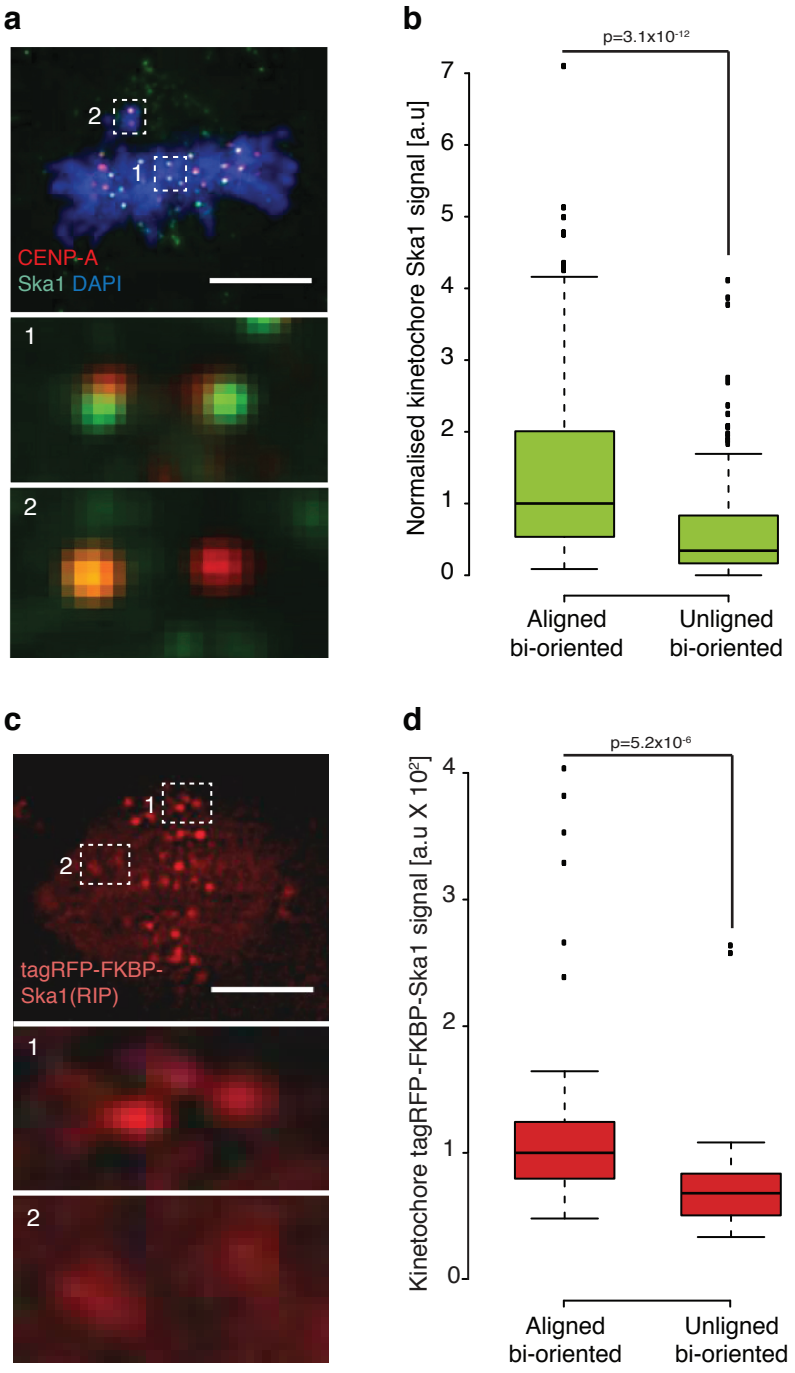

Figure 22: Ska1 is enriched at aligned bi-oriented kinetochores

(a) Immunofluorescence image of a prometaphase HeLa K cell stained with DAPI and antibodies against CENP-A (red) and Ska1 (green). Zoom boxes depict the staining intensities at aligned (1) and unaligned (2) bi-oriented kinetochore pairs respectively. Scale bar 5μm. (b) Quantification of Ska1 staining intensity at aligned and unaligned bi-oriented kinetochore pairs relative to CENP-A after background subtraction. (c) Image of a prometaphase eGFP-CENP-A expressing cell transfected with tagRFP-FKBP-Ska1, with only the transgene signal shown. Zoom boxes depict the staining intensities at aligned (1) and unaligned (2) bi-oriented kinetochore pairs respectively. Scale bar 5μm. (d) Quantification of tagRFP-FKBP-Ska1 intensities at aligned and unaligned bi-oriented kinetochore pairs after background subtraction

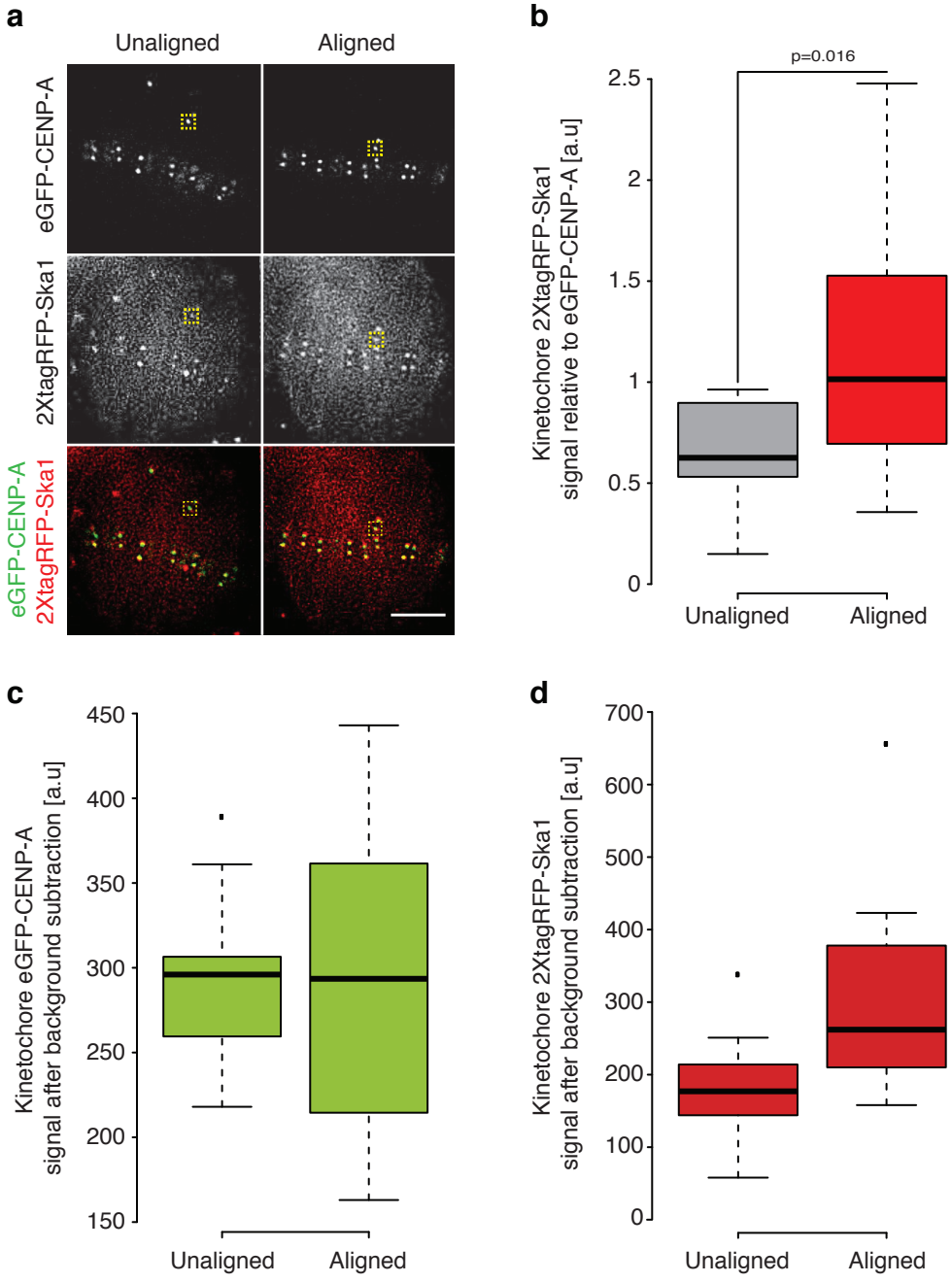

Figure 23: Ska1 matures at bi-oriented kinetochore-pairs as they congress

(a) Left: Image of a late prometaphase HeLa cell with a single unaligned kinetochore pair expressing eGFP-CENP-A and transfected with 2×tagRFP-Ska1. Right: Image of the same cell after the kinetochore pair has aligned at the spindle equator. Scale bar 5μm. (b) Quantification of 2×tagRFP-Ska1 intensity at the same kinetochores when in an unaligned state and after alignment at the spindle equator. Measurements were taken relative to eGFP-CENP-A after background subtraction. (c) Quantification of kinetochore eGFP-CENP-A signal after background subtraction at the kinetochores followed for live cell Ska1 loading shown pannel a. This demonstrates that changes in CENP-A signal cannot account for the calculated increase in 2XtagRFP-Ska1 intensity.
(d) Quantification of kinetochore 2xtagRFP-Ska1 signal after background subtraction at the kinetochores followed for live cell Ska1 loading shown pannel a. This demonstrates that an increase in tagRFP signal is responsible for the calculated increase in Ska1 at kinetochores as they congress.

each channel at the unaligned and aligned populations. In agreement with Ska1 loading, the tagRFP signal can be seen to increase while the eGFP signal remains roughly constant (Fig 23c,d) (n=12 kinetochores from 10 cells per condition). Thus, congressing bi-oriented kinetochore-pairs progressively load the Ska complex as they approach the spindle equator. These additional complexes may be 'swept-up' from the microtubule pool as the kinetochore tracks the shrinking K-fiber. In this regard, deletion of the Ska1 microtubule binding domain (Ska1ΔMTBD), which specifically prevents its recruitment to the spindle, reduces the kinetochore bound pool (relative to eGFP-CENP-A) at aligned sister-pairs by ~70% (n=173 kinetochores from 30 cells expressing Ska1ΔMTBD and 134 kinetochores from 25 cells expressing Ska1WT), a level comparable to that measured when microtubules are depolymerized with nocodazole (Fig 24a-g) (n=300 kinetochores from 30 cells per condition). The residual kinetochore-bound pool of Ska complex is probably loaded through the previously reported Ndc80 loop-Ska interaction (Zhang et al., 2012).

This raised the possibility that Ska complex maturation is coupled to the recruitment of microtubules. Ideally, we would have correlated Ska complex and α-tubulin intensities at single kinetochores in different spindle positions. However, our Ska1 antibody was ineffective with gluteraldehyde fixation, and the noise from non-K-fibre microtubules confounds quantification in cells fixed with paraformaldehyde. To overcome this, we used cold treatment to remove non-kinetochore microtubules, fixed the cells using paraformaldehyde, and then quantified the Ska1 and α-tubulin signals at

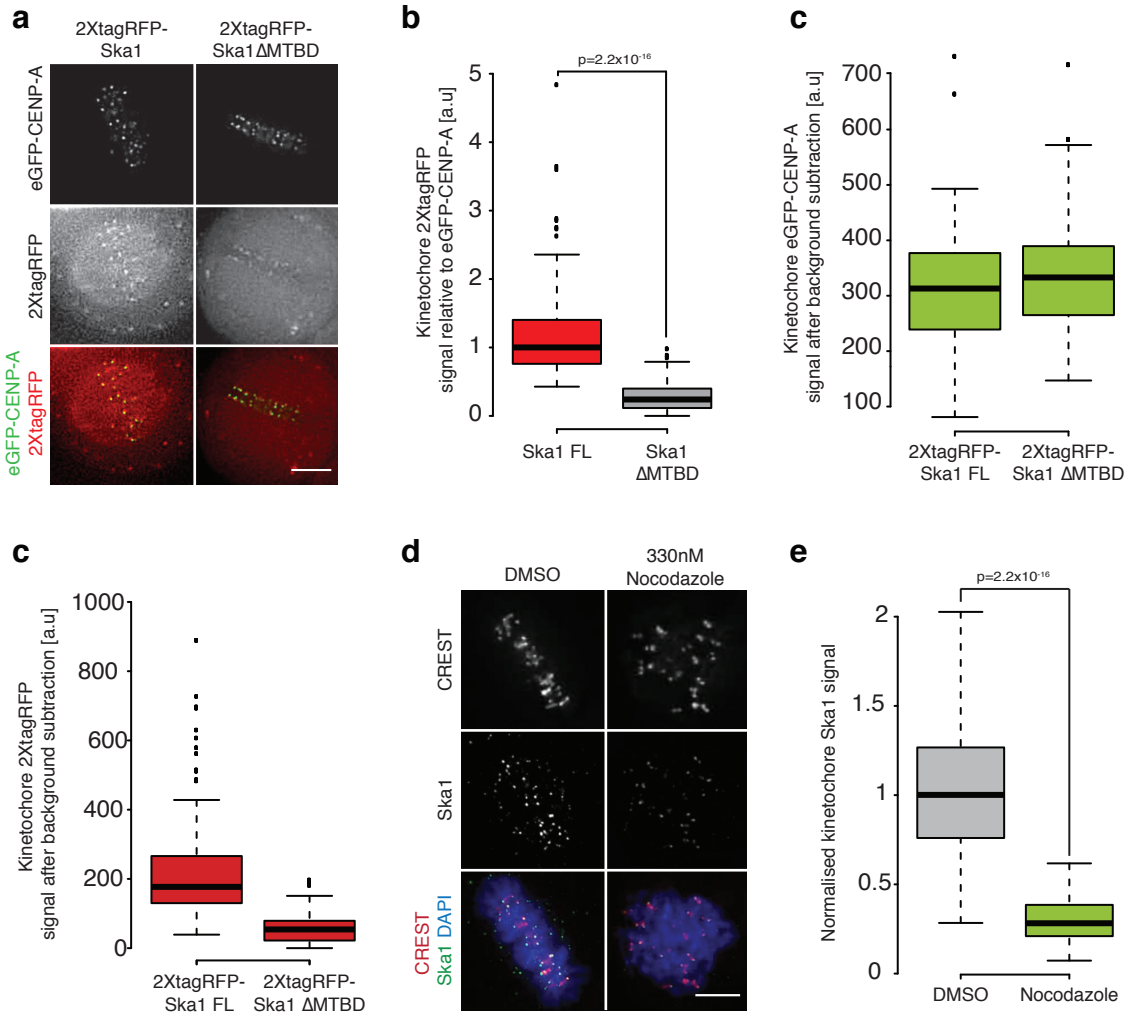

Figure 24: Ska1 may be loaded from the spindle onto the kinetochore

(a) Images of metaphase HeLa cells expressing eGFP-CENP-A and transfected with either 2×tagRFP-Ska1 or 2×tagRFP-Ska1ΔMTBD. Scale bar 5μm. (b) Quantification of kinetochore 2×tagRFP signal in cell expressing 2×tagRFP-Ska1 or 2×tagRFP-Ska1 ΔMTBD relative to eGFP-CENP-A after background subtraction. (c) Quantification of kinetochore eGFP-CENP-A signal after background subtraction at the kinetochores used to quantify 2xtagRFP-Ska1 and 2xtagRFP-Ska1ΔMTBD signal in pannel a. (d) Quantification of kinetochore 2xtagRFP signal after background subtraction at the kinetochores used to quantify 2xtagRFP-Ska1 and 2xtagRFP-Ska1ΔMTBD signal in pannel a. (e) Immunofluorescence images of a HeLa K cell treated with either DMSO or 330nM nocodazole for 16 hr and stained with DAPI, CREST antisera and an antibody against Ska1. Scale bar 5μm. (f) Quantification of Ska1 kinetochore staining intensity in cells treated with either DMSO or 330nM nocodazole for 16 hr relative to CREST after background subtraction.

single aligned kinetochores (Fig 25a,b). It is important to note that a limitation of this approach is that spindle length decreases in the cold, forming a broad metaphase plate that contains a mix of sister-pairs that were aligned and unaligned prior to treatment (Fig 25a). Despite this, our analysis revealed a strong linear correlation (R^2=0.3444) between the levels of Ska1 and α-tubulin (Fig 25a,b). Together, these data demonstrate that bi-oriented kinetochores can exist in both mature and immature states, and this is correlated with both congression and the number of K-fibre microtubules.

3.8 *Ska1 maturation correlates with loss of Bub1 from kinetochores*

It is well established that unattached kinetochores in prometaphase generate a 'wait anaphase' signal via the spindle assembly checkpoint (SAC) (London and Biggins, 2014b; Musacchio, 2015), thus allowing for sister-pairs to bi-orient prior to segregation. Interestingly however, cells also delay anaphase until all chromosomes have aligned, even in cases when unaligned kinetochores are bi-oriented and therefore satisfying the SAC. One idea is that this delay reflects the kinetics of Securin and CyclinB degradation. However, our observation of unaligned bi-oriented kinetochore-pairs in an immature state raises the possibility that they may still signal via the SAC. To test this, we stained cells with anti-Bub1 (as a marker of SAC activity) and anti-Ska1 (as a marker of maturity). First, we

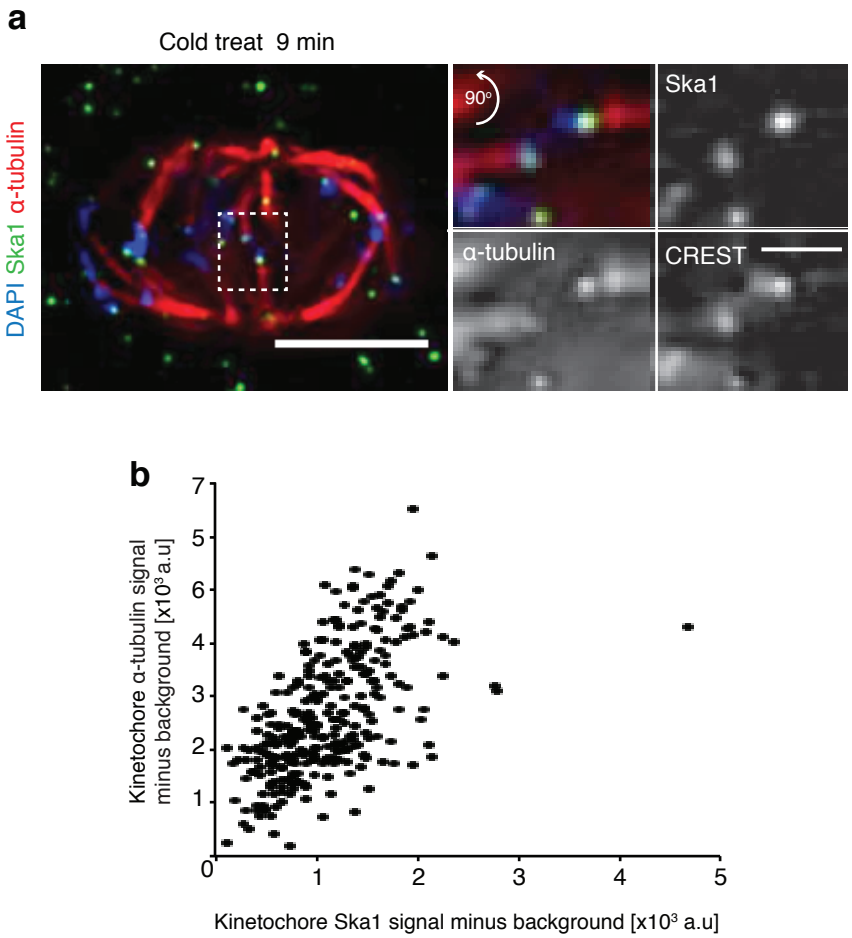

Figure 25: Ska1 loading correlates with microtubule occupancy

(a) Image of a cold treated metaphase cell fixed and stained with DAPI and Abs against α-tubulin and Ska1. Zoom boxes depict the staining intensities at individual kinetochore pairs. Scale bar 5 μm (top) 1μm (bottom). (h) Scatter plot of Ska1 and kinetochore proximal α-tubulin signals at single kinetochores after background subtraction in cold treated metaphase cells, n=300 KT from 30 cells.

categorized prometaphase sister-pairs into three groups based on spindle position, orientation and inter-sister distance. They are as follows: (1) aligned/bi-oriented, (2) unaligned/bi-oriented, and (3) unaligned/non-bi-oriented. As expected, aligned/bi-oriented kinetochore pairs had high levels of Ska1 and low levels of Bub1 (Fig 26a-d). The opposite was true for unaligned/non-bioriented kinetochore pairs, which had low levels of Ska1 and high levels of Bub1 (Fig 26a-d). In agreement with our previous data, the unaligned/bi-oriented kinetochore-pairs had ~50% lower Ska1 than those aligned at the spindle equator, but significantly higher than the unaligned/non-bioriented population. Interestingly however, these kinetochores loaded Bub1 to a level comparable to that of the unaligned/non-bi-oriented population (Fig 26a-d). This behavior was also sister-kinetochore autonomous, and we could observe instances where one sister in a pair was Bub1 positive/Ska1 negative and the other sister Bub1 negative/Ska1 positive (Fig 26e). Thus demonstrating that bi-oriented kinetochores in an immature state can generate an independent SAC signal.

3.9 *Summary*

Here, we have demonstrated that the Ska complex is a load-bearing component of the kinetochore, which is progressively recruited during congression to limit the number of lead kinetochore detachment events.

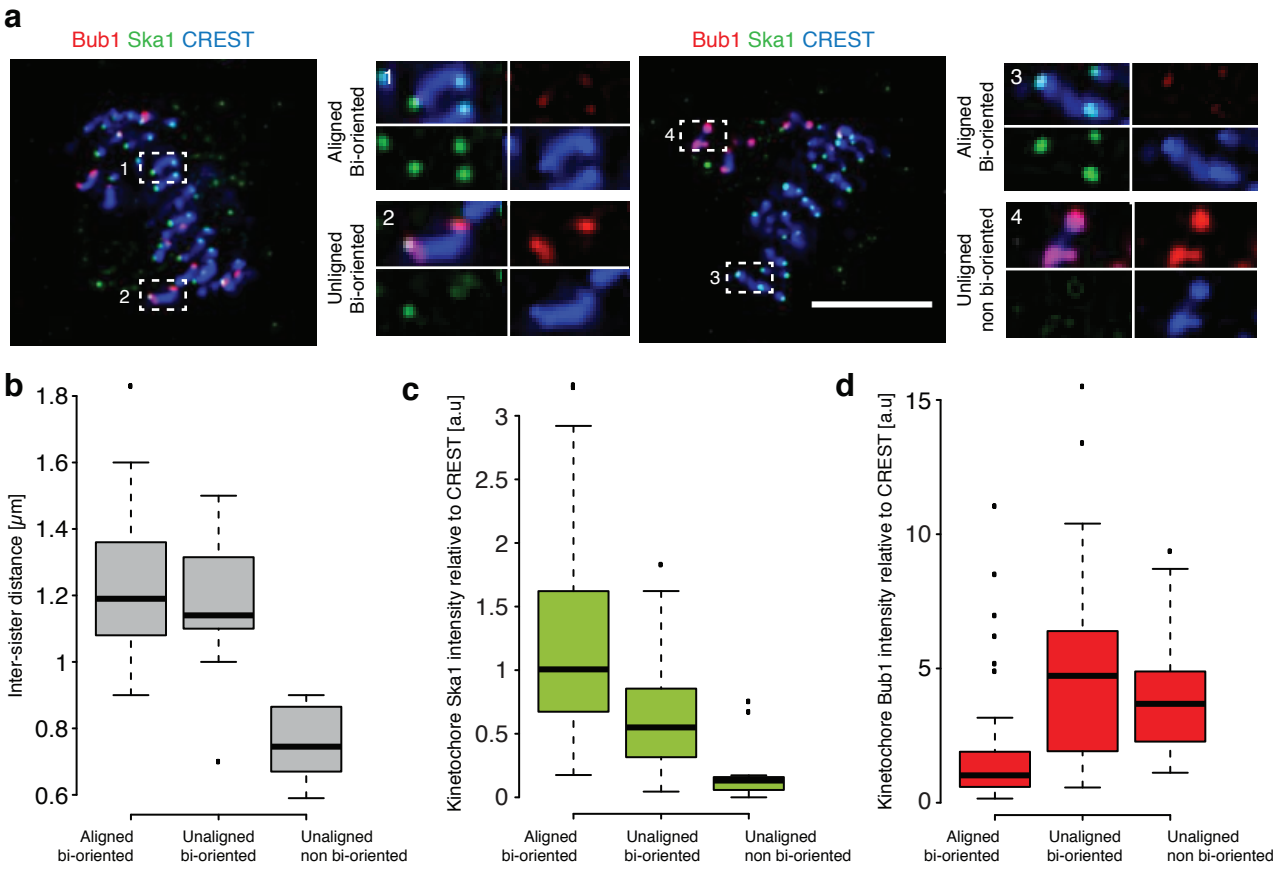

Figure 26: Ska maturation correlates with loss of Bub1 from kinetochores

(a) Immunofluorescence images of prometaphase HeLa K cells stained with antibodies against Ska1 and Bub1 and CREST antisera. Zoom boxes depict the staining intensities at aligned bi-oriented (1 & 3), unaligned bi-oriented (2) and unaligned non-bi-oriented (4) kinetochore pairs, respectively. Scale bar 5μm. (b) Quantification of CREST based inter-sister distance at the kinetochore-pair subgroups shown in (a). (c) Quantification of kinetochore Ska1 staining intensity relative to CREST after background subtraction at the kinetochore-pair subgroups defined in (a). (d) Quantification of kinetochore Bub1 staining intensity relative to CREST after background subtraction at the kinetochore-pair subgroups defined in (a). (e) Immunofluorescence images of prometaphase HeLa K cells stained with antibodies against Ska1 and Bub1 and CREST antisera. Zoom boxes depict an unaligned bi-oriented kinetochore-pair with opposing Ska1/Bub1 loading. Scale bar 5μm.

Moreover, we have shown that these detachment events are a normal feature of mitosis, and are typically followed by reattachment and successful congression in unperturbed human cells. This may reflect some kind of mechanical ‘self-check’, where by kinetochores that fail to fully mature the Ska complex or recruit too few microtubules during congression detach, halting the cell in prometaphase. This would allow the sister-pair to reform its attachment and correctly mature, ensuring that only anaphase compatible kinetochores reach the spindle equator.

Chapter 4: *Distinct contributions of the Ska complex, CENP-F and CENP-E to depolymerisation-coupled pulling*

4.1 *Introduction*

Currently, our data demonstrate that the Ska complex is required to increase the load bearing capacity of the kinetochore, which allows the leading sister to efficiently track the shortening K-fiber. However, the Ska complex is clearly not required for all congression events, as the majority of kinetochore-pairs align in its absence. This suggests that other factors contribute to congression via DCP, and these are at least in part redundant. In this regard, *in vitro* analysis of CENP-F, a factor that relocates from the nuclear envelope to the kinetochore during mitosis, has been shown to behave in a manner reminiscent of the Ska complex *in vitro* (Volkov et al., 2015). CENP-F contains two microtubule-binding domains (MTBD), one located at either terminus. Of particular interest is the N-terminal MTBD, which shows a preference for binding curved microtubule structures, tracks with the depolymerising plus-end, and can transduce this force to a bead coated in the fragment (Volkov et al., 2015). However, elucidation of its function in congression *in vivo* has been confounded by its proposed role in CENP-E and dynein recruitment to the kinetochore (Bomont et al., 2005;

Feng et al., 2006; Holt et al., 2005; Vergnolle and Taylor, 2007; Yang et al., 2005). Moreover, CENP-E is required for end-on attached kinetochores about a monopole to track depolymerising astral microtubules in response to nocodazole treatment (Gudimchuk et al., 2013), suggesting it may too contribute to DCP. Here, we demonstrate that CENP-F has an independent role in coupling the lead kinetochore to depolymerising microtubules during congression *in vivo*. Moreover, we show that CENP-E is not required for DCP *per se*, but contributes to force generation at end-on attached kinetochores.

4.2 *CENP-F is required for the maintenance of bi-orientation during congression*

To follow the behaviour of bi-oriented congressing chromosomes depleted of CENP-F, we employed the same imaging and kinetochore selection protocol described in section 3.2. Quantitative immunofluorescence revealed that CENP-F was efficiently depleted, reducing the kinetochore signal relative to CREST by >95% (Fig 27a,b) (n=200 kinetochores from 20 cells per condition). We then followed the behaviour of congressing kinetochore-pairs in CENP-F depleted cells, and observed a 20% reduction in successful congression to the spindle equator, which corresponded with a 12% (±1%) increase in flipping (n=140 kinetochores form 43 cells). The remaining 8% either stalled, failing to generate any productive force, or

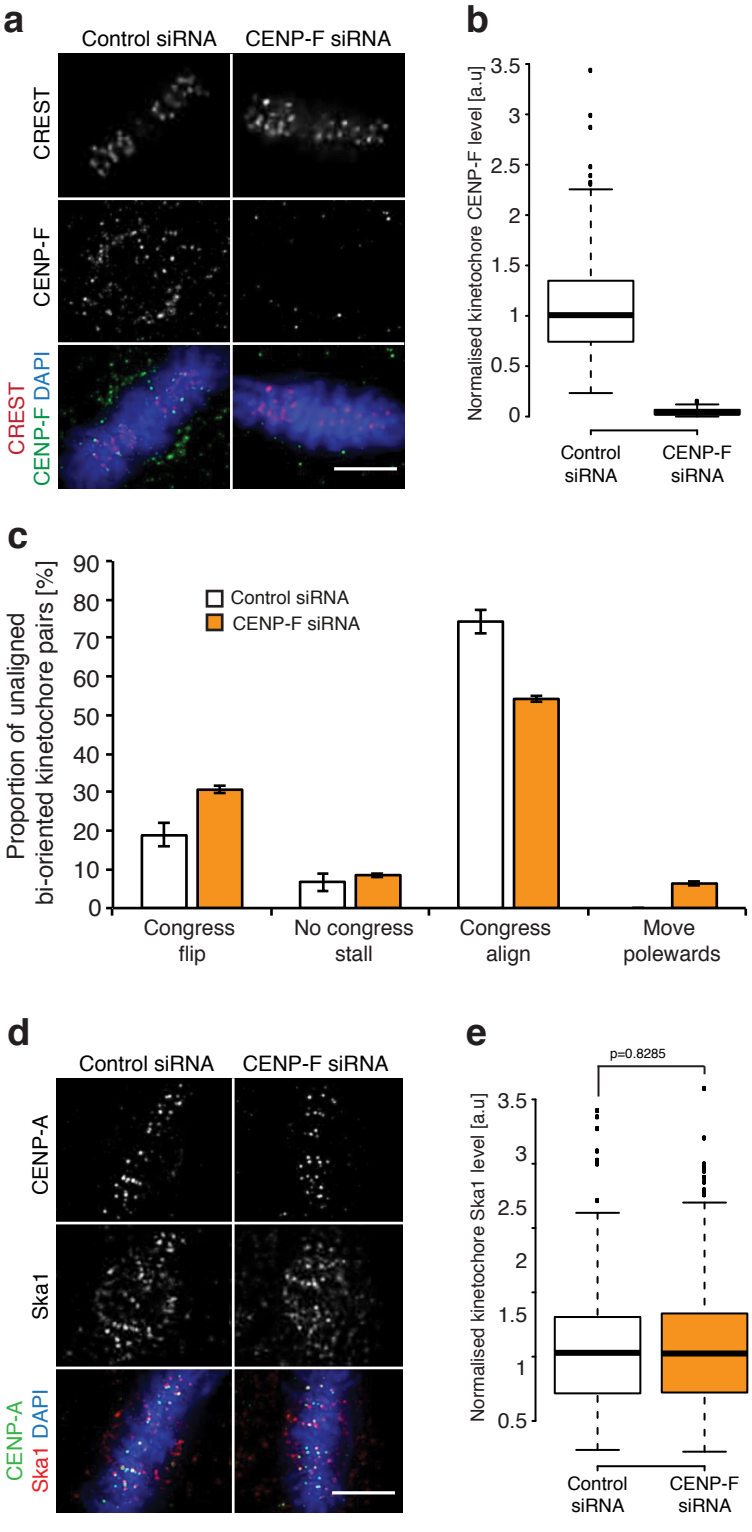

Figure 27 CENP-F contributes to the maintenance of bi-orientation during congression

(a) Immunofluorescence images of HeLa K cells treated with either control or CENP-F siRNA for 48hr and stained with DAPI, CREST antisera and an antibody against CENP-F. Scale bar 5μm. (b) Quantification of kinetochore CENP-F staining relative to CREST after background subtraction in cells treated with either control or CENP-F siRNA. (c) Quantification of bi-oriented kinetochore behaviour during congression in eGFP-CENP-A expressing HeLa cells treated with either control or CENP-F siRNA. Error bar ±SD.
(d) Immunofluorescence images of HeLa K cells treated with either control or CENP-F siRNA and stained with DAPI and antibodies against CENP-A and Ska1. Scale bar 5μm. (e) Quantification of kinetochore Ska1 staining relative to CENP-A after background subtraction in cells treated with either control or CENP-F siRNA.

were transported toward their proximal pole (Fig 27c) (n=140 kinetochores form 43 cells). Thus, CENP-F is required for the maintenance of bi-orientation during congression, albeit to a lesser extent that the Ska complex. The possibility remained that this effect was indirect, via perturbation of Ska complex loading to the kinetochore. However, quantitative immunofluorescence revealed that kinetochore bound Ska1 was unchanged upon CENP-F depletion (Fig 27d,e) (n=200 kinetochores from 20 cells per condition). Taken together, these data demonstrate a minor, Ska complex independent role for CENP-F in the maintenance of bi-orientation during congression.

4.3 *Integrating the Ska complex, CENP-F and CENP-E at end-on attached kinetochores*

Currently, our data supports a model where the Ska complex and CENP-F are required for the maintenance of lead kinetochore attachment during congression, albeit to differing degrees. A key further question is how these factors cooperate at the kinetochore to enable congression via DCP. Importantly, CENP-F has been implicated in the kinetochore loading of CENP-E (Bomont et al., 2005), a finding we confirmed in both prometaphase and metaphase HeLa cells (n=200 kinetochore pairs from 20 cells) (Fig 28a,b). Previous reports have demonstrated that mono-oriented sister kinetochores utilise CENP-E to track depolymerising astral

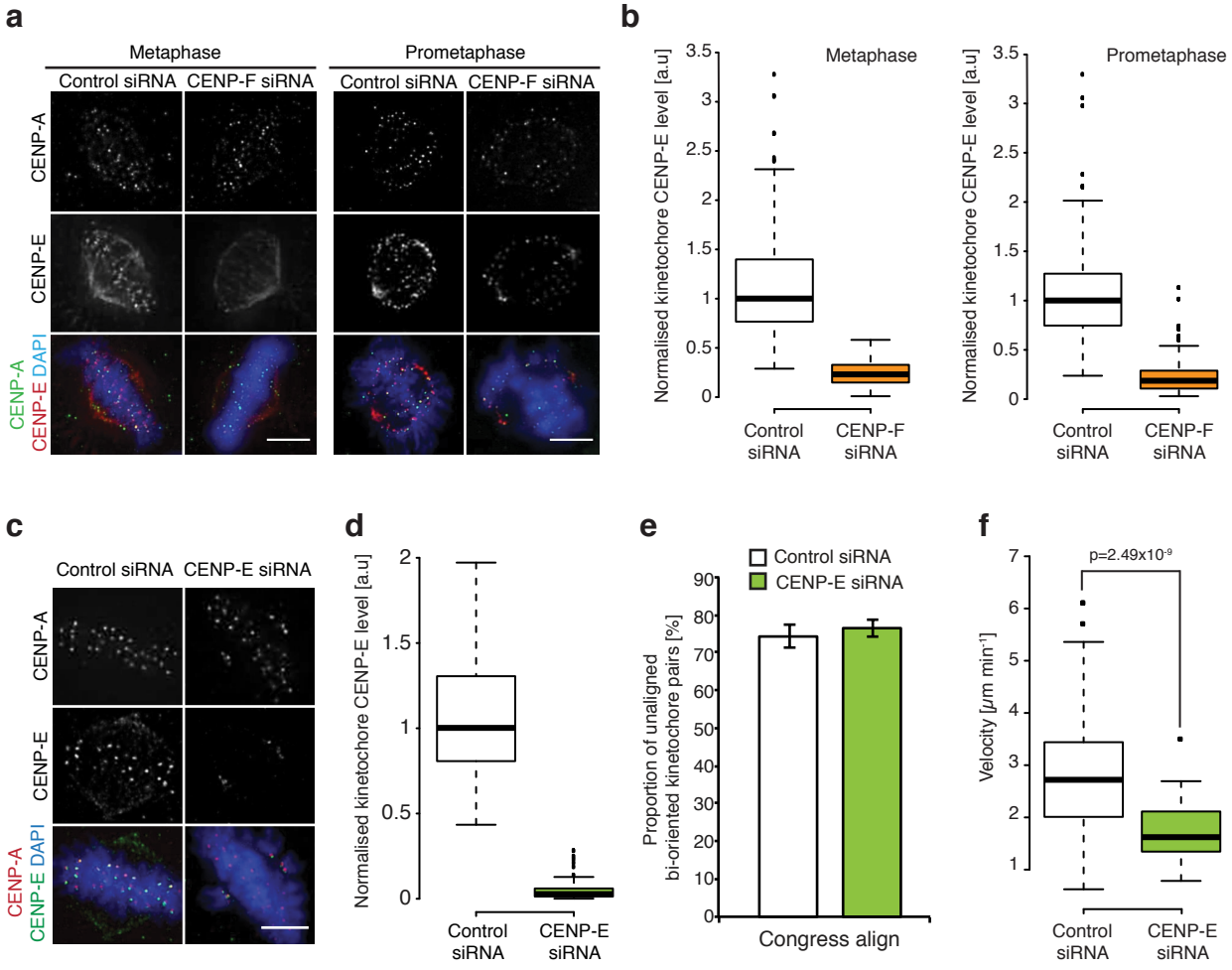

Figure 28: CENP-F recruites the force generating CENP-E to kinetochores

(a) Immunofluorescence images of metaphase (left) and prometaphase (right) HeLa K cells treated with either control or CENP-F siRNA and stained with DAPI, and antibodies against CENP-A and CENP-E. Scale Bar 5μm. (b) Quantification kinetochore CENP-E staining relative to CENP-A after background subtraction in metaphase (left) and prometaphase (right) HeLa K cells treated with either control or CENP-F siRNA. (c) Immunofluorescence images of HeLa K cells treated with either control or CENP-E siRNA and stained with DAPI, and antibodies against CENP-A and CENP-E. Scale bar 5μm.
(d) Quantification of kinetochore CENP-E staining relative to CENP-A after background subtraction in HeLa K cells treated with either control or CENP-E siRNA. (f) Quantification of the proportion of successfully congressing bi-oriented kinetochore-pairs in eGFP-CENP-A expressing HeLa cells treated with either control or CENP-E siRNA. (f) Quantification of kinetochore velocity during congression in eGFP-CENP-A expressing HeLa cells treated with either control or CENP-E siRNA. Velocity measurements were taken from tracks of processive movement that lasted at least 3 time points.

microtubules (Gudimchuk et al., 2013). However, we found that depletion of CENP-E had no effect on the congression of bi-oriented kinetochore pairs (Fig 28c-e) (Bancroft et al., 2015). One possibility is that the role for CENP-E is diminished when sisters become bi-oriented and undergo DCP, as the motor is at the microtubule plus-end and thus cannot carry out its primary function. Consistent with this idea, we find that depletion of CENP-E, while having no effect on the fidelity of congression via DCP, results in kinetochores congressing at a slower speed (from 2.93 μm min^{-1} ±1.2 μm min^{-1} in control cells to 1.7 μm min^{-1} ±0.6 μm min^{-1} in CENP-E depleted cells, n=33 kinetochore pairs from 19 cells) (Fig 28f), suggesting that the motor is contributing to a kinetochores capacity to generate force. Moreover, we find that depletion of CENP-E reduces the frequency of flip events by one third when compared to control cells (from 18.8% ±3% (n=157 kinetochore pairs from 90 cells) to 12.3% ±3.7% (n=61 kinetochore pairs from 25 cells)) and when codepleted with Ska1 (from 70% ±3.7% in Ska1 depleted cells (n=114 kinetochore pairs from 67 cells) to 41.9% ±1% in Ska1+CENP-E codepleted cells (n=138 kinetochore pairs from 39 cells)) (Fig 29a-e). Thus CENP-E is not required for congression via DCP, but has some role in generating force at end-on attached kinetochores.

This dependency of CENP-E on CENP-F may explain why CENP-F does not lead to as many flip events when compared to Ska complex (Fig 27c). Indeed, the speed of congressing chromosomes was also reduced in CENP-F depleted cells (from 2.93 μm min^{-1} ±1.2 μm min^{-1} in control cells to

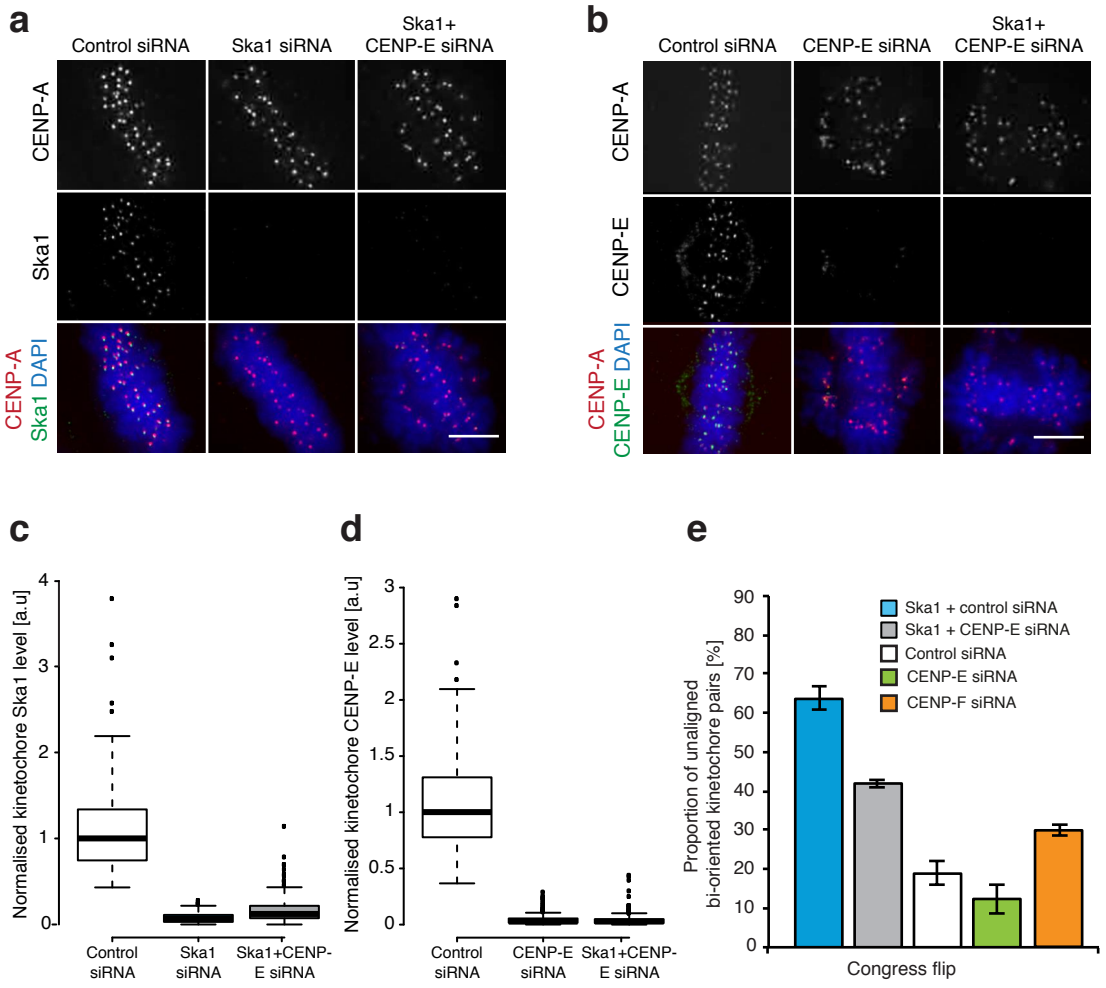

Figure 29: CENP-E depletion can rescue kinetochore flipping

a) Immunofluorescence images of HeLa K cells treated with either control, Ska1 or Ska1 + CENP-E siRNA and stained with DAPI, and antibodies against CENP-A and Ska1. Scale bar 5μm. (b) Immunofluorescence images of HeLa K cells treated with either control, CENP-E or Ska1 + CENP-E siRNA and stained with DAPI, and antibodies against CENP-A and CENP-E. Scale bar 5μm. (c) Quantification of kinetochore Ska1 staining relative to CENP-A after background subtraction in HeLa K cells treated with either control, Ska1 or Ska1 + CENP-E siRNA. (d) Quantification of kinetochore CENP-E staining relative to CENP-A after background subtraction in HeLa K cells treated with either control, CENP-E or Ska1 + CENP-E siRNA. (e) Quantification of the proportion of bi-oriented kinetochore pairs that flipped during congression in eGFP-CENP-A expressing HeLa cells treated with either control, Ska1 + control, Ska1+ CENP-E, CENP-E or CENP-F siRNA. Error bar ±SD.

2.01 μm min^{-1} ±0.84 μm min^{-1} in CENP-F depleted cells (n=35 kinetochore pairs from 30 cells) (Fig 30a). Interestingly, depletion of CENP-F does not affect the flip phenotype in Ska complex depleted cells (63.1% ±2.7% in Ska1+control siRNA (n=218 kinetochore pairs from 47 cells) and 63.9% ±1.6% in Ska1+CENP-F siRNA (n=226 kinetochore pairs from 61 cells)) even though the speeds are reduced and both proteins are efficiently depleted (n=200 kinetochores from 20 cells) (Fig 30b-f). Given that CENP-E depletion can rescue flipping, and it is absent from CENP-F depleted kinetochores, this suggests that both CENP-F and the Ska complex independently contribute to the formation of load-bearing microtubule attachments.

4.4 *Summary*

Here, we have demonstrated that CENP-F has an independent, but minor role in the formation of load-stable kinetochore-microtubule attachments. This contribution may be limited by the observed requirement of CENP-F for CENP-E kinetochore loading, as CENP-E, while being dispensable for congression via DCP, contributes to force generation at end-on attached kinetochores and can therefore partially rescue flipping. This effect probably reflects the previously reported role of CENP-E in the regulation of microtubule dynamics, both directly and though recruitment of CLASP proteins (Maffini et al., 2009).

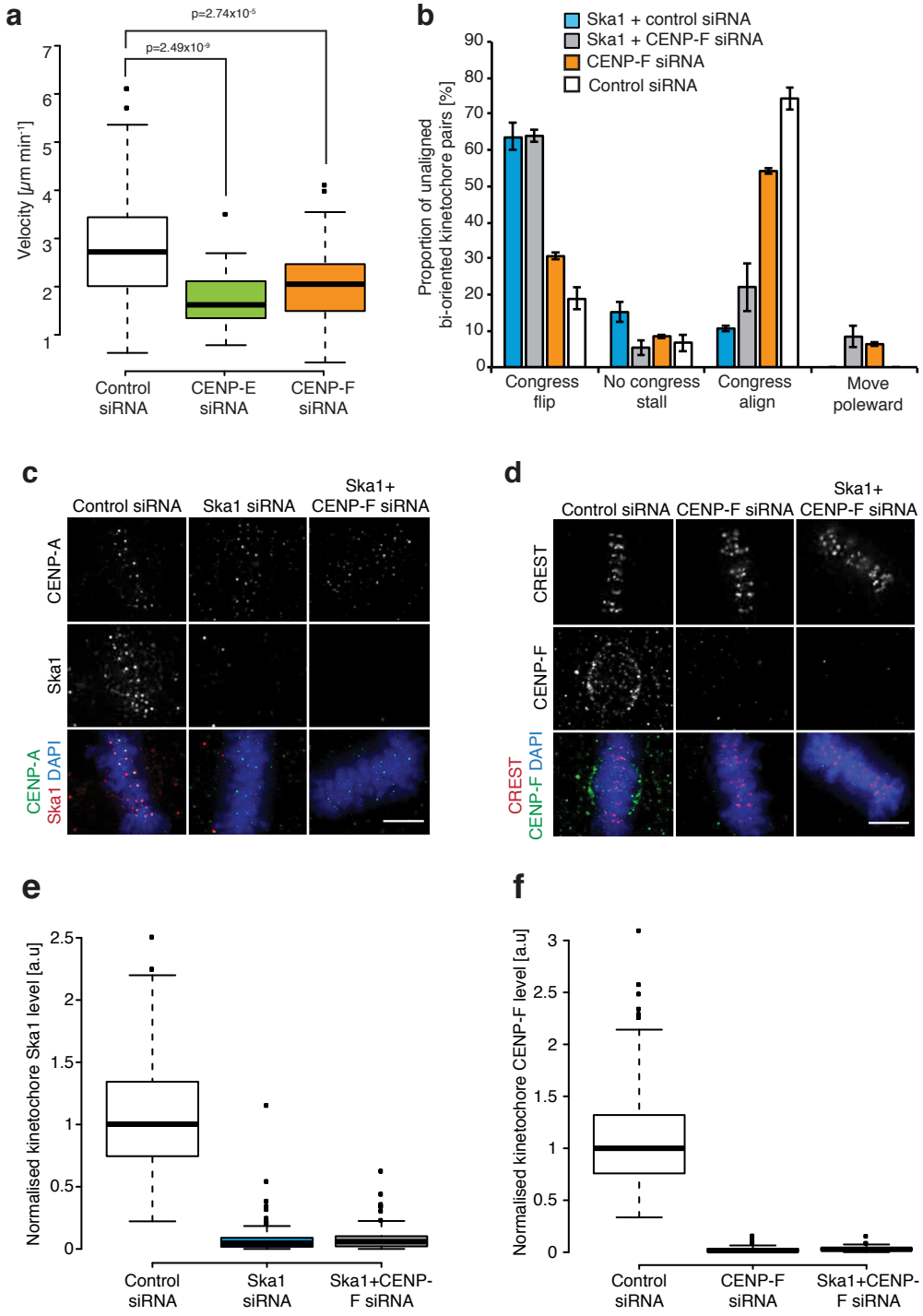

Figure 30: The Ska complex and CENP-F independently contribute to DCP

(a) Quantification of congressing kinetochore velocity in eGFP-CENP-A expressing HeLa cells treated with either control, CENP-E or CENP-F siRNA. Measurements were taken from tracks of processive movement that lasted at least 3 time points. (b) Quantification of congressing bi-oriented kinetochore behaviour during congression in cells treated with either control, CENP-F, Ska1 + control or Ska1 + CENP-F siRNA. (c) Immunofluorescence images of HeLa K cells treated with either control, Ska1 or Ska1 + CENP-F siRNA and stained with DAPI, and antibodies against CENP-A and Ska1. Scale bar 5μm. (d) Immunofluorescence images of HeLa K cells treated with either control, CENP-F or Ska1 + CENP-F siRNA and stained with DAPI, CREST antisera and an antibody against CENP-F. Scale bar 5μm. (e) Quantification of kinetochore Ska1 staining relative to CENP-A after background subtraction in HeLa K cells treated with either control, Ska1 or Ska1 + CENP-F siRNA. (f) Quantification of kinetochore CENP-F staining relative to CREST after background subtraction in HeLa K cells treated with either control, CENP-F or Ska1 + CENP-F siRNA.

Chapter 5: *Phospho-dependent force generation by CENP-Q is essential for the congression of bi-oriented kinetochore-pairs*

5.1 *Introduction*

While it is well established that several kinetochore-associated microtubule binding proteins are phospho-regulated (Chan et al., 2012; DeLuca et al., 2011; Schmidt et al., 2010; Welburn et al., 2010; Westermann et al., 2005), a modification that typically alters their recruitment and/or microtubule binding affinity. Little is known about phosphorylation events that directly regulate the function of an actively congressing kinetochore, be it laterally or end-on attached. One such event is the phosphorylation of CENP-E by Aurora A at the pole, which has been suggested to bias its walking on K-fibers oriented toward the equator (Kim et al., 2010). CENP-E is recruited to kinetochores via a currently unknown, but likely indirect, mechanism by the CENP-O subcomplex component CENP-Q. Previous work from the McAinsh lab has demonstrated that the CENP-O subcomplex is required for chromosome congression, but not for end-on attachment (McCleland et al., 2007). Suggesting that it contributed to a sub-step of DCP downstream of attachment. Indeed, by following the fates of individual kinetochore pairs depleted of CENP-Q, it was shown that CENP-Q is required for force

generation at bi-oriented kinetochore pairs, based on observations of unaligned bi-oriented chromosome stalling in its absence (Bancroft et al., 2015). This separated its role in DCP from that in CENP-E recruitment, as the same chromosome subgroup can congress when depleted of CENP-E (this study & Bancroft et al., 2015). Moreover, large-scale mass spectroscopic analysis has shown that CENP-Q is phosphorylated at serine 50 *in vivo* (Rigbolt et al., 2011). Thus, the possibility existed that the role of CENP-Q in congression was dependent upon phosphorylation at S50.

5.2 *CENP-Q^{S50A} rescues kinetochore recruitment of Plk1*

To test the significance of CENP-Q phosphorylation at S50, we mutated this residue to alanine or the phospho-mimicking aspartic acid. Prior to the analysis of congression defects associated with CENP-Q^{S50}-eGFP, we tested if this transgene could rescue the structural roles of CENP-Q in the extended CCAN, specifically, the recruitment of Plk1. In agreement with our previous data (Bancroft et al., 2015), CENP-Q depleted cells that had been transfected with an empty vector displayed an 84% reduction in kinetochore bound Plk1. In contrast, transfection with CENP-Q-eGFP rescued Plk1 loading to 50% of that observed control siRNA treated cells transfected with an empty vector, thus ruling out off target effects (Fig 31a,b) (n=300 kinetochores from 30 cells). Similarly, transfection with CENP-Q^{S50A}-eGFP rescued Plk1 loading to 62% (Fig 31c,d) (n=300 kinetochores from 30

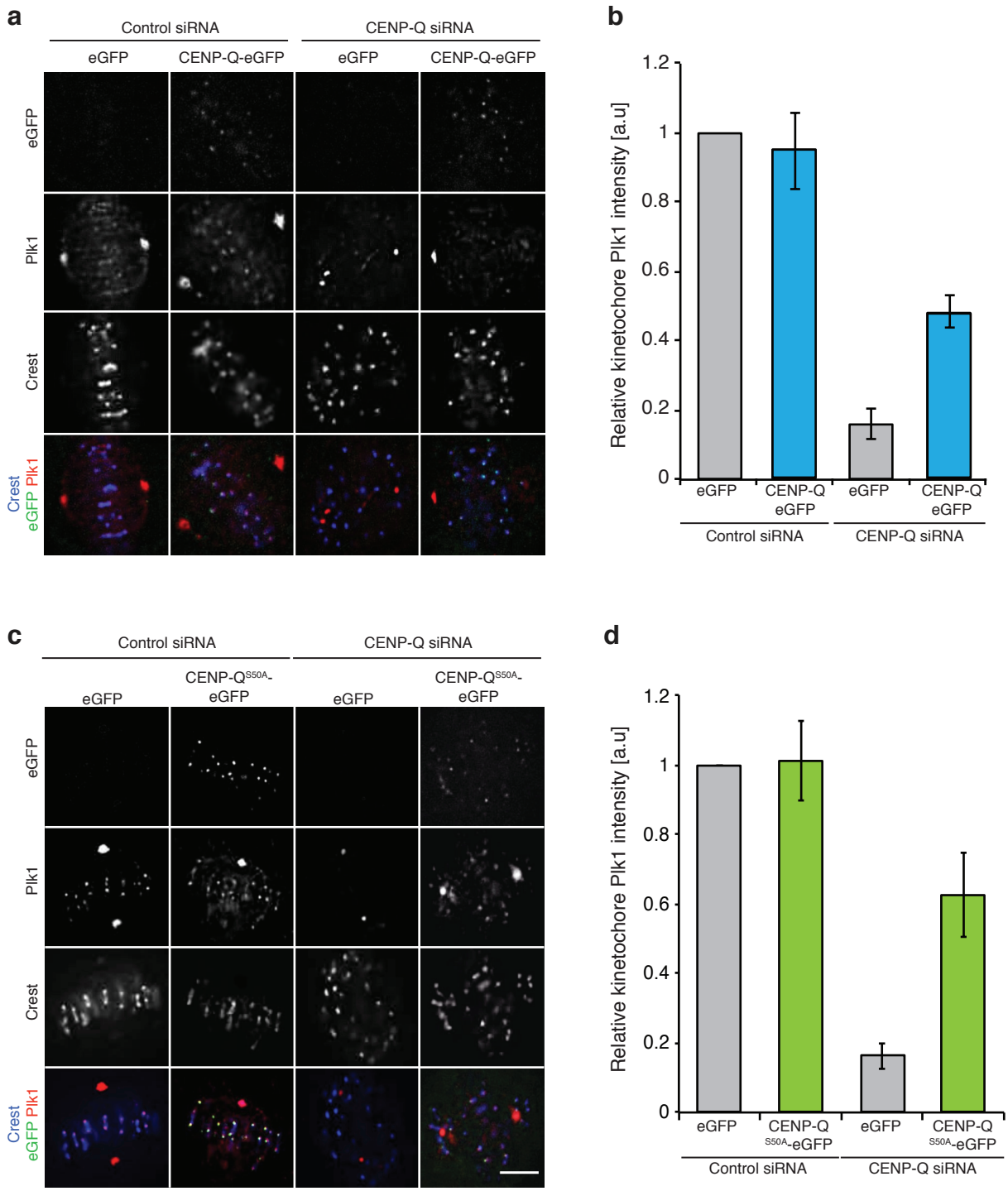

Figure 31: CENP-Q^{S50A}-eGFP can rescue kinetochore Plk1 recruitment

(a) Immunofluorescence images of Plk1 rescue experiment in HeLa K cells. Cells were treated with control or CENP-Q siRNA for 12 hr and then transfected with an siRNA resistant plasmid expressing CENP-Q-eGFP or a control eGFP expression plasmid for a further 48 hr. To reduce the effect of mitotic stage on alignment cells were arrested in metaphase with 0.1μM MG132 for 90 min prior to fixation, and stained with CREST antisera and an antibody against Plk1. Scale bar 5μm. (b) Quantification of kinetochore Plk1 levels in the CENP-Q rescue experiment. Error bar ±SD. (c) Immunofluorescence images of a CENP-QS50A–eGFP siRNA rescue experiment in HeLa K cells. Cells were treated with CENP-Q siRNA or control siRNA for 12hr and then transfected with an siRNA-resistant plasmid expressing CENP-QS50A–eGFP or a control eGFP expression plasmid for a further 48hr. To reduce the effect of the mitotic stage on alignment, cells were arrested in metaphase with 1 mM MG132 for 90min before fixation. Cells were stained with CREST antisera and an antibody against Plk1. Scale bar: 5μm. (B) Quantification of Plk1 levels in the CENP-QS50A –eGFP siRNA rescue experiment. Error bar ±SD.

cells). As Plk1 is indirectly recruited by CENP-Q, via interaction with its CENP-O subcomplex neighbour CENP-U (Park et al., 2015), this result demonstrates that cells rescued with CENP-Q^{S50A}-eGFP can form a functional CENP-O subcomplex at the kinetochore. Thus, CENP-Q^{S50A}-eGFP enables investigation of the phospho-dependent role of CENP-Q in chromosome congression independently of CENP-O subcomplex assembly and Plk1 recruitment.

5.3 *Phosphorylation of CENP-Q S50 is required for chromosome congression*

Currently, our data demonstrates that CENP-Q^{S50A}-eGFP can be used as a tool to specifically test the phospho-dependent role of CENP-Q in congression, as it rescues its structural roles within the kinetochore. To asses the role of phosphorylation at this site in congression, we transfected CENP-Q depleted cells with CENP-Q-eGFP, CENP-Q^{S50A}-eGFP or CENP-Q^{S50D}-eGFP, and monitored the phenotypic outcome in terms of CENP-E loading and the accumulation of polar chromosomes. First, we confirmed that all transgenes were equally loaded to the kinetochore, ruling out expression level as a contributor to the observed phenotypes (Fig 32a,b) ($n \geq 150$ kinetochores per condition). In line with our previous data, transfection with wild-type CENP-Q successfully rescued both the accumulation of polar chromosomes and CENP-E loading (Fig 32a,c,d) ($n \geq$

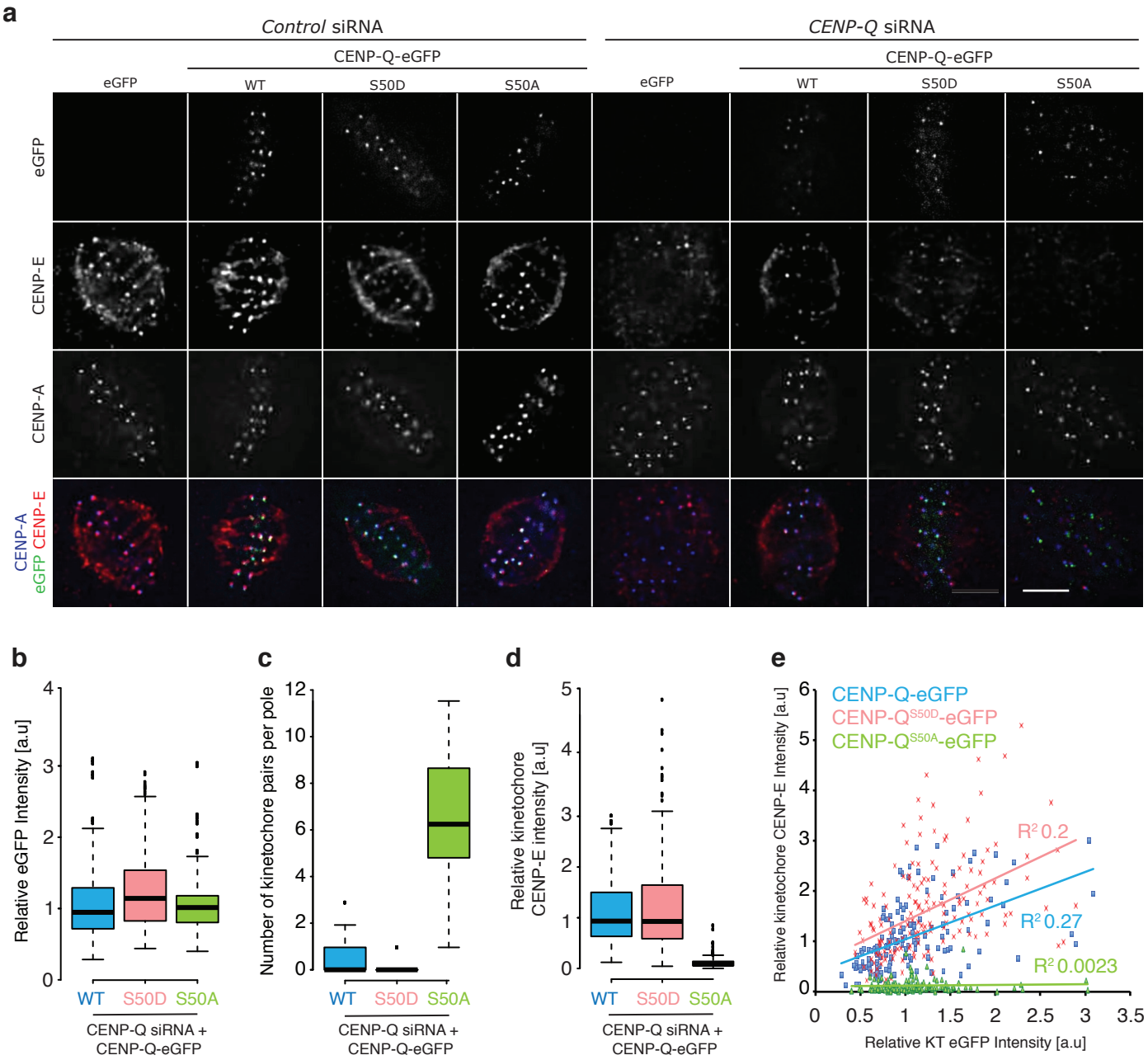

Figure 32: Phosphorylation at CENP-Q serine 50 is vital for chromosome congression

(a) Immunofluorescence images of CENP-QS50A–eGFP and CENP-QS50D–eGFP siRNA rescue experiments in HeLa K cells. Cells were treated with CENP-Q siRNA or control siRNA for 12hr and then transfected with an siRNA-resistant plasmid expressing CENP-Q–eGFP, CENP-QS50A–eGFP or CENP-QS50D–eGFP or a control eGFP expression plasmid for a further 48hr. To reduce the effect of the mitotic stage on alignment, cells were arrested in metaphase with 1 μM MG132 for 90 min before fixation. Cells were stained with antibodies against CENP-A and CENP-E. Scale bar: 5 μm. (b) Quantification of kinetochore transgene levels for each CENP-Q variant. (c) Quantification of the average number of kinetochore pairs per pole in the CENP-Q phospho-mutant rescue shown above. Dotted yellow line indicates the level in control cells. (d) Quantification of kinetochore CENP-E levels in the CENP-Q phospho-mutant rescue shown above. Dotted yellow line indicates the level in control cells. (e) A plot demonstrating the relationship between the kinetochore eGFP and CENP-E signals in cells rescued with CENP-Q–eGFP, CENP-Q–eGFPS50A or CENPQ–eGFPS50D.

150 kinetochores per condition). In contrast, transfection with CENP-Q^{S50A}-eGFP pheno-copied a CENP-Q depletion, with both a high number of polar chromosomes and low CENP-E kinetochore loading, suggesting that phosphorylation at S50 is critical for CENP-Q functionality. In agreement, transfection with the phospho-mimicking CENP-Q^{S50D}-eGFP successfully rescued the depletion phenotype, with both polar chromosome number and CENP-E levels comparable to cells rescued with wild-type CENP-Q (Fig 32c,d) ($n \geq 150$ kinetochores per condition). Finally, we plotted the level of the transgene and that of CENP-E for individual kinetochores in the rescue experiments (Fig 32e) ($n \geq 150$ kinetochores per condition). This revealed a positive correlation for both the CENP-Q-eGFP and CENP-Q^{S50D}-eGFP transgenes, demonstrating that the recruitment of CENP-E molecules is dependent upon the number of CENP-Q molecules at the kinetochore. As expected, this relationship was lost upon transfection with the CENP-Q^{S50A}-eGFP, with no CENP-E recruitment observed at high transgene levels (Fig 32e). Taken together, these data support a phospho-dependent role for CENP-Q in DCP and CENP-E kinetochore loading that is independent of Plk1 and the CENP-O subcomplex.

5.4 *Summary*

Here, we have demonstrated that; (1) the phosphorylation of CENP-Q at serine 50 is key for its role in congression and CENP-E recruitment, and (2)

CENP-Q has a direct role in congression, independent of its structural role in CENP-O subcomplex assembly and Plk1 recruitment.

Chapter 6: *Discussion*

6.1 *Summary of findings*

By combining specific molecular perturbations with single kinetochore tracking we have shown that: (1) the Ska complex, which is progressively recruited to bi-oriented kinetochores as they congress, is required for the leading sister to withstand microtubule pulling forces during migration, (2) CENP-F independently contributes to this process, however it appears to play a secondary or minor role relative to Ska, (3) force generation at end-on attached kinetochores requires MCAK, CENP-E and the kinase activity of Aurora B, and (4) the phosphorylation of CENP-Q at serine 50 is essential for chromosome congression. Together, these findings generate a model of how individual kinetochore components contribute to DCP sub-steps and how these specific functions are regulated, all of which is vital for high-fidelity chromosome segregation.

6.2 The role of the Ska complex in congression

Here, we have provided the first direct *in vivo* evidence that a kinetochore factor, the Ska complex, is specifically required to maintain microtubule attachment during congression – a key feature of DCP. Kinetochores

depleted of the Ska complex can form bi-oriented attachments and initiate congression, but frequently rotate through 90° as they approach the equator and move poleward, an event triggered by microtubule detachment at the leading kinetochore. This is in line with structural and biochemical studies that show how the Ska complex mediates coupling to depolymerising microtubule plus-end by binding and remaining attached to curved protofilaments that are extruded during microtubule disassembly (Abad et al., 2014; Jeyaprakash et al., 2012; Schmidt et al., 2012; Welburn et al., 2009) (Fig 33). This takes us beyond the idea that microtubule attachment factors, namely Ndc80, are the sole force-couplers at end-on attached kinetochores (Cheeseman and Desai, 2008; Powers et al., 2009; Welburn et al., 2009). How much force the Ska complex can transduce, and how the complex is organised at the kinetochore *in vivo* will be key in understanding its role in microtubule coupling. In this regard, structural analysis of purified recombinant Ska complex has shown that it can oligomerise into a higher order structure (Jeyaprakash et al., 2012), a behaviour that has previously been suggested to contribute to Ndc80 force-coupling (Alushin et al., 2010). However, the biological relevance of this Ska complex oligomer is yet to be determined.

Moreover, the cause of lead kinetochore detachment remains obscure. One possibility is that the leading kinetochore experiences periods of high-load during congression, and in the absence of the Ska complex this physically ruptures the attachment. How might these periods of high load occur? We

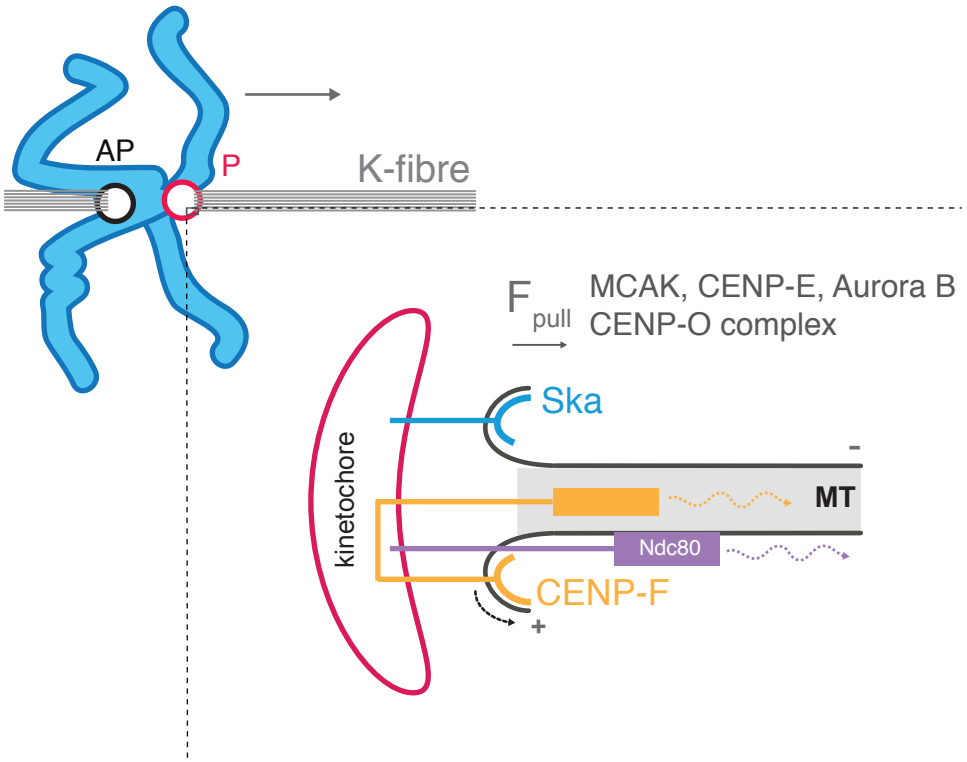

Figure 33: A molecular model of DCP mediators

Schematic depicting the contribution of kinetochore factors to DCP. Here, the Ndc80 complex first forms an end-on attachment to a microtubule. Upon depolymerisation, the Ska complex and the CENP-F amino-terminal microtubule binding domain (Volkov et al., 2015) attach to, and track with, the curving protofilaments as they peel away from the lattice, thus generating a pulling force. This coupling is essential for the maintenance of lead kinetochore attachment when under load. The carboxy-terminal microtubule-binding domain of CENP-F and Ndc80 may also contribute to force generation by binding to the microtubule lattice and diffusing away (indicated by the dotted curved arrow) from the depolymerising plus-end. In addition to these coupling factors, CENP-E, MCAK, Aurora B and phosphorylation of CENP-Q at serine 50 (Bancroft et al., 2015) are required for a force generation step (indicated by Fpull).

favour the idea that kinetochores come under increasing load due to the recruitment of new microtubules into the K-fibre. Additionally, the K-fiber may experience periods of 'depolymerisation coherence' during congression, equivalent to the recently documented 'bursts' of coherent polymerisation (Armond et al., 2015). Interestingly, our tracking experiments do show periods of high centromeric stretch during congression, where the inter-sister separation was observed to spontaneously elevate to 1.6-1.7μm. These stretching events correlated with sustained migration of the sister-pair toward the equator. Importantly, this stretching resulted from the leading kinetochore moving away from its trailing sister, suggesting that it alone has experienced an acute pulling force. Therefore, kinetochores appear to be subject to fluctuating forces during congression.

We cannot, however, rule out that we are observing error-correction, which destabilises attachments in response to loss of tension (Lampson and Cheeseman, 2011). Nevertheless, several lines of evidence argue against this model; (1) once a kinetochore-pair has bi-oriented they are not subject to error correction. This is based on the finding that key error correction targets are not rephosphorylated in response to the loss of tension or microtubule attachment (DeLuca et al., 2011). Furthermore, we observed no difference in Aurora B Ndc80 phosphorylation between aligned or unaligned bi-oriented chromosomes. (2) It is unclear how a symmetrical cue, the loss of tension across the sister pair, leads to a highly

asymmetrical response with only the P kinetochore detaching from its K-fiber, (3) we have observed detachment at high tension, a time where Aurora B substrates should be physically separated from the kinase (Liu et al., 2009), and (4) the Ska complex has recently been suggested to promote Aurora B activity (Redli et al., 2016). Therefore, despite Ska1 depletion compromising the error correction machinery, congressing kinetochores in these cells display a high rate of lead sister detachment. This line of thinking has been complicated by a recent report showing that Ska1 recruits PP1 to the kinetochore (Sivakumar et al., 2016). In the context of our model, the loss of PP1 in Ska depleted cells would prevent the stabilisation of kinetochore-microtubule attachments and favour detachment events (flips). Importantly, the authors demonstrated that depletion of the Ska complex caused a ~25% increase in the phosphorylation of Knl1 (Sivakumar et al., 2016). However, these experiments were conducted at unattached kinetochores, a state that is known to promote Aurora B dependent outer-kinetochore phosphorylation (Liu et al., 2009) and reduce kinetochore bound PP1 (DeLuca et al., 2011). Together, these factors push the kinetochore into a pro-phosphorylation state. Therefore, if the loss of PP1 in Ska depleted cells was the cause of flipping, one might expect this change in phosphorylation to be more pronounced. Indeed, in an unperturbed mitosis, Aurora B phosphorylation of Ndc80 is ~500% higher in prometaphase when compared to metaphase. Even with this augmented phosphorylation, many kinetochore-pairs

instantaneously form stable bi-oriented attachments (DeLuca et al., 2011; Magidson et al., 2011). Therefore, we suggest that the reported reduction in kinetochore bound PP1 in Ska depleted cells would have only a minimal, if any, impact on congression. Moreover, in our depletion experiments we unload the entire Ska complex from kinetochores. As the complex possess an additional microtubule binding domain at the C-terminus of Ska3, which is required for congression (Abad et al., 2016; Jeyaprakash et al., 2012), the Ska complex likely contributes to kinetochore function independently of PP1 loading. Thus, we propose a model in which excess pulling force at the leading kinetochore leads to the mechanical failure of the attachment in Ska1 depleted cells.

6.3 *Integrating the Ska complex, CENP-F, CENP-E and MCAK in DCP*

Our data clearly show that the Ska complex is not essential for congression *per se,* since the majority of kinetochores successfully align at the spindle equator in its absence. Presumably, kinetochores are congressing by other mechanisms, such as CENP-E-dependent lateral sliding, instantaneous bi-orientation or through contributions from other redundant factors (Kapoor et al., 2006; Magidson et al., 2011). In this regard, we show that CENP-F is also involved in load bearing – although this activity appears to contribute significantly less than the Ska complex. Mechanistically, CENP-F likely

utilises its amino-terminal microtubule-binding domain, which has been shown to preferentially bind to curved microtubule structures (Volkov et al., 2015) (Fig 33). In addition, CENP-F may bind the microtubule lattice via its C-terminus, and utilise a biased diffusion to track the depolymerising plus-end (Volkov et al., 2015), as suggested for the Ndc80 complex (Powers et al., 2009) (Fig 34). Interestingly, these biased-diffusion and protofilament binding pathways are not independent, as Ndc80 contributes to Ska complex loading (Zhang et al., 2012), and Ska acts as a processivity factor for Ndc80 *in vitro* (Schmidt et al., 2012). Future work using separation of function mutants in Ndc80 and CENP-F, alongside the *in vitro* reconstitution of these factors on dynamic microtubules will be required to determine their relative contribution to chromosome movement.

While the Ska complex and CENP-F are involved in the formation of load-bearing microtubule attachment, our data rule out a role for CENP-E motors in DCP. However, we do find that depletion of CENP-E, like MCAK, interferes with force-generation at bi-oriented kinetochores (inferred from the slowing of kinetochore motion when CENP-E or MCAK are depleted) (Fig 29). Moreover, this reduction in force following CENP-E depletion (or MCAK) is sufficient to reduce the frequency of kinetochore detachment in Ska depleted and control cells. The slowing of kinetochore movement following depletion of MCAK most likely reflects loss of its depolymerase activity (Hunter et al., 2003) and subsequent changes to the balance of microtubule polymerisation between the leading and trailing sister

kinetochores (Armond et al., 2015). On the other hand, it is unclear why a plus-end directed motor such as CENP-E would influence DCP, although it may reflect direct regulation of microtubule polymerisation (Sardar et al., 2010), and/or recruitment of CLASP proteins (Maffini et al., 2009). Nevertheless, this role of CENP-E in DCP is consistent with previous work showing that CENP-E is required for mono-oriented kinetochores to track shrinking astral-microtubules (Gudimchuk et al., 2013). It is tempting to speculate that the requirements for CENP-E at end-on attached kinetochores are influenced by attachment state (mono- vs. bi-oriented) and/or spatial position within the spindle. Indeed, the role of CENP-E in lateral sliding is proposed to be phospho-regulated in a spatially dependent manner (Kim et al., 2010).

Interestingly, we also confirm here that CENP-E requires CENP-F for kinetochore–binding (Bomont et al., 2005). This loss of CENP-E and the resulting slowing of kinetochore movement may well be limiting the observed effect of CENP-F depletion at end-on attached kinetochores. Importantly, all these phenotypes are distinct from depletion of the microtubule-binding CCAN subunit CENP-Q (Bancroft et al., 2015) or inactivation of Aurora-B kinase activity (this study) (Fig 33). In both cases the kinetochores can bi-orientate but are unable to initiate movement, suggesting problems in regulation of microtubule dynamics (and force generation). Overall, monitoring the fates of kinetochores using live cell imaging takes the field beyond the generic “congression problem”

phenotype, and allows much more specific functions to be assigned to kinetochore and spindle factors. The challenge is going to be untangling the hierarchical dependencies that are evident and how the phosphorylation of many factors modulates their activities during DCP.

6.4 *Phosphorylation of CENP-Q serine 50 is essential for chromosome congression*

Previous work from the McAinsh lab implicated CENP-Q in a force generation step at end-on attached kinetochores (Bancroft et al., 2015). However, this observation was confounded by the simultaneous loss of other CENP-O subcomplex members and Plk1 from CENP-Q depleted kinetochores. Our observation that a non-phosphorylatable mutant of CENP-Q serine 50 fails to rescue the CENP-Q depletion phenotype, despite being properly loaded to kinetochores, raises two key points; (1) the role of CENP-Q in congression is distinct from its structural roles in the kinetochore, and (2) phosphorylation of CENP-Q at S50 is critical for this function in congression (Fig 33). Given that CENP-E is also lost of cells rescued with CENP-Q S50A, it is tempting to speculate that phosphorylation at this site directly licences the binding of CENP-E to CENP-Q. However, CENP-E remains bound in cells depleted of CENP-L or CENP-H, factors that are required for CENP-Q recruitment to the

kinetochore (Amaro et al., 2010; McCleland et al., 2007). Moreover, the loss of CENP-E from CENP-Q depleted kinetochores is partially rescued by treatment with nocodazole, suggesting that microtubules are required for CENP-E unloading (Bancroft et al., 2015). As such, a more likely mechanism is that CENP-Q regulates microtubule dynamics to permit CENP-E loading, an idea that is supported by observations of direct microtubule binding by the CENP-O complex (Amaro et al., 2010; Zhu et al., 2013). Moreover, this would account for the reported CENP-E independent role of CENP-Q in force generation during DCP (Bancroft et al., 2015). How phosphorylation at S50 affects the microtubule binding activity of CENP-Q, and what kinase targets S50 are key further questions. With respect to the latter, the most likely candidate is the CENP-U bound pool of Plk1. However, despite CENP-Q being a target of Plk1 *in vitro* (Kang et al., 2011b), stable isotope labelling by amino acids in cell culture (SILAC) experiments demonstrated that S50 was not sensitive to depletion or inhibition of Plk1 (Santamaria et al., 2011). Future work that combines phospho-specific antibody staining with small molecule inhibitors *in vivo* will undoubtedly shed light on the kinase. Moreover, such staining would also provide insight into the temporal regulation of this phosphorylation at specific kinetochore sub-groups, an event that may specifically licence CENP-Q mediated force-generation in defined spindle regions.

6.5 *The contribution of flipping to wild-type congression*

During our initial analysis of DCP behaviour, we unexpectedly found that wild-type kinetochore-pairs have a ~20% baseline level of flipping. In addition, flipping could be observed in unperturbed RPE1 cells, however, at a much lower rate due to the accelerated speed of prometaphase and the reported instantaneous bi-orientation of sister-pairs following NEB (Magidson et al., 2011). Nevertheless, these data demonstrate that flipping is a normal step in chromosome congression. This raises the question, how could the detachment of a kinetochore from its associated K-fiber be beneficial? Such metastable attachments seem counter intuitive, as one would expect robust attachments to prevent the deleterious loss of chromosomes. However, if attachments were too tight it may prevent the correction of merotely, as Aurora B phosphorylation of attachment proteins may not sufficiently reduce microtubule affinity at the erroneous site. Therefore, flipping could simply be the consequence of this affinity trade off. Another idea is based on the observation that the Ska complex is progressively recruited to bi-oriented kinetochores as they congress from an unaligned to an aligned position. This shows that once kinetochores bi-orient they progressively load Ska complexes in a maturation step that depends on active congression (Fig 34). We propose that this is to accommodate for the increased pulling forces the kinetochore would experience as the K-fiber increases in microtubule number and undergoes

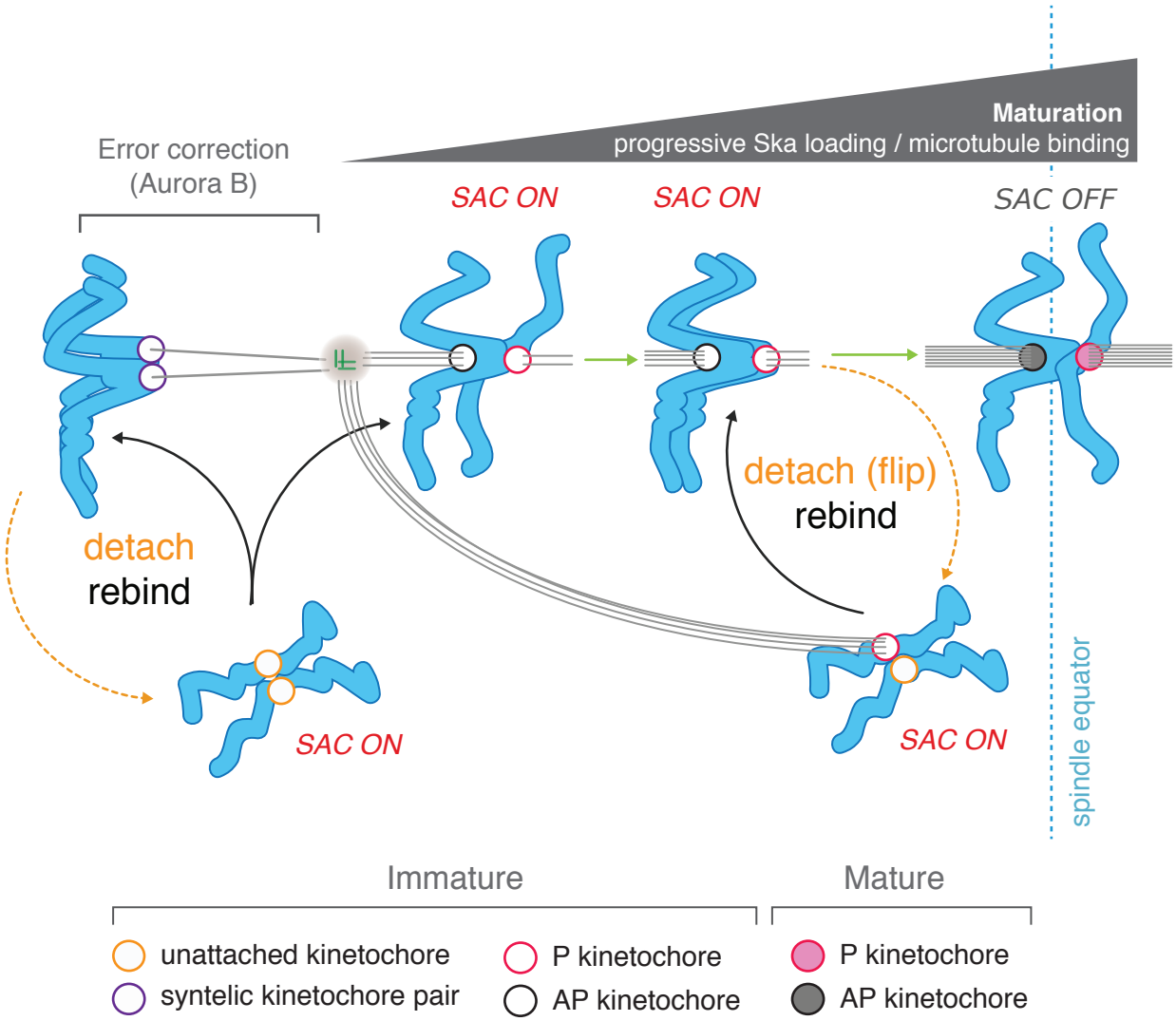

Figure 34: A model for bi-oriented kinetochore maturation and attachment regulation during congression

Behind the pole, the canonical Aurora B error correction pathway destabilizes erroneous attachments (such as syntelic) in response to a lack of tension, promoting the formation of bi-oriented attachments. These unaligned bi-oriented kinetochore pairs then utilise DCP to congress to the spindle equator. During this migration each kinetochore progressively loads the Ska complex and recruits microtubules, reaching full maturity once at the metaphase plate. This progressive Ska complex recruitment confers increasing load-bearing capacity on the structure, enabling kinetochores to efficiently track the depolymerising K-fiber microtubules, which are increasing in number and stability. These unaligned, immature kinetochore-pairs also signal the SAC during congression, therefore creating a 'wait anaphase' signal until all chromosomes have aligned. We propose that this maturation is part of a mechanical microtubule attachment self-check. If the kinetochore does not recruit sufficient Ska complexes (which is required for load-stable attachment) it will detach from its associated K-fiber. The casues the cell to arrested in prometaphase through the SAC, enabling the kinetochore-pair to reattach and fully mature prior to alignment. This would ensure that only load-stable, and therefore anaphase compatible, kinetochore-pairs reach the metaphase plate.

periods of coherence. Slow maturation would therefore decrease the load-bearing capacity of the structure, and may lead to detachment (Fig 34). These mechanics would therefore only allow for mature kinetochores, in terms of Ska complex number and bound microtubules, to persist through to anaphase, as those that flip would activate the SAC. Indeed, flip events in wild-type cells are typically followed by attachment and successful congression, whereas in Ska1 depleted cells, kinetochores are trapped in a futile detachment-reattachment-detachment cycle that prevents mitotic progression. Thus, episodes of detachment-attachment in wild type cells may represent some kind of mechanical self-check on the attachment (Fig 34). Developing the tools to monitor maturation state and microtubule occupancy at actively congressing kinetochores will be vital for further validation of this model.

Our data also suggests that the Ska complex has a bimodal recruitment pathway. In terms of temporal organisation, we suggest that Ndc80 loads an initial pool to unattached sister-pairs (Zhang et al., 2012), and upon bi-orientation and congression via DCP, additional Ska complex are ‘swept-up’ from the microtubule lattice. Future experiments in which the movement of K-fibre associated Ska complex is followed using photo-activatable flurophores can be used to directly test this idea. Moreover, correlating kinetochore movement directionality with Ska complex enrichment would show if K-fiber tracking is indeed responsible for its loading. As one would expect P-movement to be associated with complex recruitment.

How these newly loaded complexes are retained at the kinetochore is also unclear, as overexpression of Ska1ΔMTBD, which is loaded to kinetochores but not the spindle, cannot push Ska1 recruitment to a level beyond that observed for endogenous Ska complex in nocodazole. This suggests that the cytoplasmic pool of the Ska complex is not limiting its microtubule independent recruitment by Ndc80. Instead, this Ndc80 loading pathway appears to be saturated. As such, the Ska complex may have an additional interaction partner(s) at the kinetochore, or its oligomerisation at the kinetochore may be key for complex retention. This model also predicts that kinetochores congressing via CENP-E sliding would be Ska immature but located within the metaphase plate. In agreement, we do observe aligned kinetochores with low Ska1 levels. Analysis of the microtubule attachment state at these aligned, Ska1 immature kinetochore-pairs using correlative light electron microscopy will be key in determining if this is true.

The loss of attachment during flipping, in theory, reverts the kinetochore to a completely immature state. In this regard, we have shown that unaligned non-bi-oriented sister-pairs have roughly half the number of Ska complexes compared to their bi-oriented counterparts, and ~75% less than those aligned and bi-oriented. As such, it will be important to assess how the maturation status of these flipping kinetochores changes after detachment. One would predict that the RZZ pathway of SAC activation would be reactivated, as the microtubule-dependent dynein silencing pathway would be abrogated. Whether the Ska complex is subsequently unloaded is an

open question, however, given that its maturation is key for successful congression, its removal from the kinetochore would seem disadvantageous. This idea also raises questions about how maturation is linked to microtubule occupancy, and if bi-orientation induces irreversible structural changes in the kinetochore that allow for the maintenance of maturation in a microtubule independent manner.

6.6 *Linking Ska complex maturation to SAC signalling*

Our data provides evidence that immature (judged by Ska1 loading) bi-oriented kinetochores can generate a SAC signal (shown through Bub1 loading). Importantly, this signal is not linked to congression, as Ska1 mature kinetochores, regardless of spindle position, typically have low Bub1. However, given that Ska1 matures as chromosomes congress, the unloading of Bub1 often correlates with alignment at the metaphase plate. This behaviour is kinetochore autonomous, with individual sisters within a pair often observed with opposite Ska1/Bub1 loading profiles. Suggesting that kinetochores do not communicate their maturation or SAC state to their sister, and the dynamics of both are likely regulated by microtubule binding at the single kinetochore level. Recently, it has been suggested that two kinetochore state dependent SAC pathways operate to ensure a robust wait-anaphase signal is produced (Silio et al., 2015). Here, the RZZ pathway loads Mad1:Mad2 to unattached kinetochores, whereas the KBB

pathway loads Bub1:Bub3 to kinetochores that are oriented but unaligned (which are analogous to the immature bi-oriented reported here). The relationship between Ska1 maturation and Bub1 loading provides compelling further evidence that the KBB pathway operates downstream of bi-orientation to generate a SAC signal when kinetochores are immature (Fig 34). This idea that may explain why cells delay anaphase until all chromosomes are aligned, even when unaligned kinetochores are bi-oriented, as these would be immature and therefore generate an attachment independent SAC signal. It will be important to test Mad2 levels at these immature bi-oriented kinetochores, as previous work has suggested that it is unloaded as soon as the K-K axis orients along the spindle axis (Magidson et al., 2015). Nevertheless, is has been shown that high steady-state Mad1:Mad2 is not required for SAC signalling, and a robust 'wait-anaphase' signal can be generated by non-detectable levels of the complex (Martin-Lluesma et al., 2002). While it is very unlikely that Ska complex maturation and SAC signalling are causally linked, they may share a common molecular signal, such as microtubule occupancy or another factor that displays maturation dependent dynamicity.

6.7 *Conclusion and future directions*

From its origins in the polar repulsion and traction fiber models, congression can now be though of as a multi-step process that involves an

array of spindle positions, attachments states and molecular mediators. Here, we have focused on bi-oriented chromosomes utilising depolymerisation-coupled pulling to congress to the equator. By employing single-kinetochore tracking with specific molecular perturbations, we have assigned precise functions to individual kinetochore components. How these factors are integrated at the microtubule plus-end, how they are temporally phospho-regulated, and how they are conserved across multiple cell types are key further questions.

While it is clear that two congression mechanisms exist, the relative contributions of these processes are still poorly understood in the context of pole-to-plate movement. As such, identifying direct markers of lateral and end-on attachment states that can be followed in live cells will greatly improve our understanding. Such markers will likely be associated with the precise molecular alterations induced by the formation of a stable end-on attachment. How these changes occur, and whether they be structural, dependent on tension, or biochemical signals will be influential not only in our understanding of congression, but contribute to models of maturation, error correction and checkpoint signalling. All of which need to be tightly regulated to ensure the error free transmission of genetic material.

References

Abad, M.A., B. Medina, A. Santamaria, J. Zou, C. Plasberg-Hill, A. Madhumalar, U. Jayachandran, P.M. Redli, J. Rappsilber, E.A. Nigg, and A.A. Jeyaprakash. 2014. Structural basis for microtubule recognition by the human kinetochore Ska complex. *Nature communications*. 5:2964.

Abad, M.A., J. Zou, B. Medina-Pritchard, E.A. Nigg, J. Rappsilber, A. Santamaria, and A.A. Jeyaprakash. 2016. Ska3 Ensures Timely Mitotic Progression by Interacting Directly With Microtubules and Ska1 Microtubule Binding Domain. *Scientific reports*. 6:34042.

Adams, R.R., S.P. Wheatley, A.M. Gouldsworthy, S.E. Kandels-Lewis, M. Carmena, C. Smythe, D.L. Gerloff, and W.C. Earnshaw. 2000. INCENP binds the Aurora-related kinase AIRK2 and is required to target it to chromosomes, the central spindle and clevage furrow. *Current biology : CB*. 10:1075-1078.

Ahonen, L.J., A.M. Kukkonen, J. Pouwels, M.A. Bolton, C.D. Jingle, P.T. Stukenberg, and M.J. Kallio. 2009. Perturbation of Incenp function impedes anaphase chromatid movements and chromosomal passenger protein flux at centromeres. *Chromosoma*. 118:71-84.

Ainsztein, A.M., S.E. Kandels-Lewis, A.M. Mackay, and W.C. Earnshaw. 1998. INCENP centromere and spindle targeting: identification of essential conserved motifs and involvement of heterochromatin protein HP1. *J Cell Biol*. 143:1763-1774.

Akera, T., Y. Goto, M. Sato, M. Yamamoto, and Y. Watanabe. 2015. Mad1 promotes chromosome congression by anchoring a kinesin motor to the kinetochore. *Nat Cell Biol*. 17:1124-1133.

Alushin, G.M., V. Musinipally, D. Matson, J. Tooley, P.T. Stukenberg, and E. Nogales. 2012. Multimodal microtubule binding by the Ndc80 kinetochore complex. *Nature structural & molecular biology*. 19:1161-1167.

Alushin, G.M., V.H. Ramey, S. Pasqualato, D.A. Ball, N. Grigorieff, A. Musacchio, and E. Nogales. 2010. The Ndc80 kinetochore complex forms oligomeric arrays along microtubules. *Nature*. 467:805-810.

Amano, M., A. Suzuki, T. Hori, C. Backer, K. Okawa, I.M. Cheeseman, and T. Fukagawa. 2009. The CENP-S complex is essential for the stable assembly of outer kinetochore structure. *J Cell Biol*. 186:173-182.

Amaro, A.C., C.P. Samora, R. Holtackers, E. Wang, I.J. Kingston, M. Alonso, M. Lampson, A.D. McAinsh, and P. Meraldi. 2010. Molecular control of kinetochore-microtubule dynamics and chromosome oscillations. *Nat Cell Biol*. 12:319-329.

Andrews, P.D., Y. Ovechkina, N. Morrice, M. Wagenbach, K. Duncan, L. Wordeman, and J.R. Swedlow. 2004. Aurora B regulates MCAK at the mitotic centromere. *Developmental cell*. 6:253-268.

Antonio, C., I. Ferby, H. Wilhelm, M. Jones, E. Karsenti, A.R. Nebreda, and I. Vernos. 2000. Xkid, a chromokinesin required for chromosome alignment on the metaphase plate. *Cell*. 102:425-435.

Armond, J.W., E. Vladimirou, M. Erent, A.D. McAinsh, and N.J. Burroughs. 2015. Probing microtubule polymerisation state at single kinetochores during metaphase chromosome motion. *J Cell Sci*. 128:1991-2001.

Auckland, P., and A.D. McAinsh. 2015. Building an integrated model of chromosome congression. *J Cell Sci*. 128:3363-3374.

Ault, j.G., A.J. DeMarco, E.D. Salmon, and C.L. Rieder. 1991. Studies on the ejection properties of asters: astral microtubule turnover influences the oscillatory behaviour and positioning of monoorientated chromosomes. *J. Cell. Sci*. 99:701-710.

Ault, J.G., and C.L. Rieder. 1992. Chromosome mal-orienatation and reorientation during mitosis. *Cell Motil. Cytoskeleton*. 22:155-159.

Bancroft, J., P. Auckland, C.P. Samora, and A.D. McAinsh. 2015. Chromosome congression is promoted by CENP-Q- and CENP-E-dependent pathways. *J Cell Sci*. 128:171-184.

Barisic, M., P. Aguiar, S. Geley, and H. Maiato. 2014. Kinetochore motors drive congression of peripheral polar chromosomes by overcoming random arm-ejection forces. *Nat Cell Biol*. 16:1249-1256.

Barisic, M., R. Silva e Sousa, S.K. Tripathy, M.M. Magiera, A.V. Zaytsev, A.L. Pereira, C. Janke, E.L. Grishchuk, and H. Maiato. 2015. Microtubule detrosination guides chromosomes during mitosis. *Science*. 348:799-803.

Barisic, M., B. Sohm, P. Mikolcevic, C. Wandke, V. Rauch, T. Ringer, M. Hess, G. Bonn, and S. Geley. 2010. Spindly/CCDC99 is required for efficient chromosome congression and mitotic checkpoint regulation. *Mol Biol Cell*. 21:1968-1981.

Basilico, F., S. Maffini, J.R. Weir, D. Prumbaum, A.M. Rojas, T. Zimniak, A. De Antoni, S. Jeganathan, B. Voss, S. van Gerwen, V. Krenn, L. Massimiliano, A. Valencia, I.R. Vetter, F. Herzog, S. Raunser, S. Pasqualato, and A. Musacchio. 2014. The pseudo GTPase CENP-M drives human kinetochore assembly. *eLife*. 3:e02978.

Bassett, E.A., J. DeNizio, M.C. Barnhart-Dailey, T. Panchenko, N. Sekulic, D.J. Rogers, D.R. Foltz, and B.E. Black. 2012. HJURP uses distinct CENP-A surfaces to recognize and to stabilize CENP-A/histone H4 for centromere assembly. *Developmental cell*. 22:749-762.

Beadle, G.W. 1932. A possible influence of the spindle fiber on crossing-over in drosophila. *Proc Natl Acad Sci U S A*. 18:160-165.

Beardmore, V.A., L.J. Ahonen, G.J. Gorbsky, and M.J. Kallio. 2004. Survivin dynamics increases at centromeres during G2/M phase transition and is regulated by microtubule-attachment and Aurora B kinase activity. *J Cell Sci*. 117:4033-4042.

Benison, G., P.A. Karplus, and E. Barbar. 2007. Structure and dynamics of LC8 complexes with KXTQT-motif peptides: swallow and dynein

intermediate chain compete for a common site. *Journal of molecular biology*. 371:457-468.
Bieling, P., I. Kronja, and T. Surrey. 2010. Microtubule motility on reconstituted meiotic chromatin. *Current biology : CB*. 20:763-769.
Bishop, J.D., and J.M. Schumacher. 2002. Phosphorylation of the carboxyl terminus of inner centromere protein (INCENP) by the Aurora B Kinase stimulates Aurora B kinase activity. *The Journal of biological chemistry*. 277:27577-27580.
Black, B.E., L.E. Jansen, P.S. Maddox, D.R. Foltz, A.B. Desai, J.V. Shah, and D.W. Cleveland. 2007. Centromere identity maintained by nucleosomes assembled with histone H3 containing the CENP-A targeting domain. *Mol Cell*. 25:309-322.
Bodor, D.L., J.F. Mata, M. Sergeev, A.F. David, K.J. Salimian, T. Panchenko, D.W. Cleveland, B.E. Black, J.V. Shah, and L.E. Jansen. 2014. The quantitative architecture of centromeric chromatin. *eLife*. 3:e02137.
Bomont, P., P. Maddox, J.V. Shah, A.B. Desai, and D.W. Cleveland. 2005. Unstable microtubule capture at kinetochores depleted of the centromere-associated protein CENP-F. *EMBO*. 24:3927-3939.
Brinkley, B.R., and E. Stubblefield. 1966. The fine structure of the kinetochore of a mammalian cell in vitro. *Chromosoma*. 19:28-43.
Brouhard, G.J., and A.J. Hunt. 2005. Microtubule movements on the arms of mitotic chromosomes: polar ejection forces quantified in vitro. *Proc Natl Acad Sci U S A*. 102:13903-13908.
Brust-Mascher, I., and J.M. Scholey. 2002. Microtubule flux and sliding in mitotic spindles of Drosophila embroys. *Mol Biol Cell*. 13:3967-3975.
Buffin, E., C. Lefebvre, J. Huang, M.E. Gagou, and R.E. Karess. 2005. Recruitment of Mad2 to the kinetochore requires the Rod/Zw10 complex. *Current biology : CB*. 15:856-861.
Cai, S., C.B. O'Connell, A. Khodjakov, and C.E. Walczak. 2009. Chromosome congression in the absence of kinetochore fibres. *Nat Cell Biol*. 11:832-838.
Cane, S., A.A. Ye, S.J. Luks-Morgan, and T.J. Maresca. 2013. Elevated polar ejection forces stabilize kinetochore-microtubule attachments. *J Cell Biol*. 200:203-218.
Carroll, C.W., K.J. Milks, and A.F. Straight. 2010. Dual recognition of CENP-A nucleosomes is required for centromere assembly. *J Cell Biol*. 189:1143-1155.
Carroll, C.W., M.C. Silva, K.M. Godek, L.E. Jansen, and A.F. Straight. 2009. Centromere assembly requires the direct recognition of CENP-A nucleosomes by CENP-N. *Nat Cell Biol*. 11:896-902.
Carter, A.P., C. Cho, L. Jin, and R.D. Vale. 2011. Crystal structure of the dynein motor domain. *Science*. 331:1159-1161.
Cassimeris, L., C.L. Rieder, and E.D. Salmon. 1994. Microtubule assembly and kinetochore directional instability in vertebrate monopolar

spindles: implications for the mechanism of chromosome congression. *J. Cell. Sci*. 107:285-297.
Cassimeris, L., and E.D. Salmon. 1991. Kinetochore microtubules shorten by loss of subunits at the kinetochores of prometaphase chromosomes. *J. Cell. Sci*. 98:151-158.
Centonze, V.E., and G.G. Borisy. 1991. Pole-to-chromosome movements induced at metaphase: sites of microtubule disassembly. *J. Cell. Sci*. 100:205-211.
Chan, C.S.M., and D. Botstein. 1993. Isolation and characterization of chromosome-gain and increase-in-ploidy mutants in yeast *Genetics*. 135:677-691.
Chan, G.K.T., B.T. Schaar, and T.J. Yen. 1998. Characterization of the kinetochore binding domain of CENP-E reveals interactions with the kinetochore proteins CENP-F and hBUBR1. *J Cell Biol*. 143:49-63.
Chan, Y.W., L.L. Fava, A. Uldschmid, M.H. Schmitz, D.W. Gerlich, E.A. Nigg, and A. Santamaria. 2009. Mitotic control of kinetochore-associated dynein and spindle orientation by human Spindly. *J Cell Biol*. 185:859-874.
Chan, Y.W., A.A. Jeyaprakash, E.A. Nigg, and A. Santamaria. 2012. Aurora B controls kinetochore-microtubule attachments by inhibiting Ska complex-KMN network interaction. *J Cell Biol*. 196:563-571.
Cheerambathur, D.K., R. Gassmann, B. Cook, K. Oegema, and A. Desai. 2013. Crosstalk betweem microtubule attachment complexes ensures accurate chromosome segregation. *Science*. 342:1239-1242.
Cheeseman, I.M., J.S. Chappie, E.M. Wilson-Kubalek, and A. Desai. 2006. The conserved KMN network constitutes the core microtubule-binding site of the kinetochore. *Cell*. 127:983-997.
Cheeseman, I.M., and A. Desai. 2008. Molecular architecture of the kinetochore-microtubule interface. *Nature reviews. Molecular cell biology*. 9:33-46.
Cheeseman, I.M., M. Enquist-Newman, T. Müller-Reichert, D.G. Drubin, and G. Barnes. 2001. Mitotic spindle integrity and kinetochore function linked by the Duo1p/Dam1p complex. *J Cell Biol*. 152:197-212.
Cheeseman, I.M., S. Niessen, S. Anderson, F. Hyndman, J.R. Yates, 3rd,, K. Oegema, and A. Desai. 2004. A conserved protein network controls assembly of the outer kinetochore and its ability to sustain tension. *Genes & development*. 18:2255-2268.
Chen, R.H. 2002. BubR1 is essential for kinetochore localization of other spindle checkpoint proteins and its phosphorylation requires Mad1. *J Cell Biol*. 158:487-496.
Chowdhury, S., S.A. Ketcham, T.A. Schroer, and G.C. Lander. 2015. Structural organization of the dynein-dynactin complex bound to microtubules. *Nature structural & molecular biology*. 22:345-347.

Ciferri, C., S. Pasqualato, E. Screpanti, G. Varetti, S. Santaguida, G. Dos Reis, A. Maiolica, J. Polka, J.G. De Luca, P. De Wulf, M. Salek, J. Rappsilber, C.A. Moores, E.D. Salmon, and A. Musacchio. 2008. Implications for kinetochore-microtubule attachment from the structure of an engineered Ndc80 complex. *Cell*. 133:427-439.

Cimini, D., L.A. Cameron, and E.D. Salmon. 2004. Anaphase spindle mechanics prevent mis-segregation of merotelically oriented chromosomes. *Current biology : CB*. 14:2149-2155.

Cimini, D., B. Howell, P. Maddox, A. Khodjakov, F. Degrassi, and E.D. Salmon. 2001. Merotelic kinetochore orientation is a major mechanism of aneuploidy in mitotic mammalian tissue cells *J Cell Biol*. 153:517-527.

Cimini, D., B. Moree, J.C. Canman, and E.D. Salmon. 2003. Merotelic kinetochore orientation occurs frequently during early mitosis in mammalian tissue cells and error correction is achieved by two different mechanisms. *J Cell Sci*. 116:4213-4225.

Cimini, D., X. Wan, C.B. Hirel, and E.D. Salmon. 2006. Aurora kinase promotes turnover of kinetochore microtubules to reduce chromosome segregation errors. *Current biology : CB*. 16:1711-1718.

Collin, P., O. Nashchekina, R. Walker, and J. Pines. 2013. The spindle assembly checkpoint works like a rheostat rather than a toggle switch. *Nat Cell Biol*. 15:1378-1385.

Cooke, C.A., M. Margarete, S. Heck, and W.C. Earnshaw. 1987. The inner centromere protein (INCENP) antigens: movement from inner centromere to midbody during mitosis. *J Cell Biol*. 105:2053-2067.

Cross, R.A., and A. McAinsh. 2014. Prime movers: the mechanochemistry of mitotic kinesins. *Nature reviews. Molecular cell biology*. 15:257-271.

Czaban, B.B., A. Forer, and A.S. Bajer. 1993. Ultraviolet microbeam irradiation of chromosomal spindle fibres in Haemanthus katherinae endosperm I. Behaviour of the irradiated region. *J. Cell. Sci* 105:571-578.

Czechanski, A., H. Kim, C. Byers, I. Greenstein, J. Stumpff, and L.G. Reinholdt. 2015. Kif18a is specifically required for mitotic progression during germ line development. *Developmental biology*. 402:253-262.

Darlington, C.D. 1937. Recent advances in cytology, 2nd edition. Blackston Co, Philadelphia.

DeLuca, K.F., S.M. Lens, and J.G. DeLuca. 2011. Temporal changes in Hec1 phosphorylation control kinetochore-microtubule attachment stability during mitosis. *J Cell Sci*. 124:622-634.

Dick, A.E., and D.W. Gerlich. 2013. Kinetic framework of spindle assembly checkpoint signalling. *Nat Cell Biol*. 15:1370-1377.

Ditchfield, C., V.L. Johnson, A. Tighe, R. Ellston, C. Haworth, T. Johnson, A. Mortlock, N. Keen, and S.S. Taylor. 2003. Aurora B couples

chromosome alignment with anaphase by targeting BubR1, Mad2, and Cenp-E to kinetochores. *J Cell Biol*. 161:267-280.
Dou, Z., X. Liu, W. Wang, T. Zhu, X. Wang, L. Xu, A. Abrieu, C. Fu, D.L. Hill, and X. Yao. 2015. Dynamic localization of Mps1 kinase to kinetochores is essential for accurate spindle microtubule attachment. *Proc Natl Acad Sci U S A*. 112:E4546-4555.
Du, J., A.E. Kelly, H. Funabiki, and D.J. Patel. 2012. Structural basis for recognition of H3T3ph and Smac/DIABLO N-terminal peptides by human Survivin. *Structure*. 20:185-195.
Du, Y., C.A. English, and R. Ohi. 2010. The kinesin-8 Kif18A dampens microtubule plus-end dynamics. *Current biology : CB*. 20:374-380.
Dumont, S., E.D. Salmon, and T.J. Mitchison. 2012. Deformations within moving kinetochores reveal different sits of active and passive force generation. *Science*. 337:355-358.
Dunsch, A.K., E. Linnane, F.A. Barr, and U. Gruneberg. 2011. The astrin-kinastrin/SKAP complex localizes to microtubule plus ends and facilitates chromosome alignment. *J Cell Biol*. 192:959-968.
Earnshaw, W.C., and R.L. Bernat. 1991. Chromosomal passengers: toward an integrated view of mitosis. *Chromosoma*. 100:139-146.
Earnshaw, W.C., and B.R. Migeon. 1985. Three related centromere proteins are absent from the inactive centromere of a stable isodicentric chromosome. *Chromosoma*. 92:290-296.
Earnshaw, W.C., and N. Rothfield. 1985. Identification of a family of human centromere proteins using autoimmune sera from patients with scleroderma. *Chromosoma*. 91:313-321.
Echeverri, C.J., B.M. Paschal, K.T. Vaughan, and R.B. Vallee. 1996. Molecular characterization of the 50-kD subunit of dynactin reveals function for the complex in chromosome alignment and spindle organisation in mitosis. *J Cell Biol*. 132:617-633.
Eskat, A., W. Deng, A. Hofmeister, S. Rudolphi, S. Emmerth, D. Hellwig, T. Ulbricht, V. Doring, J.M. Bancroft, A.D. McAinsh, M.C. Cardoso, P. Meraldi, C. Hoischen, H. Leonhardt, and S. Diekmann. 2012. Step-wise assembly, maturation and dynamic behavior of the human CENP-P/O/R/Q/U kinetochore sub-complex. *PloS one*. 7:e44717.
Fachinetti, D., H.D. Folco, Y. Nechemia-Arbely, L.P. Valente, K. Nguyen, A.J. Wong, Q. Zhu, A.J. Holland, A. Desai, L.E. Jansen, and D.W. Cleveland. 2013. A two-step mechanism for epigenetic specification of centromere identity and function. *Nat Cell Biol*. 15:1056-1066.
Fang, J., Y. Liu, Y. Wei, W. Deng, Z. Yu, L. Huang, Y. Teng, T. Yao, Q. You, H. Ruan, P. Chen, R.M. Xu, and G. Li. 2015. Structural transitions of centromeric chromatin regulate the cell cycle-dependent recruitment of CENP-N. *Genes & development*. 29:1058-1073.
Fang, L., A. Seki, and G. Fang. 2009. SKAP associates with kinetochores and promotes the metaphase-to-anaphase transition. *Cell cycle*. 8:2819-2827.

Feng, J., H. Huang, and T.J. Yen. 2006. CENP-F is a novel microtubule-binding protein that is essential for kinetochore attachments and affects the duration of the mitotic checkpoint delay. *Chromosoma*. 115:320-329.

Ferreira, J.G., A.J. Pereira, and H. Maiato. 2014. Microtubule plus-end tracking proteins and their roles in cell division. *Int Rev Cell Mol Biol*. 309:59-140.

Fischle, W., B.S. Tseng, H.L. Dormann, B.M. Ueberheide, B.A. Garcia, J. Shabanowitz, D.F. Hunt, H. Funabiki, and C.D. Allis. 2005. Regulation of HP1-chromatin binding by histone H3 methylation and phosphorylation. *Nature*. 438:1116-1122.

Flemming, W. 1882. Zellsubstanz, Kern und Zelltheilung. *Leipzig*.

Folco, H.D., C.S. Campbell, K.M. May, C.A. Espinoza, K. Oegema, K.G. Hardwick, S.I. Grewal, and A. Desai. 2015. The CENP-A N-tail confers epigenetic stability to centromeres via the CENP-T branch of the CCAN in fission yeast. *Current biology : CB*. 25:348-356.

Foltz, D.R., L.E. Jansen, B.E. Black, A.O. Bailey, J.R. Yates, 3rd, and D.W. Cleveland. 2006. The human CENP-A centromeric nucleosome-associated complex. *Nat Cell Biol*. 8:458-469.

Fremont, S., A. Gerard, M. Galloux, K. Janvier, R.E. Karess, and C. Berlioz-Torrent. 2013. Beclin-1 is required for chromosome congression and proper outer kinetochore assembly. *EMBO reports*. 14:364-372.

Fujita, Y., T. Hayashi, T. Kiyomitsu, Y. Toyoda, A. Kokubu, C. Obuse, and M. Yanagida. 2007. Priming of centromere for CENP-A recruitment by human hMis18alpha, hMis18beta, and M18BP1. *Developmental cell*. 12:17-30.

Fukagawa, T., and W.C. Earnshaw. 2014. The centromere: chromatin foundation for the kinetochore machinery. *Developmental cell*. 30:496-508.

Fukagawa, T., Y. Mikami, A. Nishihashi, V. Regnier, T. Haraguchi, Y. Hiraoka, N. Sugata, K. Todokoro, W. Brown, and T. Ikemura. 2001. CENP-H, a constitutive centromere component, is required for centromere targeting of CENP-C in vertebrate cells. *EMBO*. 20:4603-4617.

Funabiki, H., and A.W. Murray. 2000. The Xenopus chromokinesin Xkid is essential for metaphase chromosome alignment and must be degraded to allow anaphase chromosome movement. *Cell*. 102:411-424.

Gaitanos, T.N., A. Santamaria, A.A. Jeyaprakash, B. Wang, E. Conti, and E.A. Nigg. 2009. Stable kinetochore-microtubule interactions depend on the Ska complex and its new component Ska3/C13Orf3. *The EMBO journal*. 28:1442-1452.

Ganem, N.J., K. Upton, and D.A. Compton. 2005. Efficient mitosis in human cells lacking poleward microtubule flux. *Current biology : CB*. 15:1827-1832.

Ganguly, A., R. Bhattacharya, and F. Cabral. 2012. Control of MCAK degradation and removal from centromeres. *Cytoskeleton*. 69:303-311.

Gascoigne, K.E., K. Takeuchi, A. Suzuki, T. Hori, T. Fukagawa, and I.M. Cheeseman. 2011. Induced ectopic kinetochore assembly bypasses the requirement for CENP-A nucleosomes. *Cell*. 145:410-422.

Gassmann, R., A.J. Holland, D. Varma, X. Wan, F. Civril, D.W. Cleveland, K. Oegema, E.D. Salmon, and A. Desai. 2010. Removal of Spindly from microtubule-attached kinetochores controls spindle checkpoint silencing in human cells. *Genes & development*. 24:957-971.

Gonen, S., B. Akiyoshi, M.G. Iadanza, D. Shi, N. Duggan, S. Biggins, and T. Gonen. 2012. The structure of purified kinetochores reveals multiple microtubule-attachment sites. *Nature structural & molecular biology*. 19:925-929.

Gorbsky, G.J., P.J. Sammak, and G.G. Borisy. 1987. Chromosomes move poleward in anaphase along stationary microtubules that coordinately diassemble from their kinetochore ends *J Cell Biol*. 104:9-18.

Gregan, J., S. Polakova, L. Zhang, I.M. Tolic-Norrelykke, and D. Cimini. 2011. Merotelic kinetochore attachment: causes and effects. *Trends in cell biology*. 21:374-381.

Grishchuk, E.L., M.I. Molodtsov, F.I. Ataullakhanov, and J.R. McIntosh. 2005. Force production by disassembling microtubules. *Nature*. 438:384-388.

Grishchuk, E.L., I.S. Spiridonov, V.A. Volkov, A. Efremov, S. Westermann, D. Drubin, G. Barnes, F.I. Ataullakhanov, and J.R. McIntosh. 2008. Different assemblies of the DAM1 complex follow shortening microtubules by distinct mechanisms. *Proc Natl Acad Sci U S A*. 105:6918-6923.

Gudimchuk, N., B. Vitre, Y. Kim, A. Kiyatkin, D.W. Cleveland, F.I. Ataullakhanov, and E.L. Grishchuk. 2013. Kinetochore kinesin CENP-E is a processive bi-directional tracker of dynamic microtubule tips. *Nat Cell Biol*. 15:1079-1088.

Guimaraes, G.J., Y. Dong, B.F. McEwen, and J.G. Deluca. 2008. Kinetochore-microtubule attachment relies on the disordered N-terminal tail domain of Hec1. *Current biology : CB*. 18:1778-1784.

Hafner, J., M.I. Mayr, M.M. Mockel, and T.U. Mayer. 2014. Pre-anaphase chromosome oscillations are regulated by the antagonistic activities of Cdk1 and PP1 on Kif18A. *Nature communications*. 5:4397.

Hanisch, A., H.H.W. Silljé, and E.A. Nigg. 2006. Timely anaphase onset requires a novel spindle and kinetochore complex comprising Ska1 and Ska2. *EMBO*. 25:5504-5515.

Harrington, J.J., G. Van Bokkelen, R.W. Mays, K. Gustashaw, and H.F. Willard. 1997. Formation of de novo centromeres and construction of first-generation human artificial microchromosomes. *Nature Genetics*. 15:345-355.

Hauf, S., R.W. Cole, S. LaTerra, C. Zimmer, G. Schnapp, R. Walter, A. Heckel, J. van Meel, C.L. Rieder, and J.M. Peters. 2003. The small molecule Hesperadin reveals a role for Aurora B in correcting kinetochore-microtubule attachment and in maintaining the spindle assembly checkpoint. *J Cell Biol*. 161:281-294.

Hayashi, T., Y. Fujita, O. Iwasaki, Y. Adachi, K. Takahashi, and M. Yanagida. 2004. Mis16 and Mis18 are required for CENP-A loading and histone deacetylation at centromeres. *Cell*. 118:715-729.

Hayashi-Takanaka, Y., K. Yamagata, N. Nozaki, and H. Kimura. 2009. Visualizing histone modifications in living cells: spatiotemporal dynamics of H3 phosphorylation during interphase. *J Cell Biol*. 187:781-790.

Hays, T.S., and E.D. Salmon. 1990. Poleward force at the kinetochore in metaphase depends on the number of kinetochore microtubules. *J Cell Biol*. 110:391-404.

Hays, T.S., D. Wise, and E.D. Salmon. 1982. Traction force on a kinetochore at metaphase acts as a linear function of kinetochore fiber length *J Cell Biol*. 93:374-382.

Hellwig, D., S. Emmerth, T. Ulbricht, V. Doring, C. Hoischen, R. Martin, C.P. Samora, A.D. McAinsh, C.W. Carroll, A.F. Straight, P. Meraldi, and S. Diekmann. 2011. Dynamics of CENP-N kinetochore binding during the cell cycle. *J Cell Sci*. 124:3871-3883.

Hemmerich, P., S. Weidtkamp-Peters, C. Hoischen, L. Schmiedeberg, I. Erliandri, and S. Diekmann. 2008. Dynamics of inner kinetochore assembly and maintenance in living cells. *J Cell Biol*. 180:1101-1114.

Hill, T.L. 1985. Theoretical problems related to the attachment of microtubules to kinetochores. *Proc Natl Acad Sci U S A*. 82:4404-4408.

Hirota, T., J.J. Lipp, B.H. Toh, and J.M. Peters. 2005. Histone H3 serine 10 phosphorylation by Aurora B causes HP1 dissociation from heterochromatin. *Nature*. 438:1176-1180.

Hiruma, Y., C. Sacritan, S.T. Pachis, A. Adamopoulos, T. Kuijt, E. von Castelmur, A. Perrakis, and G.J. Kops. 2015. Competition between MPS1 and microtubules at kinetochores regulates spindle checkpoint signalling. *Science*. 348:1264-1267.

Holt, S.V., M.A. Vergnolle, D. Hussein, M.J. Wozniak, V.J. Allan, and S.S. Taylor. 2005. Silencing Cenp-F weakens centromeric cohesion, prevents chromosome alignment and activates the spindle checkpoint. *J Cell Sci*. 118:4889-4900.

Honda, R., R. Korner, and E.A. Nigg. 2003. Exploring the functional interactions between Aurora B, INCENP, and survivin in mitosis *Mol Biol Cell*. 14:3325-3341.

Honnappa, S., S.M. Gouveia, A. Weisbrich, F.F. Damberger, N.S. Bhavesh, H. Jawhari, I. Grigoriev, F.J. van Rijssel, R.M. Buey, A. Lawera, I. Jelesarov, F.K. Winkler, K. Wuthrich, A. Akhmanova, and M.O.

Steinmetz. 2009. An EB1-binding motif acts as a microtubule tip localization signal. *Cell*. 138:366-376.
Hooke, R. 1665. Micrographia. *London*.
Hori, T., M. Amano, A. Suzuki, C.B. Backer, J.P. Welburn, Y. Dong, B.F. McEwen, W.H. Shang, E. Suzuki, K. Okawa, I.M. Cheeseman, and T. Fukagawa. 2008a. CCAN makes multiple contacts with centromeric DNA to provide distinct pathways to the outer kinetochore. *Cell*. 135:1039-1052.
Hori, T., M. Okada, K. Maenaka, and T. Fukagawa. 2008b. CENP-O Class Proteins Form a Stable Complex and Are Required for Proper Kinetochore Function. *Mol Biol Cell* 19:843-854.
Howell, B.J. 2001. Cytoplasmic dynein/dynactin drives kinetochore protein transport to the spindle poles and has a role in mitotic spindle checkpoint inactivation. *J Cell Biol*. 155:1159-1172.
Howell, B.J., D.B. Hoffman, G. Fang, A.W. Murray, and E.D. Salmon. 2000. Visualization of Mad2 Dynamics at Kinetochores, along Spindle Fibers, and at Spindle Poles in Living Cells. *J Cell Biol*. 150:1233-1249.
Howell, B.J., B. Moree, E.M. Farrar, S. Stewart, G. Fang, and E.D. Salmon. 2004. Spindle checkpoint protein dynamics at kinetochores in living cells. *Current biology : CB*. 14:953-964.
Hoyt, M.A., L. Totis, and B.T. Roberts. 1991. S. cerevisiae genes required for cell cycle arrest in response to loss of microtubule function. *Cell*. 66:507-517.
Hu, H., Y. Liu, M. Wang, J. Fang, H. Huang, N. Yang, Y. Li, J. Wang, X. Yao, Y. Shi, G. Li, and R.M. Xu. 2011. Structure of a CENP-A-histone H4 heterodimer in complex with chaperone HJURP. *Genes & development*. 25:901-906.
Huang, H., J. Feng, J. Famulski, J.B. Rattner, S.T. Liu, G.D. Kao, R. Muschel, G.K. Chan, and T.J. Yen. 2007. Tripin/hSgo2 recruits MCAK to the inner centromere to correct defective kinetochore attachments. *J Cell Biol*. 177:413-424.
Huang, Y., W. Wang, P. Yao, X. Wang, X. Liu, X. Zhuang, F. Yan, J. Zhou, J. Du, T. Ward, H. Zou, J. Zhang, G. Fang, X. Ding, Z. Dou, and X. Yao. 2012. CENP-E kinesin interacts with SKAP protein to orchestrate accurate chromosome segregation in mitosis. *The Journal of biological chemistry*. 287:1500-1509.
Hunter, A.W., M. Caplow, D.L. Coy, W.O. Hancock, S. Diez, L. Wordeman, and J. Howard. 2003. The kinesin-related protein MCAK is a microtubule depolymerase that forms an ATP-hydrolyzing complex at microtubule ends. *Mol Cell*. 11:445-457.
Iemura, K., and K. Tanaka. 2015. Chromokinesin Kid and kinetochore kinesin CENP-E differentially support chromosome congression without end-on attachment to microtubules. *Nature communications*. 6:6447.

Jaqaman, K., E.M. King, A.C. Amaro, J.R. Winter, J.F. Dorn, H.L. Elliott, N. McHedlishvili, S.E. McClelland, I.M. Porter, M. Posch, A. Toso, G. Danuser, A.D. McAinsh, P. Meraldi, and J.R. Swedlow. 2010. Kinetochore alignment within the metaphase plate is regulated by centromere stiffness and microtubule depolymerases. *J Cell Biol*. 188:665-679.

Jeyaprakash, A.A., C. Basquin, U. Jayachandran, and E. Conti. 2011. Structural basis for the recognition of phosphorylated histone h3 by the survivin subunit of the chromosomal passenger complex. *Structure*. 19:1625-1634.

Jeyaprakash, A.A., U.R. Klein, D. Lindner, J. Ebert, E.A. Nigg, and E. Conti. 2007. Structure of a Survivin-Borealin-INCENP core complex reveals how chromosomal passengers travel together. *Cell*. 131:271-285.

Jeyaprakash, A.A., A. Santamaria, U. Jayachandran, Y.W. Chan, C. Benda, E.A. Nigg, and E. Conti. 2012. Structural and functional organization of the Ska complex, a key component of the kinetochore-microtubule interface. *Mol Cell*. 46:274-286.

Johnson, V.L., M.I. Scott, S.V. Holt, D. Hussein, and S.S. Taylor. 2004. Bub1 is required for kinetochore localization of BubR1, Cenp-E, Cenp-F and Mad2, and chromosome congression. *J Cell Sci*. 117:1577-1589.

Johnston, K., A. Joglekar, T. Hori, A. Suzuki, T. Fukagawa, and E.D. Salmon. 2010. Vertebrate kinetochore protein architecture: protein copy number. *J Cell Biol*. 189:937-943.

Kabeche, L., and D.A. Compton. 2013. Cyclin A regulates kinetochore microtubules to promote faithful chromosome segregation. *Nature*. 502:110-113.

Kang, J., J. Chaudhary, H. Dong, S. Kim, C.A. Brautigam, and H. Yu. 2011a. Mitotic centromeric targeting of HP1 and its binding to Sgo1 are dispensable for sister-chromatid cohesion in human cells. *Mol Biol Cell*. 22:1181-1190.

Kang, Y.H., C.H. Park, T.S. Kim, N.K. Soung, J.K. Bang, B.Y. Kim, J.E. Park, and K.S. Lee. 2011b. Mammalian polo-like kinase 1-dependent regulation of the PBIP1-CENP-Q complex at kinetochores. *The Journal of biological chemistry*. 286:19744-19757.

Kapoor, T.M., M.A. Lampson, P. Hergert, L. Cameron, D. Cimini, E.D. Salmon, B.F. McEwen, and A. Khodjakov. 2006. Chromosomes can congress to the metaphase plate before biorientation. *Science*. 311:388-391.

Kato, H., J. Jiang, B.R. Zhou, M. Rozendaal, H. Feng, R. Ghirlando, T.S. Xiao, A.F. Straight, and Y. Bai. 2013. A conserved mechanism for centromeric nucleosome recognition by centromere protein CENP-C. *Science*. 340:1110-1113.

Kawashima, S.A., T. Tsukahara, M. Langegger, S. Hauf, T.S. Kitajima, and Y. Watanabe. 2007. Shugoshin enables tension-generating attachment of kinetochores by loading Aurora to centromeres. *Genes & development*. 21:420-435.

Kelly, A.E., C. Ghenoiu, J.Z. Xue, C. Zierhut, H. Kimura, and H. Funabiki. 2010. Survivin reads phosphorylated histone H3 threonine 3 to activate the mitotic kinase Aurora B. *Science*. 330:235-239.

Kelly, A.E., S.C. Sampath, T.A. Maniar, E.M. Woo, B.T. Chait, and H. Funabiki. 2007. Chromosomal enrichment and activation of the aurora B pathway are coupled to spatially regulate spindle assembly. *Developmental cell*. 12:31-43.

Kemmler, S., M. Stach, M. Knapp, J. Ortiz, J. Pfannstiel, T. Ruppert, and J. Lechner. 2009. Mimicking Ndc80 phosphorylation triggers spindle assembly checkpoint signalling. *The EMBO journal*. 28:1099-1110.

Kern, D.M., P.K. Nicholls, D.C. Page, and I.M. Cheeseman. 2016. A mitotic SKAP isoform regulates spindle positioning at astral microtubule plus ends. *J Cell Biol*. 213:315-328.

Khodjakov, A., I.S. Gabashvili, and C.L. Rieder. 1999. " Dumb" Versus "Smart kinetochore models for chromosome congression during mitosis in vertebrate somatic cells. *Cell Motility and the Cytoskeleton*. 43:179-185.

Khodjakov, A., and C.L. Rieder. 1996 Kinetochores Moving Away from Their Associated Pole Do Not Exert a Significant Pushing Force on the Chromosome. *J. Cell. Biol.* 135:315-327.

Kim, H., C. Fonseca, and J. Stumpff. 2014. A unique kinesin-8 surface loop provides specificity for chromosome alignment. *Mol Biol Cell*. 25:3319-3329.

Kim, S., H. Sun, D.R. Tomchick, H. Yu, and X. Luo. 2012. Structure of human Mad1 C-terminal domain reveals its involvement in kinetochore targeting. *Proc Natl Acad Sci U S A*. 109:6549-6554.

Kim, S., and H. Yu. 2015. Multiple assembly mechanisms anchor the KMN spindle checkpoint platform at human mitotic kinetochores. *J Cell Biol*. 208:181-196.

Kim, Y., J.E. Heuser, C.M. Waterman, and D.W. Cleveland. 2008. CENP-E combines a slow, processive motor and a flexible coiled coil to produce an essential motile kinetochore tether. *J Cell Biol*. 181:411-419.

Kim, Y., A.J. Holland, W. Lan, and D.W. Cleveland. 2010. Aurora kinases and protein phosphatase 1 mediate chromosome congression through regulation of CENP-E. *Cell*. 142:444-455.

Kiyomitsu, T., and I.M. Cheeseman. 2012. Chromosome- and spindle-pole-derived signals generate an intrinsic code for spindle position and orientation. *Nat Cell Biol*. 14:311-317.

Kiyomitsu, T., O. Iwasaki, C. Obuse, and M. Yanagida. 2010. Inner centromere formation requires hMis14, a trident kinetochore protein

that specifically recruits HP1 to human chromosomes. *J Cell Biol*. 188:791-807.
Kiyomitsu, T., C. Obuse, and M. Yanagida. 2007. Human Blinkin/AF15q14 is required for chromosome alignment and the mitotic checkpoint through direct interaction with Bub1 and BubR1. *Developmental cell*. 13:663-676.
Klare, K., J.R. Weir, F. Basilico, T. Zimniak, L. Massimiliano, N. Ludwigs, F. Herzog, and A. Musacchio. 2015. CENP-C is a blueprint for constitutive centromere-associated network assembly within human kinetochores. *J Cell Biol*. 210:11-22.
Kline-Smith, S.L., A. Khodjakov, P. Hergert, and C.E. Walczak. 2004. Depletion of centromeric MCAK leads to chromosome congresson and segregation defects due to improper kinetochore attachments. *Mol Biol Cell*. 15:1146-1159.
Knowlton, A.L., W. Lan, and P.T. Stukenberg. 2006. Aurora B is enriched at merotelic attachment sites, where it regulates MCAK. *Current biology : CB*. 16:1705-1710.
Kon, T., T. Oyama, R. Shimo-Kon, K. Imamula, T. Shima, K. Sutoh, and G. Kurisu. 2012. The 2.8 A crystal structure of the dynein motor domain. *Nature*. 484:345-350.
Kon, T., K. Sutoh, and G. Kurisu. 2011. X-ray structure of a functional full-length dynein motor domain. *Nature structural & molecular biology*. 18:638-642.
Kops, G.J., Y. Kim, B.A. Weaver, Y. Mao, I. McLeod, J.R. Yates, 3rd, M. Tagaya, and D.W. Cleveland. 2005. ZW10 links mitotic checkpoint signaling to the structural kinetochore. *J Cell Biol*. 169:49-60.
Krenn, V., K. Overlack, I. Primorac, S. van Gerwen, and A. Musacchio. 2014. KI motifs of human Knl1 enhance assembly of comprehensive spindle checkpoint complexes around MELT repeats. *Current biology : CB*. 24:29-39.
Krenn, V., A. Wehenkel, X. Li, S. Santaguida, and A. Musacchio. 2012. Structural analysis reveals features of the spindle checkpoint kinase Bub1-kinetochore subunit Knl1 interaction. *J Cell Biol*. 196:451-467.
Kuijt, T.E.F., M. Omerzu, A.T. Saurin, and G.J. Kops. 2014. Conditional targeting of MAD1 to kinetochores is sufficient to reactivate the spindle assembly checkpoint in metaphase. *Chromosoma*. 123:471-480.
Lampert, F., P. Hornung, and S. Westermann. 2010. The Dam1 complex confers microtubule plus end-tracking activity to the Ndc80 kinetochore complex. *J Cell Biol*. 189:641-649.
Lampson, M.A., and I.M. Cheeseman. 2011. Sensing centromere tension: Aurora B and the regulation of kinetochore function. *Trends in cell biology*. 21:133-140.
Lampson, M.A., and T.M. Kapoor. 2005. The human mitotic checkpoint protein BubR1 regulates chromosome-spindle attachments. *Nat Cell Biol*. 7:93-98.

Lampson, M.A., K. Renduchitala, A. Khodjakov, and T.M. Kapoor. 2004. Correcting improper chromosome-spindle attachments during cell division. *Nat Cell Biol*. 6:232-237.

Lan, W., X. Zhang, S.L. Kline-Smith, S.E. Rosasco, G.A. Barrett-Wilt, J. Shabanowitz, D.F. Hunt, C.E. Walczak, and P.T. Stukenberg. 2004. Aurora B phosphorylates centromeric MCAK and regulates its localization and microtubule depolymerization activity. *Current biology : CB*. 14:273-286.

Levesque, A.A., and D.A. Compton. 2001. The chromokinesin Kid is necessary for chromosome arm orientation and oscillation, but not congression, on mitotic spindles. *J Cell Biol*. 154:1135-1146.

Li, J., W. Lee, and J.A. Cooper. 2005. NudEL targets dynein to microtubule ends through LIS1. *Nat Cell Biol*. 7:686-690.

Li, R., and A.W. Murray. 1991. Feedback control of mitosis in budding yeast. *Cell*. 66:519-531.

Li, Y., W. Yu, Y. Liang, and X. Zhu. 2007. Kinetochore dynein generates a poleward pulling force to facilitate congression and full chromosome alignment. *Cell research*. 17:701-712.

Liang, Y., W. Yu, Y. Li, L. Yu, Q. Zhang, F. Wang, Z. Yang, J. Du, Q. Huang, X. Yao, and X. Zhu. 2007. Nudel modulates kinetochore association and function of cytopasmic dynein in M phase. *Mol Biol Cell*. 18:2656-2666.

Liao H., Winkfein R.J., Mack G., Rattner J.B., and Y. T.J. 1995. CENP-F is a protein of the nuclear matrix that assembles onto kinetochores at late G2 and is rapidly degraded after mitosis. *J Cell Biol*. 130:507-518.

Liu, D., X. Ding, J. Du, X. Cai, Y. Huang, T. Ward, A. Shaw, Y. Yang, R. Hu, C. Jin, and X. Yao. 2007. Human NUF2 interacts with centromere-associated protein E and is essential for a stable spindle microtubule-kinetochore attachment. *The Journal of biological chemistry*. 282:21415-21424.

Liu, D., G. Vader, M.J.M. Vromans, M. Lampson, and S.M.A. Lens. 2009. Sensing Chromosome Bi-Orientation by Spatial Separation of Aurora B Kinase from Kinetochore Substrates. *Science*. 323:1350-1353.

Liu, D., M. Vleugel, C.B. Backer, T. Hori, T. Fukagawa, I.M. Cheeseman, and M.A. Lampson. 2010. Regulated targeting of protein phosphatase 1 to the outer kinetochore by KNL1 opposes Aurora B kinase. *J Cell Biol*. 188:809-820.

Liu, S.T., J.B. Rattner, S.A. Jablonski, and T.J. Yen. 2006. Mapping the assembly pathways that specify formation of the trilaminar kinetochore plates in human cells. *J Cell Biol*. 175:41-53.

Logsdon, G.A., E.J. Barrey, E.A. Bassett, J.E. DeNizio, L.Y. Guo, T. Panchenko, J.M. Dawicki-McKenna, P. Heun, and B.E. Black. 2015. Both tails and the centromere targeting domain of CENP-A are required for centromere establishment. *J Cell Biol*. 208:521-531.

Loncarek, J., O. Kisurina-Evgenieva, T. Vinogradova, P. Hergert, S. La Terra, T.M. Kapoor, and A. Khodjakov. 2007. The centromere geometry essential for keeping mitosis error free is controlled by spindle forces. *Nature*. 450:745-749.

London, N., and S. Biggins. 2014a. Mad1 kinetochore recruitment by Mps1-mediated phosphorylation of Bub1 signals the spindle checkpoint. *Genes & development*. 28:140-152.

London, N., and S. Biggins. 2014b. Signalling dynamics in the spindle checkpoint response. *Nature reviews. Molecular cell biology*. 15:736-747.

London, N., S. Ceto, J.A. Ranish, and S. Biggins. 2012. Phosphoregulation of Spc105 by Mps1 and PP1 regulates Bub1 localization to kinetochores. *Current biology : CB*. 22:900-906.

Luo, X., and H. Yu. 2008. Protein metamorphosis: the two-state behavior of Mad2. *Structure*. 16:1616-1625.

M.J.Schleden. 1838. Beiträge zur Phytogenesis. *Müller´s Arch. Anat. Physiol. Wiss. Med*:136-176.

Maddox, P.S., F. Hyndman, J. Monen, K. Oegema, and A. Desai. 2007. Functional genomics identifies a Myb domain-containing protein family required for assembly of CENP-A chromatin. *J Cell Biol*. 176:757-763.

Maffini, S., A.R. Maia, A.L. Manning, Z. Maliga, A.L. Pereira, M. Junqueira, A. Shevchenko, A. Hyman, J.R. Yates, 3rd, N. Galjart, D.A. Compton, and H. Maiato. 2009. Motor-independent targeting of CLASPs to kinetochores by CENP-E promotes microtubule turnover and poleward flux. *Current biology : CB*. 19:1566-1572.

Magidson, V., C.B. O'Connell, J. Loncarek, R. Paul, A. Mogilner, and A. Khodjakov. 2011. The spatial arrangement of chromosomes during prometaphase facilitates spindle assembly. *Cell*. 146:555-567.

Magidson, V., R. Paul, N. Yang, J.G. Ault, C.B. O'Connell, I. Tikhonenko, B.F. McEwen, A. Mogilner, and A. Khodjakov. 2015. Adaptive changes in the kinetochore architecture facilitate proper spindle assembly. *Nat Cell Biol*. 17:1134-1144.

Maldonado, M., and T.M. Kapoor. 2011. Constitutive Mad1 targeting to kinetochores uncouples checkpoint signalling from chromosome biorientation. *Nat Cell Biol*. 13:475-482.

Malvezzi, F., G. Litos, A. Schleiffer, A. Heuck, K. Mechtler, T. Clausen, and S. Westermann. 2013. A structural basis for kinetochore recruitment of the Ndc80 complex via two distinct centromere receptors. *The EMBO journal*. 32:409-423.

Manuelidis, L. 1978a. Chromosomal location of complex and simple repeated human DNAs. *Chromosoma*. 66:23-32.

Manuelidis, L. 1978b. Complex and simple sequences in human repeated DNAs. *Chromosoma*. 66:1-21.

Mao, Y., A. Abrieu, and D.W. Cleveland. 2003. Activating and Silencing the Mitotic Checkpoint through CENP-E-Dependent Activation/Inactivation of BubR1. *Cell*. 114:87-98.
Maresca, T.J., and E.D. Salmon. 2009. Intrakinetochore stretch is associated with changes in kinetochore phosphorylation and spindle assembly checkpoint activity. *J Cell Biol*. 184:373-381.
Marshall, O.J., A.C. Chueh, L.H. Wong, and K.H. Choo. 2008. Neocentromeres: new insights into centromere structure, disease development, and karyotype evolution. *American journal of human genetics*. 82:261-282.
Martin-Lluesma, S., V. Stucke, M.,, and E.A. Nigg. 2002. Role of Hec1 in Spindle Checkpoint Signaling and Kinetochore Recruitment of Mad1/Mad2. *Science*. 297:2267-2270.
Masuoto, H., M. Ikeno, M. Nakano, T. Okazaki, B. Grimes, H. Cooke, and N. Suzuki. 1998. Assay of centromere function using a human artificial chromosome. *Chromosoma*. 107:406-416.
Mayr, M.I., S. Hummer, J. Bormann, T. Gruner, S. Adio, G. Woehlke, and T.U. Mayer. 2007. The human kinesin Kif18A is a motile microtubule depolymerase essential for chromosome congression. *Current biology : CB*. 17:488-498.
McCleland, M.L., S. Borusu, A.C. Amaro, J.R. Winter, M. Belwal, A.D. McAinsh, and P. Meraldi. 2007. The CENP-A NAC/CAD kinetochore complex controls chromosome congression and spindle bipolarity. *The EMBO Journal*. 26:5033-5047.
McEwen, B.F., Heagle, A. B., Cassels, G. O., Buttle, K. F. & Rieder, C. L. . 1997. Kinetochore fober maturation in PtK1 cells and its implications for the mechanisms of chromosome congression and anaphase onset. *Journal of cell biology*. 137:1567-1580.
McIntosh, J.R. 2016. Mitosis. *Cold Spring Harbor perspectives in biology*. 8.
McIntosh, J.R., E.L. Grishchuk, M.K. Morphew, A.K. Efremov, K. Zhudenkov, V.A. Volkov, I.M. Cheeseman, A. Desai, D.N. Mastronarde, and F.I. Ataullakhanov. 2008. Fibrils connect microtubule tips with kinetochores: a mechanism to couple tubulin dynamics to chromosome motion. *Cell*. 135:322-333.
McKinley, K.L., and I.M. Cheeseman. 2014. Polo-like kinase 1 licenses CENP-A deposition at centromeres. *Cell*. 158:397-411.
McKinley, K.L., N. Sekulic, L.Y. Guo, T. Tsinman, B.E. Black, and I.M. Cheeseman. 2015. The CENP-L-N Complex Forms a Critical Node in an Integrated Meshwork of Interactions at the Centromere-Kinetochore Interface. *Mol Cell*. 60:886-898.
Meadows, J.C., L.A. Shepperd, V. Vanoosthuyse, T.C. Lancaster, A.M. Sochaj, G.J. Buttrick, K.G. Hardwick, and J.B. Millar. 2011. Spindle checkpoint silencing requires association of PP1 to both Spc7 and kinesin-8 motors. *Developmental cell*. 20:739-750.

Milks, K.J., B. Moree, and A.F. Straight. 2009. Dissection of CENP-C-directed centromere and kinetochore assembly. *Mol Biol Cell*. 20:4246-4255.

Miller, S.A., M.L. Johnson, and P.T. Stukenberg. 2008. Kinetochore attachments require an interaction between unstructured tails on microtubules and Ndc80(Hec1). *Current biology : CB*. 18:1785-1791.

Miranda, J.J., P. De Wulf, P.K. Sorger, and S.C. Harrison. 2005. The yeast DASH complex forms closed rings on microtubules. *Nature structural & molecular biology*. 12:138-143.

Mitchison, T., L. Evans, E. Schulze, and M. Kirschner. 1986. Sites of Microtubule Assembly and Disassembly in the Mitotic Spindle. *Cell*. 45:515-527.

Mitchison, T.J. 1989. Polewards microtubule flux in the mitotic spindle: evidence from photoactivation of fluorescence. *J Cell Biol*. 109:637-652.

Mitchison, T.J., and E.D. Salmon. 1992. Poleward Kinetochore Fiber Movement Occurs during Both Metaphase and Anaphase-A in Newt Lung Cell Mitosis. *J. Cell. Biol.* 119:569-582.

Moudgil, D.K., N. Westcott, J.K. Famulski, K. Patel, D. Macdonald, H. Hang, and G.K. Chan. 2015. A novel role of farnesylation in targeting a mitotic checkpoint protein, human Spindly, to kinetochores. *J Cell Biol*. 208:881-896.

Moyle, M.W., T. Kim, N. Hattersley, J. Espeut, D.K. Cheerambathur, K. Oegema, and A. Desai. 2014. A Bub1-Mad1 interaction targets the Mad1-Mad2 complex to unattached kinetochores to initiate the spindle checkpoint. *J Cell Biol*. 204:647-657.

Murata-Hori, M., and Y.L. Wang. 2002. Both midzone and astral microtubules are involved in the delivery of cytokinesis signals: insights from the mobility of aurora B. *J Cell Biol*. 159:45-53.

Musacchio, A. 2015. The Molecular Biology of Spindle Assembly Checkpoint Signaling Dynamics. *Current biology : CB*. 25:R1002-1018.

Nagpal, H., T. Hori, A. Furukawa, K. Sugase, A. Osakabe, H. Kurumizaka, and T. Fukagawa. 2015. Dynamic changes in CCAN organization through CENP-C during cell-cycle progression. *Mol Biol Cell*. 26:3768-3776.

Nicklas, R.B. 1988. The forces that move chromosomes in mitosis. *Annu Rev Biophys Chem*. 17:431-449.

Nicklas, R.B., and P. Arana. 1992. Evolution and the meaning of metaphase. *J Cell Sci*. 102:681-690.

Nicklas, R.B., and C.A. Koch. 1969. Chromosome micromanipulation . 3. Spindle fiber tension and the reorientation of mal-oriented chromosomes. *J Cell Biol*. 43:40-50.

Nishino, T., F. Rago, T. Hori, K. Tomii, I.M. Cheeseman, and T. Fukagawa. 2013. CENP-T provides a structural platform for outer kinetochore assembly. *The EMBO journal*. 32:424-436.

Nishino, T., K. Takeuchi, K.E. Gascoigne, A. Suzuki, T. Hori, T. Oyama, K. Morikawa, I.M. Cheeseman, and T. Fukagawa. 2012. CENP-T-W-S-X forms a unique centromeric chromatin structure with a histone-like fold. *Cell*. 148:487-501.

Nunes Bastos, R., S.R. Gandhi, R.D. Baron, U. Gruneberg, E.A. Nigg, and F.A. Barr. 2013. Aurora B suppresses microtubule dynamics and limits central spindle size by locally activating KIF4A. *J Cell Biol*. 202:605-621.

Obuse, C., O. Iwasaki, T. Kiyomitsu, G. Goshima, Y. Toyoda, and M. Yanagida. 2004. A conserved Mis12 centromere complex is linked to heterochromatic HP1 and outer kinetochore protein Zwint-1. *Nat Cell Biol*. 6:1135-1141.

Oguchi, Y., S. Uchimura, T. Ohki, S.V. Mikhailenko, and S. Ishiwata. 2011. The bidirectional depolymerizer MCAK generates force by disassembling both microtubule ends. *Nat Cell Biol*. 13:846-852.

Okada, M., I.M. Cheeseman, T. Hori, K. Okawa, I.X. McLeod, J.R. Yates, 3rd, A. Desai, and T. Fukagawa. 2006. The CENP-H-I complex is required for the efficient incorporation of newly synthesized CENP-A into centromeres. *Nat Cell Biol*. 8:446-457.

Oliveira, R.A., R.S. Hamilton, A. Pauli, I. Davis, and K. Nasmyth. 2010. Cohesin cleavage and Cdk inhibition trigger formation of daughter nuclei. *Nat Cell Biol*. 12:185-192.

Östergren, G. 1945. Equilibrium of trivalents and the mechanism of chromosome movements *Hereditas*. 31:498.

Östergren, G. 1951. The mechanism of co-orientation in bivalents and multivalents. The theory of orientation by pulling. . *Hereditas*. 37:85-156.

Overlack, K., I. Primorac, M. Vleugel, V. Krenn, S. Maffini, I. Hoffmann, G.J. Kops, and A. Musacchio. 2015. A molecular basis for the differential roles of Bub1 and BubR1 in the spindle assembly checkpoint. *eLife*. 4:e05269.

Palmer, D.K., and R.L. Margolis. 1985. Kinetochore components recognized by huan autoantibodies are present on mononucleosomes. *Mol Biol Cell*:173-186.

Palmer, D.K., K. O'Day, and R.L. Margolis. 1990. The centromere specific histone CENP-A is selectively retained in discrete foci in mammalian sperm nuceli. *Chromosoma*. 100:32-36.

Palmer, D.K., K. O'Day, H.L. Trong, H. Charbnneau, and R.L. Margolis. 1991. Purification of the centromere-specific protein CENP-A and demonstration that it is a distinctive histone. *Proc Natl Acad Sci U S A*. 88:3734-3738.

Palmer, D.K., K. O'Day, M.H. Wener, B.S. Andrews, and R.L. Margolis. 1987. A 17-kD Centromere Protein (CENP-A) Copurifies with

Nucleosome Core Particles and with Histones. *J. Cell. Biol.* 104:805-815.
Park, C.H., J.E. Park, T.S. Kim, Y.H. Kang, N.K. Soung, M. Zhou, N.H. Kim, J.K. Bang, and K.S. Lee. 2015. Mammalian Polo-like Kinase 1 (Plk1) Promotes Proper Chromosome Segregation by Phosphorylating and Delocalizing the PBIP1-CENP-Q Complex from Kinetochores. *The Journal of biological chemistry*.
Paweletz, N. 2001. Walther Flemming: pioneer of mitosis research. *Nature Reviews Molecular Cell Biology*. 2:72-75.
Pereira, A.J., and H. Maiato. 2012. Maturation of the kinetochore-microtubule interface and the meaning of metaphase. *Chromosome research : an international journal on the molecular, supramolecular and evolutionary aspects of chromosome biology*. 20:563-577.
Perpelescu, M., and T. Fukagawa. 2011. The ABCs of CENPs. *Chromosoma*. 120:425-446.
Pesenti, M.E., J.R. Weir, and A. Musacchio. 2016. Progress in the structural and functional characterization of kinetochores. *Current opinion in structural biology*. 37:152-163.
Petrovic, A., S. Mosalaganti, J. Keller, M. Mattiuzzo, K. Overlack, V. Krenn, A. De Antoni, S. Wohlgemuth, V. Cecatiello, S. Pasqualato, S. Raunser, and A. Musacchio. 2014. Modular assembly of RWD domains on the Mis12 complex underlies outer kinetochore organization. *Mol Cell*. 53:591-605.
Petrovic, A., S. Pasqualato, P. Dube, V. Krenn, S. Santaguida, D. Cittaro, S. Monzani, L. Massimiliano, J. Keller, A. Tarricone, A. Maiolica, H. Stark, and A. Musacchio. 2010. The MIS12 complex is a protein interaction hub for outer kinetochore assembly. *J Cell Biol*. 190:835-852.
Pfarr, C.M., M. Coue, P.M. Grissom, T.S. Hays, M.E. Porter, and J.R. McIntosh. 1990. Cytoplasmic dynein is localized to kinetochores during mitosis. *Nature*. 345:263-265.
Pinsky, B.A., C.R. Nelson, and S. Biggins. 2009. Protein phosphatase 1 regulates exit from the spindle checkpoint in budding yeast. *Current biology : CB*. 19:1182-1187.
Powers, A.F., A.D. Franck, D.R. Gestaut, J. Cooper, B. Gracyzk, R.R. Wei, L. Wordeman, T.N. Davis, and C.L. Asbury. 2009. The Ndc80 kinetochore complex forms load-bearing attachments to dynamic microtubule tips via biased diffusion. *Cell*. 136:865-875.
Primorac, I., J.R. Weir, E. Chiroli, F. Gross, I. Hoffmann, S. van Gerwen, A. Ciliberto, and A. Musacchio. 2013. Bub3 reads phosphorylated MELT repeats to promote spindle assembly checkpoint signaling. *eLife*. 2:e01030.
Przewloka, M.R., Z. Venkei, V.M. Bolanos-Garcia, J. Debski, M. Dadlez, and D.M. Glover. 2011. CENP-C is a structural platform for kinetochore assembly. *Current biology : CB*. 21:399-405.

Raaijmakers, J.A., M.E. Tanenbaum, A.F. Maia, and R.H. Medema. 2009. RAMA1 is a novel kinetochore protein involved in kinetochore-microtubule attachment. *J Cell Sci*. 122:2436-2445.

Raaijmakers, J.A., M.E. Tanenbaum, and R.H. Medema. 2013. Systematic dissection of dynein regulators in mitosis. *J Cell Biol*. 201:201-215.

Rago, F., K.E. Gascoigne, and I.M. Cheeseman. 2015. Distinct organization and regulation of the outer kinetochore KMN network downstream of CENP-C and CENP-T. *Current biology : CB*. 25:671-677.

Ran, F.A., P.D. Hsu, J. Wright, V. Agarwala, D.A. Scott, and F. Zhang. 2013. Genome engineering using the CRISPR-Cas9 system. *Nature protocols*. 8:2281-2308.

Redli, P.M., I. Gasic, P. Meraldi, E.A. Nigg, and A. Santamaria. 2016. The Ska complex promotes Aurora B activity to ensure chromosome biorientation. *J Cell Biol*. 215:77-93.

Remak, R. 1855. Untersuchungen über die Entwickelung der Wirbelthiere. *Berlin*.

Rieder, C.L., R.W. Cole, A. Khodjakov, and G. Sluder. 1995. The checkpoint delaying anaphase in response to chromosome monoorientation is mediated by an inhibitory signal produced by unattached kinetochores. *J Cell Biol*. 130:941-948.

Rieder, C.L., E.A. Davison, L.C.W. Jensen, L. Cassimeris, and E.D. Salmon. 1986. Oscillatory Movements of Monooriented Chromosomes and Their Position Relative to the Spindle Pole Result from the Ejection Properties of the Aster and Half-Spindle. *J. Cell. Biol.* 103:581-591.

Rieder, C.L., and H. Maiato. 2004. Stuck in division or passing through: what happens when cells cannot satisfy the spindle assembly checkpoint. *Developmental cell*. 7:637-651.

Rigbolt, K., T.A. Prokorova, Akimov.V., J. Henningsen, P.T. Johansen, I. Kratchmarova, M. Kassem, M. Mann, J.V. Olsen, and B. Blagoev. 2011. System-wide temporal characterization of the proteome and phosphoproteome of human embryonic stem cell differentiation. *Sci Signal*. 4:rs3.

Rogers, G.C., S.L. Rogers, T.A. Schwimmer, S.C. Ems-McClung, C.E. Walczak, R.D. Vale, J.M. Scholey, and D.J. Sharp. 2004. Two mitotic kinesins cooperate to drive sister chromatid separation during anaphase. *Nature*. 427:364-370.

Rosenberg, J.S., F.R. Cross, and H. Funabiki. 2011. KNL1/Spc105 recruits PP1 to silence the spindle assembly checkpoint. *Current biology : CB*. 21:942-947.

Santamaria, A., B. Wang, S. Elowe, R. Malik, F. Zhang, M. Bauer, A. Schmidt, H.H. Sillje, R. Korner, and E.A. Nigg. 2011. The Plk1-dependent phosphoproteome of the early mitotic spindle. *Molecular & cellular proteomics : MCP*. 10:M110 004457.

Sardar, H.S., V.G. Luczak, M.M. Lopez, B.C. Lister, and S.P. Gilbert. 2010. Mitotic kinesin CENP-E promotes microtubule plus-end elongation. *Current biology : CB*. 20:1648-1653.

Savoian, M.S., M.L. Goldberg, and C.L. Rieder. 2000. The rate of poleward chromosome motion is attenuated in Drosophila zw10 and rod mutants. *Nat Cell Biol*. 2:948-952.

Schleiffer, A., M. Maier, G. Litos, F. Lampert, P. Hornung, K. Mechtler, and S. Westermann. 2012. CENP-T proteins are conserved centromere receptors of the Ndc80 complex. *Nat Cell Biol*. 14:604-613.

Schmidt, J.C., H. Arthanari, A. Boeszoermenyi, N.M. Dashkevich, E.M. Wilson-Kubalek, N. Monnier, M. Markus, M. Oberer, R.A. Milligan, M. Bathe, G. Wagner, E.L. Grishchuk, and I.M. Cheeseman. 2012. The kinetochore-bound Ska1 complex tracks depolymerizing microtubules and binds to curved protofilaments. *Developmental cell*. 23:968-980.

Schmidt, J.C., T. Kiyomitsu, T. Hori, C.B. Backer, T. Fukagawa, and I.M. Cheeseman. 2010. Aurora B kinase controls the targeting of the Astrin-SKAP complex to bioriented kinetochores. *J Cell Biol*. 191:269-280.

Schneider, A. 1873. Untersuchungen über Plathelminthen. *Jahrb. Oberhess. Ges. Naturwiss. Heilk*. 14:69-81.

Schroeder, C.M., J.M. Ostrem, N.T. Hertz, and R.D. Vale. 2014. A Ras-like domain in the light intermediate chain bridges the dynein motor to a cargo-binding region. *eLife*. 3:e03351.

Schroer, T.A. 2004. Dynactin. *Annual review of cell and developmental biology*. 20:759-779.

Schwaan, T. 1839. Mikroskopische Untersuchungen über die Uebereinstimmung in der Struktur und dem Wachsthum der Thiere und Pflanzen. *Berlin*.

Screpanti, E., A. De Antoni, G.M. Alushin, A. Petrovic, T. Melis, E. Nogales, and A. Musacchio. 2011. Direct binding of Cenp-C to the Mis12 complex joins the inner and outer kinetochore. *Current biology : CB*. 21:391-398.

Sessa, F., M. Mapelli, C. Ciferri, C. Tarricone, L.B. Areces, T.R. Schneider, P.T. Stukenberg, and A. Musacchio. 2005. Mechanism of Aurora B activation by INCENP and inhibition by hesperadin. *Mol Cell*. 18:379-391.

Shah, J.V., E. Botvinick, Z. Bonday, F. Furnari, M. Berns, and D.W. Cleveland. 2004. Dynamics of centromere and kinetochore proteins; implications for checkpoint signaling and silencing. *Current biology : CB*. 14:942-952.

Sharp-Baker, H., and R. Chen. 2001. Spindle checkpoint protein Bub1 is required for kinetochore localization of Mad1, Mad2, Bub3, and CENP-E, independently of its kinase activity. *J Cell Biol*. 153:1239-1249.

Shelden, E., and P. Wadsworth. 1992. Microinjection of Biotin-tubulin into Anaphase Cells Induces Transient Elongation of Kinetochore Microtubules and Reversal of Chromosome-to-Pole Motion. *J. Cell. Biol.* 116:1409-1420.

Shepperd, L.A., J.C. Meadows, A.M. Sochaj, T.C. Lancaster, J. Zou, G.J. Buttrick, J. Rappsilber, K.G. Hardwick, and J.B. Millar. 2012. Phosphodependent recruitment of Bub1 and Bub3 to Spc7/KNL1 by Mph1 kinase maintains the spindle checkpoint. *Current biology : CB*. 22:891-899.

Shrestha, R.L., and V.M. Draviam. 2013. Lateral to end-on conversion of chromosome-microtubule attachment requires kinesins CENP-E and MCAK. *Current biology : CB*. 23:1514-1526.

Shuaib, M., K. Ouararhni, S. Dimitrov, and A. Hamiche. 2010. HJURP binds CENP-A via a highly conserved N-terminal domain and mediates its deposition at centromeres. *Proc Natl Acad Sci U S A*. 107:1349-1354.

Silio, V., A.D. McAinsh, and J.B. Millar. 2015. KNL1-Bubs and RZZ Provide Two Separable Pathways for Checkpoint Activation at Human Kinetochores. *Developmental cell*. 35:600-613.

Silva, M.C., D.L. Bodor, M.E. Stellfox, N.M. Martins, H. Hochegger, D.R. Foltz, and L.E. Jansen. 2012. Cdk activity couples epigenetic centromere inheritance to cell cycle progression. *Developmental cell*. 22:52-63.

Simon, J.R., and E.D. Salmon. 1990. The structure of microtubule ends during the elongation and shortening phases of dynamic instability examined by negative-stain electron microscopy. *J. Cell. Sci*. 96:571-582.

Sivakumar, S., J.R. Daum, A.R. Tipton, S. Rankin, and G.J. Gorbsky. 2014. The Spindle and Kinetochore-associated (Ska) complex enhances binding of the Anaphase-Promoting Complex/Cyclosome (APC/C) to chromosomes and promotes mitotic exit. *Mol Biol Cell*. 25:594-605.

Sivakumar, S., P.L. Janczyk, Q. Qu, C.A. Brautigam, P.T. Stukenberg, H. Yu, and G.J. Gorbsky. 2016. The human SKA complex drives the metaphase-anaphase cell cycle transition by recruiting protein phosphatase 1 to kinetochores. *eLife*. 5.

Skibbens, R.V., V.P. Skeen, and E.D. Salmon. 1993. Directional Instability of Kinetochore Motility during Chromosome Congression and Segregation in Mitotic Newt Lung Cells: A Push-Pull Mechanism. *J. Cell. Biol.* 122:859-876.

Smith, C.A., A.D. McAinsh, and N.J. Burroughs. 2016. Human kinetochores are swivel joints that mediate microtubule attachments. *eLife*.

Spurck, T.P., O.G. Stonington, J.A. Snyder, J.D. Pickett-Heaps, A. Bajer, and J. Mole-Bajer. 1990. UV Microbeam Irradiations of the Mitotic Spindle. II. Spindle Fiber Dynamics and Force Production. *J. Cell. Biol.* 111:1505-1518.

Starr, D.A., B.C. Williams, T.S. Hays, and M.L. Goldberg. 1998. ZW10 helps recruit Dynactin and Dynein to the kinetochore. *J Cell Biol*. 142:763-774.

Stehman, S.A., Y. Chen, R.J. McKenney, and R.B. Vallee. 2007. NudE and NudEL are required for mitotic progression and are involved in dynein recruitment to kinetochores. *J Cell Biol*. 178:583-594.

Steuer, E.R., L. Wordeman, T.A. Schroer, and M.P. Sheetz. 1990. Localization of cytoplasmic dynein to mitotic spindle and kinetochores. *Nature*. 345:266-268.

Stumpff, J., Y. Du, C.A. English, Z. Maliga, M. Wagenbach, C.L. Asbury, L. Wordeman, and R. Ohi. 2011. A tethering mechanism controls the processivity and kinetochore-microtubule plus-end enrichment of the kinesin-8 Kif18A. *Mol Cell*. 43:764-775.

Stumpff, J., G. von Dassow, M. Wagenbach, C. Asbury, and L. Wordeman. 2008. The kinesin-8 motor Kif18A suppresses kinetochore movements to control mitotic chromosome alignment. *Developmental cell*. 14:252-262.

Stumpff, J., M. Wagenbach, A. Franck, C.L. Asbury, and L. Wordeman. 2012. Kif18A and chromokinesins confine centromere movements via microtubule growth suppression and spatial control of kinetochore tension. *Developmental cell*. 22:1017-1029.

Sudakin, V. 2001. Checkpoint inhibition of the APC/C in HeLa cells is mediated by a complex of BUBR1, BUB3, CDC20, and MAD2. *J Cell Biol*. 154:925-936.

Suijkerbuijk, S.J., M. Vleugel, A. Teixeira, and G.J. Kops. 2012. Integration of kinase and phosphatase activities by BUBR1 ensures formation of stable kinetochore-microtubule attachments. *Developmental cell*. 23:745-755.

Sullivan, K.F., M. Hechenberger, and K. Masri. 1994. Human CENP-A contains a histone H3 relative histone fold domain that is required for targeting to the centromere. *J Cell Biol*. 127:581-592.

Suzuki, A., B.L. Badger, and E.D. Salmon. 2015. A quantitative description of Ndc80 complex linkage to human kinetochores. *Nature communications*. 6:8161.

Suzuki, A., B.L. Badger, X. Wan, J.G. DeLuca, and E.D. Salmon. 2014. The architecture of CCAN proteins creates a structural integrity to resist spindle forces and achieve proper Intrakinetochore stretch. *Developmental cell*. 30:717-730.

Suzuki, A., T. Hori, T. Nishino, J. Usukura, A. Miyagi, K. Morikawa, and T. Fukagawa. 2011. Spindle microtubules generate tension-dependent changes in the distribution of inner kinetochore proteins. *J Cell Biol*. 193:125-140.

Tachiwana, H., S. Muller, J. Blumer, K. Klare, A. Musacchio, and G. Almouzni. 2015. HJURP involvement in de novo CenH3(CENP-A) and CENP-C recruitment. *Cell reports*. 11:22-32.

Tanaka, K., H.L. Chang, A. Kagami, and Y. Watanabe. 2009. CENP-C functions as a scaffold for effectors with essential kinetochore functions in mitosis and meiosis. *Developmental cell*. 17:334-343.

Tanaka, K.U., N. Rachidi, C. Janke, G. Pereira, M. Galova, E. Schiebel, M.J.F. Stark, and K. Nasmyth. 2002. Evidence that the Ipl1-Sli15 (Aurora kinase-INCENP) complex promotes chromosome bi-orientation by altering kinetochore-spindle pole connections. *Cell*. 108:317-329.

Theis, M., M. Slabicki, M. Junqueira, M. Paszkowski-Rogacz, J. Sontheimer, R. Kittler, A.K. Heninger, T. Glatter, K. Kruusmaa, I. Poser, A.A. Hyman, M.T. Pisabarro, M. Gstaiger, R. Aebersold, A. Shevchenko, and F. Buchholz. 2009. Comparative profiling identifies C13orf3 as a component of the Ska complex required for mammalian cell division. *The EMBO journal*. 28:1453-1465.

Tien, J.F., N.T. Umbreit, D.R. Gestaut, A.D. Franck, J. Cooper, L. Wordeman, T. Gonen, C.L. Asbury, and T.N. Davis. 2010. Cooperation of the Dam1 and Ndc80 kinetochore complexes enhances microtubule coupling and is regulated by aurora B. *J Cell Biol*. 189:713-723.

Tirnauer, J.S., J.C. Canman, E.D. Salmon, and T.J. Mitchison. 2002. EB1 targets to kinetochores with attached, polymerising microtubules. *Mol Biol Cell*. 13:4308-4316.

Tooley, J.G., S.A. Miller, and P.T. Stukenberg. 2011. The Ndc80 complex uses a tripartite attachment point to couple microtubule depolymerization to chromosome movement. *Mol Biol Cell*. 22:1217-1226.

Toso, A., J.R. Winter, A.J. Garrod, A.C. Amaro, P. Meraldi, and A.D. McAinsh. 2009. Kinetochore-generated pushing forces separate centrosomes during bipolar spindle assembly. *J Cell Biol*. 184:365-372.

Uchida, K.S., K. Takagaki, K. Kumada, Y. Hirayama, T. Noda, and T. Hirota. 2009. Kinetochore stretching inactivates the spindle assembly checkpoint. *J Cell Biol*. 184:383-390.

Umbreit, N.T., M.P. Miller, J.F. Tien, J.C. Ortola, L. Gui, K.K. Lee, S. Biggins, C.L. Asbury, and T.N. Davis. 2014. Kinetochores require oligomerization of Dam1 complex to maintain microtubule attachments against tension and promote biorientation. *Nature communications*. 5:4951.

Urnavicius, L., K. Zhang, A.G. Diamant, C. Motz, M.A. Schlager, M. Yu, N.A. Patel, C.V. Robinson, and A.P. Carter. 2015. The structure of the dynactin complex and its interaction with dynein. *Science*. 347:1441-1446.

van der Waal, M.S., R.C. Hengeveld, A. van der Horst, and S.M. Lens. 2012. Cell division control by the Chromosomal Passenger Complex. *Experimental cell research*. 318:1407-1420.

VandenBeldt, K.J., R.M. Barnard, P.J. Hergert, X. Meng, H. Maiato, and B.F. McEwen. 2006. Kinetochores use a novel mechanism for coordinating the dynamics of individual microtubules. *Current biology : CB*. 16:1217-1223.

Vanoosthuyse, V., and K.G. Hardwick. 2009. A novel protein phosphatase 1-dependent spindle checkpoint silencing mechanism. *Current biology : CB*. 19:1176-1181.

Vergnolle, M.A., and S.S. Taylor. 2007. Cenp-F links kinetochores to Ndel1/Nde1/Lis1/dynein microtubule motor complexes. *Current biology : CB*. 17:1173-1179.

Vladimirou, E., E. Harry, N. Burroughs, and A.D. McAinsh. 2011. Springs, clutches and motors: driving forward kinetochore mechanism by modelling. *Chromosome research : an international journal on the molecular, supramolecular and evolutionary aspects of chromosome biology*. 19:409-421.

Vleugel, M., M. Omerzu, V. Groenewold, M.A. Hadders, S.M. Lens, and G.J. Kops. 2015. Sequential multisite phospho-regulation of KNL1-BUB3 interfaces at mitotic kinetochores. *Mol Cell*. 57:824-835.

Vleugel, M., E. Tromer, M. Omerzu, V. Groenewold, W. Nijenhuis, B. Snel, and G.J. Kops. 2013. Arrayed BUB recruitment modules in the kinetochore scaffold KNL1 promote accurate chromosome segregation. *J Cell Biol*. 203:943-955.

Volkov, V.A., P.M. Grissom, V.K. Arzhanik, A.V. Zaytsev, K. Renganathan, T. McClure-Begley, W.M. Old, N. Ahn, and J.R. McIntosh. 2015. Centromere protein F includes two sites that couple efficiently to depolymerizing microtubules. *J Cell Biol*. 209:813-828.

von Mohl, H. 1835. Über die Vermehrung der Pflanzenzellen durch Theilung. *Tübingen*.

Waldeyer, H.W. 1888. Über Karyokinese und ihre Beziehungen zu den Befruchtungsvorgängen. *Arch. Mikrosk. Anat.* 32:1-22.

Wandke, C., M. Barisic, R. Sigl, V. Rauch, F. Wolf, A.C. Amaro, C.H. Tan, A.J. Pereira, U. Kutay, H. Maiato, P. Meraldi, and S. Geley. 2012. Human chromokinesins promote chromosome congression and spindle microtubule dynamics during mitosis. *J Cell Biol*. 198:847-863.

Wang, F., J. Dai, J.R. Daum, E. Niedzialkowska, B. Banerjee, P.T. Stukenberg, G.J. Gorbsky, and J.M. Higgins. 2010. Histone H3 Thr-3 phosphorylation by Haspin positions Aurora B at centromeres in mitosis. *Science*. 330:231-235.

Wang, X., X. Zhuang, D. Cao, Y. Chu, P. Yao, W. Liu, L. Liu, G. Adams, G. Fang, Z. Dou, X. Ding, Y. Huang, D. Wang, and X. Yao. 2012. Mitotic regulator SKAP forms a link between kinetochore core complex KMN and dynamic spindle microtubules. *The Journal of biological chemistry*. 287:39380-39390.

Waters, J.C., R.V. Skibbens, and E.D. Salmon. 1996. Oscillating mitotic newt lung cell kinetochores are, on average, under tension and rarely push. *J. Cell. Sci*. 109:2823-2831.

Weaver, B.A. 2003. Centromere-associated protein-E is essential for the mammalian mitotic checkpoint to prevent aneuploidy due to single chromosome loss. *J Cell Biol*. 162:551-563.

Wei, R.R., J.R. Schnell, N.A. Larsen, P.K. Sorger, J.J. Chou, and S.C. Harrison. 2006. Structure of a central component of the yeast kinetochore: the Spc24p/Spc25p globular domain. *Structure*. 14:1003-1009.

Weir, J.R., A.C. Faesen, K. Klare, A. Petrovic, F. Basilico, J. Fischbock, S. Pentakota, J. Keller, M.E. Pesenti, D. Pan, D. Vogt, S. Wohlgemuth, F. Herzog, and A. Musacchio. 2016. Insights from biochemical reconstitution into the architecture of human kinetochores. *Nature*. 537:249-253.

Welburn, J.P., E.L. Grishchuk, C.B. Backer, E.M. Wilson-Kubalek, J.R. Yates, 3rd, and I.M. Cheeseman. 2009. The human kinetochore Ska1 complex facilitates microtubule depolymerization-coupled motility. *Developmental cell*. 16:374-385.

Welburn, J.P., M. Vleugel, D. Liu, J.R. Yates, 3rd, M.A. Lampson, T. Fukagawa, and I.M. Cheeseman. 2010. Aurora B phosphorylates spatially distinct targets to differentially regulate the kinetochore-microtubule interface. *Mol Cell*. 38:383-392.

Westermann, S., A. Avila-Sakar, H.W. Wang, H. Niederstrasser, J. Wong, D.G. Drubin, E. Nogales, and G. Barnes. 2005. Formation of a dynamic kinetochore- microtubule interface through assembly of the Dam1 ring complex. *Mol Cell*. 17:277-290.

Westhorpe, F.G., C.J. Fuller, and A.F. Straight. 2015. A cell-free CENP-A assembly system defines the chromatin requirements for centromere maintenance. *J Cell Biol*. 209:789-801.

Westhorpe, F.G., and A.F. Straight. 2013. Functions of the centromere and kinetochore in chromosome segregation. *Current opinion in cell biology*. 25:334-340.

Whyte, J., J.R. Bader, S.B. Tauhata, M. Raycroft, J. Hornick, K.K. Pfister, W.S. Lane, G.K. Chan, E.H. Hinchcliffe, P.S. Vaughan, and K.T. Vaughan. 2008. Phosphorylation regulates targeting of cytoplasmic dynein to kinetochores during mitosis. *J Cell Biol*. 183:819-834.

Williams, J.C., P.L. Roulhac, A.G. Roy, R.B. Vallee, M.C. Fitzgerald, and W.A. Hendrickson. 2007. Structural and thermodynamic characterization of a cytoplasmic dynein light chain-intermediate chain complex. *Proc Natl Acad Sci U S A*. 104:10028-10033.

Wise, D., L. Cassimeris, C.L. Rieder, P. Wadsworth, and E.D. Salmon. 1991. Chromosome fiber dynamics and congression oscillations in metaphase PtK2 cells at 23 degrees C. *Cell Motil. Cytoskeleton*. 18:131-142.

Wood, K.W., R. Sakowicz, and L.S.B. Goldstein. 1997. CENP-E Is a Plus End–Directed Kinetochore Motor Required for Metaphase Chromosome Alignment. *Cell*. 91:357-366.
Wordeman, L., M. Wagenbach, and G. von Dassow. 2007. MCAK facilitates chromosome movement by promoting kinetochore microtubule turnover. *J Cell Biol*. 179:869-879.
Wynne, D.J., and H. Funabiki. 2015. Kinetochore function is controlled by a phospho-dependent coexpansion of inner and outer components. *J Cell Biol*. 210:899-916.
Yajima, J., M. Edamatsu, N. Watai-Nishii, T. Yamamoto, and Y.Y. Toyoshima. 2003. The human chromokinesin Kid is a plus end-directed microtubule-based motor. *EMBO*. 22:1067-1074.
Yamagishi, Y., C.H. Yang, Y. Tanno, and Y. Watanabe. 2012. MPS1/Mph1 phosphorylates the kinetochore protein KNL1/Spc7 to recruit SAC components. *Nat Cell Biol*. 14:746-752.
Yamamoto, T.G., S. Watanabe, A. Essex, and R. Kitagawa. 2008. SPDL-1 functions as a kinetochore receptor for MDF-1 in Caenorhabditis elegans. *J Cell Biol*. 183:187-194.
Yanagishi, Y., T. Honda, Y. Tanno, and S. Watanabe. 2010. Two histone marks establish the inner centromere and chromosome bi-orientation. *Science*. 330:239-243.
Yang, Z., J. Guo, Q. Chen, C. Ding, J. Du, and X. Zhu. 2005. Silencing mitosin induces misaligned chromosomes, premature chromosome decondensation before anaphase onset, and mitotic cell death. *Molecular and cellular biology*. 25:4062-4074.
Yang, Z., U.S. Tulu, P. Wadsworth, and C.L. Rieder. 2007. Kinetochore dynein is required for chromosome motion and congression independent of the spindle checkpoint. *Current biology : CB*. 17:973-980.
Ye, A.A., J. Deretic, C.M. Hoel, A.W. Hinman, D. Cimini, J.P. Welburn, and T.J. Maresca. 2015. Aurora A Kinase Contributes to a Pole-Based Error Correction Pathway. *Current biology : CB*. 25:1842-1851.
Zaytsev, A.V., J.E. Mick, E. Maslennikov, B. Nikashin, J.G. DeLuca, and E.L. Grishchuk. 2015. Multisite phosphorylation of the NDC80 complex gradually tunes its microtubule-binding affinity. *Mol Biol Cell*. 26:1829-1844.
Zeitlin, S.G., R.D. Shelby, and K.F. Sullivan. 2001. CENP-A is phosphorylated by Aurora B kinase and plays an unexpected role in completion of cytokinesis. *J Cell Biol*. 155:1147-1157.
Zhang, G., C.D. Kelstrup, X.W. Hu, M.J. Kaas Hansen, M.R. Singleton, J.V. Olsen, and J. Nilsson. 2012. The Ndc80 internal loop is required for recruitment of the Ska complex to establish end-on microtubule attachment to kinetochores. *J Cell Sci*. 125:3243-3253.
Zhang, G., T. Lischetti, D.G. Hayward, and J. Nilsson. 2015. Distinct domains in Bub1 localize RZZ and BubR1 to kinetochores to regulate the checkpoint. *Nature communications*. 6:7162.

Zhang, G., T. Lischetti, and J. Nilsson. 2014. A minimal number of MELT repeats supports all the functions of KNL1 in chromosome segregation. *J Cell Sci*. 127:871-884.

Zhang, X., W. Lan, S.C. Ems-McClung, P.T. Stukenberg, and C.E. Walczak. 2007. Aurora B phosphorylates multiple sites on mitotic centromere-associated kinesin to spatially and temporally control its function. *Mol Biol Cell*. 18:3264-3276.

Zhejian, J., H. Gao, and H. Yu. 2015. Kinetochore attachment sensed by competitive Mps1 and microtubule binding to Ndc80. *Science*. 348:1260-1264.

Zhu, T., Z. Dou, B. Qin, C. Jin, X. Wang, L. Xu, Z. Wang, L. Zhu, F. Liu, X. Gao, Y. Ke, Z. Wang, F. Aikhionbare, C. Fu, X. Ding, and X. Yao. 2013. Phosphorylation of microtubule-binding protein Hec1 by mitotic kinase Aurora B specifies spindle checkpoint kinase Mps1 signaling at the kinetochore. *The Journal of biological chemistry*. 288:36149-36159.

Appendix 1

A1 *Kinetochore ultrastructure*

A1.1 *The centromere*

Kinetochores are assembled on a chromosomal location classically described as a region of suppressed meiotic recombination (Beadle, 1932), which has come to be defined as the primary constriction of mitotic chromosomes, or centromere (Fukagawa and Earnshaw, 2014). Genetically, humans have a regional centromere, composed of an array of a 171 base-pair sequence termed α-satellite DNA (Manuelidis, 1978a; Manuelidis, 1978b). These monomers are arranged linearly, forming higher order repeat structures that are key for centromere function (Masuoto et al., 1998). In agreement, expression of cloned α-satellite DNA enabled linear minichromosomes to be stably inherited through multiple cellular generations in human cells (Harrington et al., 1997). However, while contributing to centromeric activity, these α-satellite arrays are not sufficient for centromere function. Instead, an epigenetic mark conferred by nucleosomes containing the histone variant centromere protein (CENP) –A (Earnshaw and Rothfield, 1985; Palmer and Margolis, 1985; Palmer et al., 1990; Palmer et al., 1991; Palmer et al., 1987; Sullivan et al., 1994) primarily dictates centromere functionality. Consistent with this idea, CENP-A is found at active centromeres of dicentric chromosomes (Earnshaw and

Migeon, 1985), all identified neocentromeres (Marshall et al., 2008), and is essential for the loading of all known kinetochore components (Fachinetti et al., 2013; Liu et al., 2006). CENP-A is deposited within the centromeric region by a dedicated histone chaperone, HJURP (holiday junction recognition protein) (Bassett et al., 2012; Hu et al., 2011; Shuaib et al., 2010), and the three-subunit Mis18 complex (consisting of MIS18α, MIS18β and MIS18-binding protein 1) (Fujita et al., 2007; Hayashi et al., 2004; Maddox et al., 2007) in a manner that is dependent on cyclin-dependent kinase (CDK) (Silva et al., 2012) and polo-like kinase (Plk) 1 (McKinley and Cheeseman, 2014) activity. Centromeric DNA binding is mediated by the CENP-A targeting domain (CATD), which is located within the first loop and second helix of the histone fold domain (Black et al., 2007). Once loaded, CENP-A is remarkably stable, and does not exchange with the cytoplasmic pool (Bodor et al., 2014).

A1.2 ***The core constitutive centromere associated network***

The role of CENP-A as the foundation for kinetochore assembly depends upon its interaction with several members of the core constitutive centromere associated network (CCAN), namely CENP-C, CENP-T and CENP-N. CENP-C is the largest CCAN subunit (~106kDa), and has been suggested to be the blueprint for kinetochore assembly (Klare et al., 2015). This is based on the correlation between the binding sites for other

kinetochore components along the CENP-C primary sequence and their position relative to the inner kinetochore. In this regard, a central motif promotes docking to CENP-A, an interaction that is dependent on both the CATD and C-terminus of CENP-A (Carroll et al., 2010; Kato et al., 2013; Logsdon et al., 2015; Tachiwana et al., 2015; Westhorpe et al., 2015), the latter interacting with an aromatic dipeptide on the CENP-C C-terminus (Kato et al., 2013). Upstream of this region are the binding sites for the CENP-H/I/K/M complex and CENP-L/N (Klare et al., 2015; McKinley et al., 2015; Milks et al., 2009; Nagpal et al., 2015), which are predominantly members of the extended CCAN (see below). Finally, the N-terminal region directly interacts with the Mis12 complex (Przewloka et al., 2011; Screpanti et al., 2011), which is a scaffold for outer kinetochore assembly (see below). Consistent with a blueprint role *in vivo*, CENP-C is recruited to CENP-A nucleosomes independently of all CCAN components in mitosis (Basilico et al., 2014; Klare et al., 2015), and depletion of CENP-C results in the significant reduction or loss of all CCAN components from the kinetochore (Basilico et al., 2014; Carroll et al., 2010; Gascoigne et al., 2011; Klare et al., 2015; Tanaka et al., 2009). In addition to CENP-C, the CATD is also required for the loading of CENP-N (Carroll et al., 2009). This interaction is cell cycle specific, as an RG loop (Arg80/Gly81) within the CATD that is key for the CENP-A-CENP-N interaction is obscured until the centromeric chromatin switches to an open state during the G1/S transition (Fang et al., 2015). It must be noted however, that CENP-N and CENP-C

are not sufficient to build a kinetochore, as ectopic CENP-A incorporation into chromosome arms, while recruiting CENP-C and CENP-N, loads no other kinetochore components (Gascoigne et al., 2011). Instead, CENP-T, which binds the N-terminus of CENP-A downstream of CENP-C (Folco et al., 2015; Logsdon et al., 2015), has emerged as a critical bridge between CENP-A and the CCAN. In this regard, ectopic localisation of the N-termini of CENP-T and CENP-C to chromatin in human cells is sufficient to build a pseudokinetochore, which can interact with microtubules and facilitate chromosome segregation (Gascoigne et al., 2011). The roles of CENP-T are thought to be carried out in complex with CENP-W, CENP-S and CENP-X. CENP-T and CENP-W dimerise, and CENP-S and CENP-X form a heterotetramer via the interaction of histone fold domains in each protein (Nishino et al., 2012). Moreover, CENP-T/W and CENP-S/X can form a heterotetrameric complex that can supercoil DNA in a manner reminiscent of nucleosomal histones, raising the possibility that CENP-T/W/S/X acts as another chromatin bound foundation for kinetochore assembly (Nishino et al., 2012). In terms of hierarchy, CENP-T or CENP-W deficient cells fail to recruit CENP-S/X (Hori et al., 2008a), whereas depletion of CENP-S or CENP-X has no effect on CENP-T loading (Amano et al., 2009). Indeed, CENP-S/X requires the additional presence of CENP-K for kinetochore localisation, but CENP-T does not (Amano et al., 2009; Hori et al., 2008a). This suggests that CENP-T may bind DNA independently, and in cooperation with other factors facilitate the loading CENP-S/X to form the

CENP-T/W/S/X complex. In addition, it remains possible that subpopulations of CENP-T/W and CENP-S/X function independently of CENP-T/W/S/X (Westhorpe and Straight, 2013). Nevertheless, all CENP-A interacting members of the CCAN have been shown to either directly or indirectly interact with one another, suggesting that the core CCAN may form a stable, cooperative complex around the CENP-A nucleosome (Pesenti et al., 2016).

A1.3 *Building the extended CCAN*

Built upon the core CCAN is a series of factors known as the extended CCAN, which consists of CENP-L, the CENP-HIKM complex and CENP-O subcomplex (consisting of CENPs-O/P/Q/R/U) (Basilico et al., 2014; Hori et al., 2008b; Perpelescu and Fukagawa, 2011). Over the past decade, significant analysis of biochemical interactions and depletion phenotypes has begun to untangle the interdependencies and relationships between these CCAN components. In this regard, CENP-L and CENP-HIKM appear to be upstream of the CENP-O subcomplex, and, somewhat unexpectedly, display multiple centromere localisation routes. First, CENP-N, whose depletion significantly impairs kinetochore function (Carroll et al., 2009; Foltz et al., 2006; McCleland et al., 2007), contributes to CENP-HIKM loading through a mechanism dependent on the direct interaction of CENP-N with an intermediary molecule, CENP-L (Carroll et al., 2009; Foltz et al.,

2006; Okada et al., 2006). Second, recent work on the 'kinetochore blueprint' factor CENP-C has identified a PEST domain located within its N-terminal half as an interaction domain for CENP-HIKM (Klare et al., 2015). These CENP-N/L and CENP-C localisation routes for CENP-HIKM are not independent, as *in vitro* reconstitution of the mammalian kinetochore revealed the existence of the CENP-CHIKMLN complex (Weir et al., 2016), which stably binds CENP-A nucleosome. In addition to these interactions, it is suggested that CENP-C contributes to CENP-HIKM loading via CENP-T, as depletion of CENP-C in interphase resulted in a 75% reduction in kinetochore bound CENP-T/W (and a 80% reduction in CENP-HIKM) (Klare et al., 2015). Nevertheless, the residual CENP-C independent pools of CENP-T/W and CENP-HIKM suggest the presence of multiple recruitment pathways that originate from distinct scaffolds on the CENP-A nucleosome. In this regard, the histone fold domains that allow for CENP-T/W dimerization have also been shown to promote binding to CENP-HIKM (Basilico et al., 2014; Hori et al., 2008a; Nishino et al., 2013). This interaction appears to be independent of its tetramerisation partner CENP-S/X, as depletion of CENP-T/W significantly impairs kinetochore assembly, whereas depletion of CENP-S/X does not (Amano et al., 2009). Thus, the core CCAN possesses multiple linkages to the extended CCAN member, CENP-HIKM. Moving further downstream, CENP-HIKM is implicated in the centromere localisation of the CENP-O subcomplex, potentially via the interaction of CENP-K with CENP-O (Eskat et al., 2012; Okada et al.,

2006). Consistent with CENP-O/P/Q/R/U forming a stable complex at the terminus of the extended CCAN, CENP-O depletion specifically impairs CENP-P/Q/R/U localisation, while leaving other CCAN members bound at the centromere (Bancroft et al., 2015; Foltz et al., 2006; Hori et al., 2008b; Okada et al., 2006). Additionally, the CENP-O subcomplex is required for the kinetochore targeting of non-CCAN proteins Plk1(Bancroft et al., 2015; Park et al., 2015) and CENP-E (Bancroft et al., 2015), via a phospho-regulated interaction with CENP-U and a currently unknown mechanism, respectively.

A1.4 *Recruitment of the KMN network by CCAN components*

Unlike the core and extended CCAN components, outer kinetochore proteins are only recruited to the centromere during mitosis, and confer several key properties to the structure; (1) attach to spindle microtubules, (2) regulate microtubule attachment such that erroneous attachments are destabilised and bi-orientation is promoted, and (3) signal the attachment status of all kinetochores to delay anaphase onset until all chromosomes are bi-oriented and aligned at the spindle equator. Specifically, two core CCAN components, CENP-T and CENP-C, recruit the primary outer kinetochore and microtubule-binding factor, the 10 subunit KMN network (consisting of the Knl1 complex: *Knl1, Zwint*, the Ndc80 complex: *Ndc80, Nuf2, Spc24, Spc25,* and Mis12 complex: *Nsl1, Nnf1, Dsn1, Mis12*). In

humans, flies and frogs, CENP-C is the primary node for KMN loading (Milks et al., 2009; Przewloka et al., 2011; Screpanti et al., 2011). An N-terminal 21 amino acid fragment of CENP-C interacts with the Mis12 complex, and a 71 amino acid fragment that fails to associate with kinetochores perturbs the centromeric targeting of the Mis12 complex and Knl1(Screpanti et al., 2011). This is important, as the Mis12 complex is known as the 'hub' of the KMN network (Petrovic et al., 2010), as it interacts with both the Ndc80 and Knl1 complexes via adjacent binding sites located at opposite ends of the complex. Specifically, this involves short linear motifs located on the Nsl1 and Dsn1 subunits, which interact with RWD domains located on the Ndc80 components Spc24 and Spc25, as well as the C-terminus of the Knl1 complex subunit Knl1 (Ciferri et al., 2008; Kiyomitsu et al., 2010; Malvezzi et al., 2013; Nishino et al., 2013; Petrovic et al., 2014; Petrovic et al., 2010; Wei et al., 2006). Importantly however, the CENP-C truncation mutant that prevented kinetochore recruitment of the Mis12 complex and Knl1 only partially disrupted Ndc80 binding, suggesting that additional pathway(s) contributed to KMN formation (Screpanti et al., 2011). Indeed, complete outer kinetochore assembly requires the N-terminal tail of CENP-T, which interacts with the RWD domains of Spc24 and Spc25 in a Cdk1 dependent manner (Gascoigne et al., 2011; Malvezzi et al., 2013; Nishino et al., 2013; Rago et al., 2015; Schleiffer et al., 2012; Suzuki et al., 2015). Moreover, CENP-T and the Mis12 complex bind competitively to the RWD domains of the

Ndc80 complex (Malvezzi et al., 2013; Nishino et al., 2013), and therefore form two independent recruitment arms. In cells, these arms appear to be saturated, as depletion of either significantly perturbs Ndc80 kinetochore levels (Gascoigne et al., 2011; Kim and Yu, 2015; Rago et al., 2015; Suzuki et al., 2015). In summary, kinetochores possess at least two pathways for KMN network assembly, which either directly or indirectly link microtubule binding to centromeric DNA and are regulated in a manner that allows cell cycle specific activation.

A1.5 ***Dynamics of the CCAN and KMN***

Both the CCAN and KMN display cell cycle and mitotic stage dynamicity. While described as constitutive, the CCAN changes in both composition and turnover kinetics during the cell cycle, with differences primarily being reported between S and M phases. In this regard, fluorescence recovery after photobleaching experiments (FRAP) demonstrated that CENP-C and CENP-H are stabilised in S-phase (Hemmerich et al., 2008), a time at which CENP-N is also enriched (Hellwig et al., 2011; McCleland et al., 2007). Moreover, CENP-O is loaded to centromeres during DNA replication (Eskat et al., 2012), which subsequently recruits other members of the CENP-O subcomplex that have individual residency kinetics (Eskat et al., 2012). A key question here is do these changes alter centromere function? In the case of CENP-N, it binds CENP-A in the same region as the

deposition factor HJURP (Bassett et al., 2012; Carroll et al., 2010), suggesting that HJURP associated with newly recruited CENP-A may abrogate CENP-N binding. In agreement, the reduction in centromeric CENP-N correlates with the timing of new CENP-A incorporation. Moreover, certain hierarchical relationships within the kinetochore appear to be cell cycle dependent. Indeed, CENP-H and CENP-K knock-out chicken DT40 cells mislocalise CENP-C in interphase but not in mitosis, suggesting the CCAN reorganises during cell cycle progression (Fukagawa et al., 2001; Zhang et al., 2007). More recently, work in *Xenopus* extracts has identified an expandable kinetochore module, which may be involved in microtubule capture (Wynne and Funabiki, 2015). Here, the loading of CENP-C to the expandable module was dependent upon CENP-E, a relationship that is not conserved in the 'traditional' pathway of CCAN assembly. The authors suggest that this dependency enables the relocation of CENP-C away from the inner kinetochore during early prometaphase, where it can carry out additional functions. However, upon microtubule attachment it is retracted into the core region, where it binds CENP-A nucleosomes and performs its well-established structural roles (Wynne and Funabiki, 2015). It must be noted that this dramatic expansion is not observed in human retinal pigment epithelial (RPE) 1 cells (Magidson et al., 2015). However, the KMN component Ndc80 does form an elongated structure at unattached kinetochores, and this correlates with an increase in outer-kinetochore volume (using CENP-F as a marker) (Magidson et al.,

2015). In agreement with the *Xenopus* model, these structural changes were shown to be important for microtubule capture. Thus, the kinetochore displays attachment dependent gross structural variation, which is key for microtubule capture during prometaphase. End-on attachment and the application of force are also thought to alter the separation of kinetochore subunits along the sister-pair axis. Using sub pixel measurements to determine the distance between two fluorescently labelled kinetochore components (termed delta Δ), it was suggested that microtubule attachment induces intra-kinetochore 'stretch' (Maresca and Salmon, 2009; Suzuki et al., 2014; Suzuki et al., 2011; Uchida et al., 2009). Moreover, this stretch was shown to be kinetochore autonomous, changing on whether the sister was moving towards its attached pole (P movement) or away from its attached pole (AP movement) (Dumont et al., 2012). Despite gaining some traction, recent work evaluating the methodology used to calculate Δ has suggested that the kinetochore is far more rigid than previously thought (Smith et al., 2016; Suzuki et al., 2014). Smith and colleagues demonstrated that microtubule attachment and movement direction had only a small effect on Δ (5-15nm). Instead, the kinetochore behaved as a ball-and-socket joint, where KMN components could 'swivel' around the CCAN (Smith et al., 2016). This swivel had not previously been taken into account, and was demonstrated to confound the measurement of Δ at unattached kinetochores using the previous 1D method, which involved the projection of both kinetochore labels into the same plane (Smith et al.,

2016). Nevertheless, current analysis is limited to relatively few kinetochore components, and a more comprehensive analysis of subunit behaviour is needed to determine if any compliant linkages exist. In summary, the CCAN and KMN are not static units, instead, they display highly dynamic behaviours that are dependent on both cell cycle stage and microtubule occupancy at the kinetochore.

A1.6 *KMN dependent loading of outer-kinetochore complexes*

Despite containing the major microtubule-binding site within the kinetochore, several properties conferred by the KMN network are done so indirectly, via the recruitment of additional complexes. In this regard, the Ndc80 complex subunit Ndc80/Hec1 contributes to the kinetochore loading of the Ska complex (Zhang et al., 2012). This is dependent upon the Ndc80 loop region, a break in the 55nm antenna like coiled coil that links the microtubule binding and Mis12 interacting domains (Zhang et al., 2012). The Ska complex is made of Ska1, Ska2 and Ska3/RAMA1 (Hanisch et al., 2006; Raaijmakers et al., 2009; Theis et al., 2009), whose interaction forms a heterotrimer consisting of two roughly perpendicular bundles, each made of three parallel helices (Jeyaprakash et al., 2012). Two heterotrimers bind via the short N-terminal bundle in a face-to-face configuration, forming a W shaped homodimer (Jeyaprakash et al., 2012). The Ska complex possesses two microtubule-binding sites, located at the C-termini of Ska1

and Ska3, which protrude from the open face of the dimer (Abad et al., 2014; Abad et al., 2016; Jeyaprakash et al., 2012; Schmidt et al., 2012). In addition to its role in kinetochore-microtubule coupling (see below for discussion), the Ska1 microtubule binding domain (MTBD) has been proposed to act as a structural platform for protein phosphatase 1 (PP1) recruitment, despite lacking any canonical PP1 interaction motifs (Sivakumar et al., 2016).

More recently, the KMN network has been implicated in the recruitment of another microtubule binding complex, the Astrin/SKAP complex (consisting of Astrin, the dynein light chain LC8, and the small kinetochore associated protein SKAP/KNSTRN) (Dunsch et al., 2011; Fang et al., 2009; Schmidt et al., 2010). SKAP directly binds to the C-terminus of Dsn1 (Mis13), a component of the Mis12 complex (Wang et al., 2012). This interaction is proposed to mediate Astrin/SKAP complex recruitment to the kinetochore, however, this is yet to be convincingly demonstrated *in vivo*. This is because binding of the Astrin/SKAP complex to the kinetochore is dependent on microtubule occupancy (Schmidt et al., 2010), therefore, interpretation of Astrin/SKAP loss from Dsn1 depleted kinetochores is confounded by the simultaneous perturbation of microtubule attachment. This story is further complicated by the discovery of an M-phase specific short SKAP isoform, which, unlike the long isoform that has been the focus of all previous work, can efficiently rescue the SKAP siRNA phenotype in

HeLa cells (Kern et al., 2016). Thus, significantly more work is required to untangle the Astrin/SKAP loading pathway.

In addition to microtubule interaction, a key challenge faced by mitotic cells is how to delay anaphase onset until all chromosomes are bi-oriented and aligned at the spindle equator. This problem is overcome by the spindle assembly checkpoint (SAC), a complex, phospho-regulated signalling cascade that originates from the KMN network of unattached kinetochores (London and Biggins, 2014b; Musacchio, 2015). Two semi-distinct pathways generate the SAC signal, one associated with Knl1 (Knl1 Bub1 Bub3 / KBB pathway), and the other the RZZ complex (RZZ pathway, see below for a description of SAC signalling) (Silio et al., 2015). In terms of SAC organisation at the kinetochore, the Ndc80 complex calponin homology (CH) domain directly binds the kinase Mps1 (Dou et al., 2015; Hiruma et al., 2015; Kemmler et al., 2009; Zhejian et al., 2015; Zhu et al., 2013), which phosphorylates Knl1 at several Met-Glu-Leu-Thr (MELT) motifs (London et al., 2012; Shepperd et al., 2012; Yamagishi et al., 2012). These phosphodomains then provide the docking site for the hierarchical recruitment of major SAC effectors, Bub3, Bub1, BubR1, Mad1 and Mad2 (Kiyomitsu et al., 2007; Krenn et al., 2014; London and Biggins, 2014a; Moyle et al., 2014; Overlack et al., 2015; Primorac et al., 2013; Sharp-Baker and Chen, 2001; Shepperd et al., 2012; Vleugel et al., 2015; Vleugel et al., 2013; Yamagishi et al., 2012; Zhang et al., 2014). In metazoans, the RZZ complex (consisting of Rod, Zeste White 10 (ZW10) and Zwilch) also

contributes to Mad1:Mad2 loading (Buffin et al., 2005; Kops et al., 2005), an interaction that may depend on spindly (Yamamoto et al., 2008), which binds downstream of RZZ in a farnesylation dependent manner (Barisic et al., 2010; Chan et al., 2009; Moudgil et al., 2015; Yamamoto et al., 2008). Moving further upstream, association of the RZZ complex with kinetochores is mediated by the Knl1 complex member Zwint-1, which binds ZW10 (Cheeseman et al., 2004; Kops et al., 2005; Obuse et al., 2004). Recently, Beclin-1, a component of the mammalian phosphatidylinositol-3-kinease complex has been suggested to be an additional Zwint-1-RZZ interaction partner (Fremont et al., 2013). Beclin-1 directly binds zwint-1 both *in vivo* and *vitro*, and its depletion in mammalian cells results in the loss of ZW10 from kinetochores. Importantly, Beclin-1 depletion had no effect on kinetochore Zwint-1 levels, and ZW10 depletion did not alter Beclin-1 recruitment, demonstrating that Beclin-1, in terms of hierarchy, resides between Zwint-1 and RZZ (Fremont et al., 2013). Given the current model of RZZ loading, it would appear that both SAC pathways share a common structural origin, Knl1. However, recent work has demonstrated that the RZZ pathway remains functional in cells depleted of Knl1, suggesting the existence of a Knl1 independent route for RZZ loading (Silio et al., 2015). In summary, the KMN network acts as both a direct microtubule interactor and a structural platform.

A1.7 ***Kinetochore bound dynein and kinesin***

The striking ability of the spindle to self-assemble, dynamically reorganise and move chromosomes is highly dependent on the force-generating interaction of molecular motors (kinesins and dynein) with microtubules. The additive function of these motors in several spindle regions enables a series of complex events to be facilitated by the relatively simple behaviour of individual motors on microtubules. Here, I will focus on the loading of motors to the kinetochore region, discussing those critical for kinetochore functionality, namely dynein, Kif18A (a kinesin 8), MCAK (a kinesin-13, also known as Kif2C), and CENP-E (a kinesin 7). In terms of congression, these motors can be broadly grouped into two categories, those that move chromosomes (dynein and CENP-E), and those that regulate microtubule dynamics at the kinetochore (MCAK and Kif18A).

Dynein is a multi-subunit minus-end directed motor that accumulates at kinetochores prior to microtubule attachment in prometaphase (Echeverri et al., 1996; Pfarr et al., 1990; Steuer et al., 1990). The dynein motor complex is built around two heavy chain (DHC) subunits that dimerise via their N-termini (Urnavicius et al., 2015). The C-terminal two thirds of the DHC contains the motor domain, which consists of a characteristic ring of 6 AAA^+ domains (Carter et al., 2011; Kon et al., 2012; Kon et al., 2011). Emerging from the fourth AAA^+ domain is a 15nm coiled-coil protrusion termed the 'stalk', which contains the microtubule-binding region (Kon et al., 2012). To build the motor complex, each DHC wraps around part of a WD40 domain

within the intermediate chain (DIC) subunits (Urnavicius et al., 2015). The N-termini of two DICs form an extended region, which binds three light chain (DLC) dimers (Benison et al., 2007; Chowdhury et al., 2015; Williams et al., 2007). A portion of each DHC also extends past the DICs and binds the intermediate light chains (DILC), which are structurally related to Ras G-proteins (Schroeder et al., 2014). *In vivo,* this complex associates with the essential regulatory cofactor dynactin, a 23-subunit complex built around a short actin filament that was originally identified as a dynein transport activator (Schroer, 2004). Dynein recruitment to kinetochores occurs via two independent pathways, one mediated by the RZZ complex, and other by a complex consisting of dynein, a platelet-activating factor LIS1, and the nuclear distribution proteins Nde1 and Ndel1. It must be noted, however, that the organisation of the latter pathway remains somewhat controversial, despite similarities in the mitotic defect observed when Nde1, Ndel1, LIS1 or DHC are individually depleted (Barisic et al., 2014; Li et al., 2005; Raaijmakers et al., 2013; Vergnolle and Taylor, 2007). The presence of LIS1 at kinetochores is critical for the loading of dynein (Li et al., 2005), but is not required for the association of Ndel1 or Nde1 (Vergnolle and Taylor, 2007). This suggests that LIS1 is immediately upstream of dynein, and potentially down stream of Nde1/Ndel1. However, while some demonstrate that Ndel1 loads LIS1 (Liang et al., 2007), and therefore dynein, to kinetochores, others show that Ndel1 depletion has no effect on DHC levels and dynein recruitment is entirely dependent upon Nde1(Vergnolle and

Taylor, 2007). Thus throwing into question the relationship between Ndel1 and LIS1. Moreover, a recent study demonstrated that depletion of Nde1 or Ndel1 either individually or together had only a mild, non-additive effect on DHC loading, and this cannot account for the observed reduction in DHC after knockdown of LIS1 (Raaijmakers et al., 2013). This is again disputed by observations from Nde1/Ndel1 antibody injected in LLC-PK1 cells, where dynein was almost completely lost from the kinetochore (Stehman et al., 2007). As such, the hierarchy between Nde1/Ndel1 and LIS1 is still under debate. In addition, the fibrous corona component CENP-F has been implicated in the recruitment of the dynein/Nde1/Ndel1/LIS1 complex (Vergnolle and Taylor, 2007). CENP-F directly binds both Ndel1 and Nde1 and is required for their kinetochore localisation. Building on this, Vergnolle and colleagues suggest that CENP-F acts in a linear pathway that loads Nde1 followed by dynein (Vergnolle and Taylor, 2007), however, given the contradicting results regarding the dependency of dynein on Nde1, this conclusion is uncertain. These inconsistencies may be due to cell type specific effects, as most investigations have employed a cell line specific to that study. As such, a more detailed analysis, which includes the comparison of multiple cell types and the use of mutants deficient in specific binding properties is needed to evaluate the true Nde1/Ndel1/LIS/dynein loading relationship at the kinetochore. In a comparably simplistic model, RZZ is also implicated in the recruitment of dynein. This is mediated via (1), the direct interaction of RZZ with DIC1

and the p50/dynamitin subunit of the regulatory dynactin complex (Starr et al., 1998; Whyte et al., 2008), and (2) via recruitment of spindly, which is required for dynein loading to the kinetochore (Chan et al., 2009).

CENP-E is a microtubule dependent plus-end directed motor of the kinesin-7 family (Kim et al., 2008; Wood et al., 1997). Initially, it was demonstrated in HeLa cells that CENP-E directly binds the checkpoint protein BubR1 (Chan et al., 1998), an observation that was later confirmed in Xenopus extracts (Mao et al., 2003). In the latter system, this interaction is dependent upon the BubR1 kinase domain (Mao et al., 2003), and is required for the loading of CENP-E to unattached kinetochores (Chen, 2002; Mao et al., 2003; Sharp-Baker and Chen, 2001). Despite being confirmed in human DLD-1 cells (Johnson et al., 2004), two subsequent studies using HeLa cells suggested that BubR1 depletion had no effect on CENP-E kinetochore levels (Akera et al., 2015; Lampson and Kapoor, 2005). Moreover, the role the BubR1 in kinetochore-microtubule attachment, which was originally attributed to CENP-E, was shown to be dependent on the direct regulation of the phosphatase PP2A-B56α by BubR1 (Suijkerbuijk et al., 2012). Interestingly, a recent report has implicated another SAC effector, Mad1, in the kinetochore loading of CENP-E in HeLa cells (Akera et al., 2015). Mad1 and CENP-E form a complex *in vivo*, and their interaction is dependent upon a (F/L)xxF(I/L/F) domain in Mad1 and the kinetochore targeting region of CENP-E. Here, depletion of Mad1 resulted in the complete abrogation of CENP-E binding

to the kinetochore, an observation that was conserved in yeast (Akera et al., 2015). Thus, SAC components are likely required for the loading of CENP-E, but the specific interaction factor could be cell type specific.

In addition to a SAC dependent pathway, several other kinetochore proteins directly interact with CENP-E and may facilitate its loading to kinetochores. In this regard, CENP-E has been shown to bind Nuf2 (Liu et al., 2007), SKAP (Huang et al., 2012) and CENP-F (Chan et al., 1998) both *in vivo* and *in vitro*. Depletion of CENP-F (Bomont et al., 2005; Johnson et al., 2004) or Nuf2 (Liu et al., 2007), but not SKAP (Huang et al., 2012), significantly reduces the kinetochore levels of CENP-E. Suggesting that the latter interaction does not contribute to CENP-E loading in cells. Moreover, the Nuf2 dependent pathway is independent from other members of the Ndc80 complex, as their depletion has no effect on CENP-E binding (Liu et al., 2007). Thus, the direct interaction of CENP-E with CENP-F and Nuf2 is required for its recruitment to kinetochores.

The motor-dependent regulation of microtubule dynamics at the kinetochore is facilitated by two key factors, MCAK and Kif18A (see below for discussion). Both factors have distinct recruitment pathways, which likely reflects the fact that MCAK, unlike Kif18A and the majority of other kinesins, is non-motile (Hunter et al., 2003). As such, MCAK must be actively loaded to kinetochores, a process that is microtubule independent, whereas Kif18A transports itself along the K-fiber, concentrating adjacent to at its terminus at the kinetochore (Stumpff et al., 2011). MCAK dynamically

localises to the inner centromere on mammalian chromosomes, initially occupying a central region similar to Aurora B (see below for discussion), and becoming more peripheral after bi-orientation, potentially stretching into the kinetochore (Andrews et al., 2004; Lan et al., 2004). The loading of MCAK to the centromere is dependent upon Shugoshin (Sgo) 2 (Huang et al., 2007), another inner-centromere protein that regulates chromatid cohesion by recruiting protein phosphatase (PP) 2A. In cells, depletion of Sgo2 delocalised centromeric MCAK in a microtubule independent manner (Huang et al., 2007). Interestingly, Bub1 is required for Sgo2 recruitment to the centromere, and therefore sits upstream in this pathway (Huang et al., 2007). It must be noted, however, that no interaction between Sgo2 and MCAK has yet been documented in cells or using recombinant protein, suggesting that they do not form a stable complex (Huang et al., 2007). The recruitment of MCAK is also both positivity and negatively regulated by the kinase Aurora B, which demonstrates a similar localisation pattern (see below). In this regard, phosphorylation at S110 promotes targeting, while phosphorylation at S95 limits it (Zhang et al., 2007). Temporally downstream of these events, phosphorylation at S628 by an unknown kinase is responsible for the dissociation of MCAK from the centromeric region (Ganguly et al., 2012). Thus, MCAK requires several centromeric neighbours for its localisation, however, any direct interactions that mediate this process are yet to be discovered.

Kif18A is not a kinetochore-tethered motor per se, however, its specific functionality causes it to accumulate at the K-fiber plus-end adjacent to the kinetochore (Stumpff et al., 2011), a behaviour that is vital for its function (see below for discussion). The stable binding to, and accumulation at, the K-fiber plus-end is primarily mediated by loop 2 of the Kif18A motor domain (Kim et al., 2014). This behaviour is specific to Kif18A, as a chimera consisting of the Kif4A motor domain and the C-terminal tail of Kif18A failed demonstrate similar behaviour *in vivo* (Kim et al., 2014). It is important to note that in full length Kif18A, the C-terminus acts as processivity factor that provides a motor-independent microtubule-binding site (Stumpff et al., 2011). This loading profile is also under phospho-control, with phosphorylation at S674/S684 by Cdk1 negatively regulating the motors accumulation, an action that is antagonised by a Kif18A bound pool of PP1 (Hafner et al., 2014). Thus, while not being tethered to the kinetochore, Kif18A is predisposed to accumulate within this region after microtubule attachment.

A1.8 ***The inner centromere***

The idea of an inner centromere localised ‘control hub’ for chromosome segregation was first suggested in 1991 by the chromosome passenger hypothesis (Earnshaw and Bernat, 1991). In the subsequent decades, this idea gained traction with the discovery of the chromosome passenger

complex (CPC, consisting of Aurora B, INCENP, borealin and survivin), which is located at the inner centromere, and is involved in the regulation of chromosome structure, the correction of erroneous kinetochore-microtubule attachments, and SAC signalling (van der Waal et al., 2012). The CPC can be divided into two functional modules, the first is an enzymatic component made of the Ser/Thr kinase Aurora B, which interacts with the highly conserved IN box at the C-terminus of INCENP (Adams et al., 2000). The second is a regulatory/targeting component, consisting of the INCENP N-terminus, survivin and borealin (Jeyaprakash et al., 2007). The CPC first localises to pericentric heterochromatin during late S-phase via direct interaction of INCENP with HP1 (Ainsztein et al., 1998; Beardmore et al., 2004; Cooke et al., 1987; Hayashi-Takanaka et al., 2009; Kang et al., 2011a; Zeitlin et al., 2001), which is bound to histone H3 at the trimethylated residue Lys9 (Fischle et al., 2005; Hirota et al., 2005). As cells enter mitosis, Aurora B phosphorylation of histone H3 at Ser10 abrogates the HP1-Lys9 interaction (Fischle et al., 2005; Hirota et al., 2005), switching centromeric CPC loading to an M-phase specific pathway. Here, CPC enrichment is dependent upon the phosphorylation of two histone tails, namely H3T3 by haspin kinase (Kelly et al., 2010; Wang et al., 2010; Yanagishi et al., 2010), which generates the docking site for survivin (Du et al., 2012; Jeyaprakash et al., 2011), and H2AT120 by Bub1 (Kawashima et al., 2007; Yanagishi et al., 2010). The phospho-histone profiles overlap at

the inner-centromere, therefore maximising the CPC concentration within this region.